Use of End-of-Waste Foamed Fibers and Aggregates into a Cementitious Mortar

Bartolomeo Coppola

Unione Europea

Ministero dell'Istruzione, dell'Università e della Ricerca

UNIVERSITÀ DEGLI STUDI DI SALERNO

UNIVERSITÉ DE LIÈGE

FONDO SOCIALE EUROPEO

Programma Operativo Nazionale 2000/2006
"Ricerca Scientifica, Sviluppo Tecnologico, Alta Formazione"
Regioni dell'Obiettivo 1 – Misura III.4
"Formazione superiore ed universitaria"

Department of Industrial Engineering (UNISA)

Ph.D. Course in Chemical Engineering
(XV Cycle-New Series, XXIX Cycle)

Department of Architecture, Geology, Environment and Constructions (ArGEnCo) (ULG)

Ph.D. Course in Engineering Science and Technology

USE OF END-OF-WASTE FOAMED FIBERS AND AGGREGATES INTO A CEMENTITIOUS MORTAR

Supervisors
Prof. Luciano Di Maio (UNISA)
Prof. Luc Courard (ULG)

Ph.D. student
Bartolomeo Coppola

Scientific Referees
Prof. Maria Rossella Nobile
Prof. Enzo Martinelli

Ph.D. Course Coordinators
Prof. Ernesto Reverchon (UNISA)
Prof. Frédéric Nguyen (ULG)

To my family and Giovanna, my love

Acknowledgments

At the end of these three years, it is difficult to express in few words my gratitude and appreciation to all of those who participated to the realization, directly or indirectly, of this work.

I would like to begin by expressing my gratitude to my supervisors, Prof. Luciano Di Maio and Prof. Luc Courard, for their valuable supervision and guidance on my research activities. Prof. Di Maio, I have to thank you for a countless number of reasons but the most important are the opportunities given to me to live many different experiences and, in particular, for your friendship. Prof. Courard, I have to thank you for the warm welcome in your research group in Liège: the LMC equipe (Monique, Amaury, Fabienne and Véronique) is for me like a second family. A special thank goes to my dear friend Frédéric Michel, he was always present for everything: to discuss of work or not, for jogging, for lunch, for a ride home, etc. I would also like to thank Prof. Loredana Incarnato and Prof. Paola Scarfato for providing valuable comments and feedbacks for my work, but also valuable discussions on the life and the future. I would like to thank the persons who shared with me every day of these three years in the lab I1, Valentina Volpe, Valentina Iozzino, Sara and Annarita, without you everything would be different. I would also like to thank all the other people that I met during these three years in the labs of the DIIN: Prof. Roberto Pantani, Felice, Sara, Vito, Lucia, Emilia, Nicola, Annalisa, Debora, Rita, Mariella, Simona, Gabriella, Marcella, Maria. A special thank goes also to my Belgian colleagues and friends, Sophie, Zengfeng, Vincent. I would like to thank the Italian researchers and friends in Belgium, Marina, Laura and Velia, hoping that Italian University can recognize our talent, one day. Antonella and Ada, thank you for sharing joys and efforts of these three years of Ph.D.

Finally, it is impossible for me to express all my gratitude, my friendship and my regard to those who made me feel at home and loved during my stays in Belgium: Malou, Pierre René, Simon, Henri, Anne, Monique, Jean, Jacqueline, Céline.

I conclude by thanking my family, my friends and Giovanna for their support, their understanding and love during all these years.

List of publications

B. Coppola, L. Di Maio, L. Courard, P. Scarfato, L. Incarnato, "*Nanocomposite fiber reinforced mortars*". 22nd International Conference on Composites/Nano Engineering (ICCE-22), Malta, July 13-19 2014.

B. Coppola, L. Di Maio, P. Scarfato, L. Incarnato, "*Durabilità e sostenibilità di malte cementizie rinforzate con fibre di basalto*". Smart Expo Ambiente Mediterraneo (SAM), Salerno, September 11-12 2014.

B. Coppola, L. Di Maio, P. Scarfato, L. Incarnato, "*Processability, morphology and mechanical behavior of polypropylene/clay nanocomposite fibers*". Proceedings of the 8th ECNP International Conference on Nanostructured Polymers and Nanocomposites, Dresden, September 16-19 2014. ISBN: 978-3-9816007-1-1.

B. Coppola, L. Di Maio, P. Scarfato, L. Incarnato, "*Influenza di fibre nanocomposite in polipropilene sul comportamento di una malta cementizia*". Proceedings of the XII AIMAT national conference, Lecce, September 21-24 2014. ISBN: 978-8-8940-4020-3.

B. Coppola, L. Di Maio, P. Scarfato, L. Incarnato, "*Rheological and mechanical behavior of polypropylene/clay fibers*". The Europe Africa 2014 regional conference of the international Polymer Processing Society (PPS-2014). Tel Aviv, October 19-23 2014.

B. Coppola, P. Scarfato, L. Incarnato, L. Di Maio, "*Durability and mechanical properties of nanocomposite fiber reinforced concrete*". CSE - City Safety Energy– 2, 2014: 127-136. ISSN: 2283-8767.

B. Coppola, L. Di Maio, L. Courard, P. Scarfato, L. Incarnato, "*Use of foamed polypropylene fibers to improve fiber/matrix bond for cementitious composites*". Proceedings of the 20th International Conference on Composite Materials (ICCM-20). Copenhagen, July 19-24 2015.

B. Coppola, L. Di Maio, P. Scarfato, L. Incarnato, "*Use of polypropylene fibers coated with nano-silica particles into a cementitious mortar*". Proceedings of the international conference celebrating the $(35x2)^{th}$ birthday of G. Titomanlio. Salerno, October 15-17 2015. ISBN: 978-0-7354-1342-9 DOI: 10.1063/1.4937334.

B. Coppola, L. Di Maio, L. Courard, P. Scarfato, L. Incarnato, "*Lightweight cementitious mortar made with foamed plastic waste aggregates*". Proceedings of the International Workshop on Durability and Sustainability of Concrete Structures (IW-DSCS). Bologna, October 1-3 2015. ISBN: 978-1-942727-44-6 ISSN: 01932527.

B. Coppola, L. Courard, F. Michel, L. Incarnato, L. Di Maio, "*Investigation on the use of foamed plastic waste as natural aggregates replacement in lightweight mortar*". Composites Part B: Engineering 99, 2016: 75-83. ISSN: 13598368 DOI: 10.1016/j.compositesb.2016.05.058.

B. Coppola, L. Di Maio, P. Scarfato, L. Incarnato, "*Production and characterization of polyethylene/organoclay oriented fiber*". Proceedings of the VIII international conference on "Times Of Polymers and composites": From Aerospace to Nanotechnology (TOP-2016). Vol. 1736 (1): p. 020155, May 2016. ISBN: 978-0-7354-1390-0 DOI: 10.1063/1.4949730

B. Coppola, L. Di Maio, P. Scarfato, L. Incarnato, "*Polyethylene/Layered-Silicate Nanocomposite Oriented Fibers: Morphology And Mechanical Characterization*". Proceedings of the XIII AIMAT National Congress, July 13-15. Journal of Applied Biomaterials and Functional Materials 2016. Vol. 14 (3): p. e314-e393 DOI:10.5301/jabfm.5000321

B. Coppola, L. Di Maio, L. Courard, P. Scarfato, L. Incarnato, "*Development and use of foamed recycled fibers to control shrinkage cracking of cementitious mortars*". Proceedings of the 4rd Workshop "The New Boundaries of Structural Concrete". Anacapri, September 29^{th} - October 1^{st} 2016, Pag.167-174. ISBN: 978-8-8987-2014-9

B. Coppola, P. Scarfato, L. Incarnato, L. Di Maio, "*Morphology development and mechanical properties variation during cold-drawing of polyethylene-clay nanocomposite fibers*". Materials & Design *(submitted)*

List of contents

Chapter V

List of figures

List of tables

Abstract

Durability and *sustainability* of cementitious materials are two important issues in the field of construction materials. Durability is defined as the ability of cementitious materials to resist weathering action, chemical attack, abrasion or any other process of deterioration. The use of fibers is a viable solution to partially overcome the brittle behavior of such materials. At the same time it is demonstrated that fibers, by reducing cracking phenomena, allow to face the durability related issues. Different fibers have been used according to the aims of composite materials: high strength fibers are generally used for structural purposes (toughness increase) while low modulus synthetic fibers are mainly used to avoid plastic shrinkage cracking. The effectiveness of fibers reinforcing action lies mainly on the fiber/matrix interactions. Three types of interactions can be recognized: i) physical and/or chemical adhesion; ii) friction and iii) mechanical anchorage induced by deformations on the fiber surface (e.g. crimps, hooks, twisted or deformed fibers in general). Sustainability can be identified according to the definition of sustainable development stated in 1987 by Brundtland et al.: "*the development that meets the needs of the present without compromising the ability of future generations to meet their own needs*". Sustainable development should take into account economic growth, social equality and environmental protection. The construction industry involves all these fields: the main concerns are raw materials consumption and CO_2 emissions during cement production. Moreover, also the plastic production and disposal present several environmental issues. Once again, raw materials consumption and the speed with which these materials became waste.

Thus, seen the aforementioned drawbacks related to cementitious materials, this Ph.D. was aimed to study the possibility of using end-of-waste materials (i.e when waste ceases to be waste and becomes a secondary raw material) for the production of synthetic fibers and aggregates characterized by improved mechanical interactions with the cementitious matrix. To this extent, fibers and aggregates with a rough and porous surface, able to offer interlocking positions for the cementitious matrix, were produced in laboratory by melt extrusion-foaming process. Moreover, some chemical treatments (alkaline hydrolysis and sol-gel deposition of nano-silica) were performed on fibers, to improve chemical adhesion with the cement paste. Finally, taking into account the need for reducing the

consumption of raw materials, foamed fibers and aggregates were produced starting from a polymeric end-of-waste material made of a polyolefins blend (HDPE, LDPE and PP).

Alkaline hydrolysis promoted the creation of interlocking positions on fiber surface but the best behavior was recognized for fibers with nano-silica particles on the surface. In this case, a denser ITZ and a great amount of hydration products were observed by SEM investigations. Pull-out tests confirmed the better performances of treated fibers: a higher pull-out peak load was achieved and an increase of pull-out energy was evident.

Subsequently, a foam extrusion process was used to manufacture polymeric fibers (both virgin and recycled) with a rough surface, to improve mechanical friction with the cementitious matrix. Optimizing foaming agent quantity and processing parameters was possible to produce fibers having adequate surface texture and diameter to be used in fiber reinforced mortars. Although fiber reinforced mortars workability decreases at increasing fiber volume fraction, the results demonstrated that this happens to a lower extent for mortars containing foamed fibers. Fibers mechanical properties decreased at increasing fibers porosity but fiber reinforced mortars mechanical properties, flexural and compressive strength, were not influenced by fibers addition nor their morphology. The rougher surface gives rise to a better fiber/matrix adhesion, as confirmed by pull-out tests. Durability investigations on the fiber reinforced mortars reported good results for capillary water absorption, sulfate attack and plastic shrinkage cracking. In particular, fibers length and volume fraction are key parameters in controlling plastic shrinkage cracking. Moreover, mortar samples containing foamed fibers displayed a better control of shrinkage cracking: cracks opening was delayed and the improved fiber/matrix bond was able to reduce crack width, compared to mortars containing smooth fibers.

Finally, lightweight artificial aggregates (LWAs) were produced, starting from foamed strands. At increasing LWAs substitution, a sharp decrease of density was achieved. Also workability and mechanical properties decreased, but a more ductile behaviour was recognizable. Thermal conductivity and water vapor resistance were proportional to mortars density which obviously decreased at increasing natural sand substitutions. Moreover, the use of aggregates porosity as reservoir of internal curing water showed promising preliminary results.

In brief, the results of this study demonstrate that engineered fibers with improved fiber/matrix bond allow to optimize (i.e. to reduce) fibers volume fraction in cementitious mortars. Foamed fibers characteristics can be in turn optimized by changing the manufacturing process conditions. Benefits could be not only in the control of plastic shrinkage cracking but also in the workability of fresh mortars, mechanical strength and durability of the hardened composite. In addition, using end-of-waste materials a more sustainable product can be obtained. In particular, replacing natural aggregates with plastic aggregates, is possible to reduce raw materials consumption and improve mortar properties (mainly unit weight, thermal conductivity and water vapor permeability).

Résumé

Dans le domaine de matériaux de construction, la durabilité des ouvrages en béton et le développement durable représentent deux aspects très importants. La durabilité de l'ouvrage caractérise sa capacité à conserver, pendant le temps, les fonctions d'usage pour lesquelles il a été conçu. L'utilisation des fibres dans les matériaux à base de ciment permet d'améliorer la ductilité et réduire les effets du retrait, dont la fissuration, et prolongent ainsi la durée de vie de l'élément en béton. On distingue trois grandes familles de fibres selon leur nature (métalliques, synthétiques, minérales) qui peuvent être utilisées à des fins structurelles ou non, en fonction de leurs propriétés mécaniques. Pour être efficaces, une bonne adhérence (chimique, mécanique ou par friction) fibre/matrice doit est assurée. Le développement durable a été défini dans le rapport Brundtland en 1987: «*il s'agit d'un développement qui répond aux besoins du présent sans compromettre la capacité des générations futures à répondre à leurs propres besoins*». Dans l'industrie de la construction, notamment celle du ciment, les problèmes principaux dérivent de la consommation des matières premières et des émissions de CO_2 dans l'atmosphère. De plus, la production de polymères et l'élimination des déchets plastiques posent divers problèmes environnementaux, notamment au travers de l'utilisation du pétrole et de la très faible vitesse à laquelle les produits plastiques deviennent déchets.

Étant donné les différentes problématiques mentionnées ci-dessus, le but de cette étude est la production de fibres et agrégats en plastique ayant une meilleure adhérence avec la pâte de ciment, en utilisant un matériau «*end-of-waste*» (c'est-à-dire lorsqu'un déchet cesse d'être un déchet et devient une matière première secondaire) et un processus de «*foam extrusion*». Le processus de «*foam extrusion*» a été utilisé pour produire des fibres et des agrégats avec une surface rugueuse et poreuse, sous forme de cavités dans lesquelles la matrice cimentaire peut pénétrer. De plus, certains traitements chimiques (hydrolyse alcaline et dépôt sol-gel de nano-silice) ont été effectués sur des fibres pour améliorer l'adhérence chimique avec la pâte de ciment. Enfin, prenant en compte le désir de réduire la consommation de matières premières et le but d'augmenter l'utilisation de matériaux recyclés, les fibres et les agrégats expansés ont été produits en utilisant un matériau

fin-de-déchet qui est un mélange de plusieurs polyoléfines (HDPE, LDPE et PP).

L'hydrolyse alcaline a produit de cavités sur la surface des fibres, mais le meilleur comportement a été trouvé pour les fibres avec des particules de nano-silice sur la surface. Dans ce cas, une Zone de Transition Interfaciale (ITZ) plus dense et une grande quantité de produits d'hydratation ont été observés par des investigations SEM. Les tests de pull-out ont confirmé les meilleures performances de fibres traitées: une charge maximum de pull-out plus élevée a été mesurée, avec une augmentation évidente de l'énergie d'extraction. Ensuite, un processus d'extrusion de mousse a été utilisé pour fabriquer des fibres polymères (tant vierges que recyclées) avec une surface rugueuse. L'optimisation de la quantité d'agent moussant et des paramètres de processus a permis la production de fibres ayant une texture superficielle et un diamètre adéquats. L'ouvrabilité des mortiers fibrés diminue avec l'augmentation de la quantité des fibres, mais, de manière plus faible dans le cas de mortiers renforcés avec les fibres moussées. Les propriétés mécaniques des mortiers fibrés ne sont pas influencées par l'addition des fibres ni par leur morphologie. La surface plus rugueuse offre une meilleure adhérence fibre/matrice, comme confirmé par les essais de pull-out. Les études de durabilité sur les mortiers renforcés ont rapporté de bons résultats en ce qui concerne l'absorption d'eau par capillarité, l'attaque par les sulfates et la fissuration au jeune âge. En particulier, les échantillons de mortier contenant des fibres moussées ont permis d'obtenir un meilleur contrôle de la fissuration car l'ouverture des fissures a été retardée et la bonne adhérence fibre/matrice a permis de réduire la largeur des fissures, par rapport aux mortiers contenant des fibres lisses. Enfin, des agrégats artificiels légers ont été produits à partir des fibres moussées. La substitution du sable naturel par les agrégats plastiques a engendré une forte diminution de la densité. La maniabilité et les propriétés mécaniques diminuent également, mais un comportement plus ductile est observé. La conductivité thermique et la résistance à la vapeur d'eau diminuent avec l'augmentation du taux de substitution de sable naturel, proportionnellement à la densité de mortiers. Enfin, l'utilisation de la porosité des agrégats comme réservoir d'eau a donné des résultats préliminaires prometteurs.

En résumé, les résultats de cette étude démontrent la possibilité d'optimiser la fraction volumique des fibres dans les mortiers de ciment à l'aide de fibres moussées, c'est-à-dire de fibres ayant une adhérence fibre/matrice améliorée. Les avantages pourraient être non seulement dans le contrôle de la fissuration au jeune âge, mais également dans la maniabilité des mortiers frais, la résistance mécanique et la durabilité du composite durci. En outre, en utilisant des matériaux de recyclage, on peut obtenir un produit plus durable grâce à la réduction de l'utilisation des matières premières. En particulier, le remplacement des agrégats naturels par des agrégats en polymère permet de réduire la consommation de matières premières et d'améliorer les propriétés du mortier (réduction du poids et de la conductivité thermique et augmentation de la perméabilité à la vapeur d'eau).

Chapter I
State of the art

I.1 Cementitious materials

Cementitious materials (or, more precisely, cementing materials) have been used since ancient times. The Egyptians, the Greeks and, significantly, the Romans used materials that harden after have been mixed to water. The Romans were the first producers of concrete and pozzolanic cement, that used to build structures that still exist (Neville, 1995). Nowadays, concrete is basically a mixture of water, cement, aggregates and additives (plasticizers, superplasticizer, shrinkage reducing admixtures, air entraining agents, set-retarding etc.).

Concrete is the most extensively used construction material, particularly combined with steel, thanks to a relative low price, is easily molded, has a good compressive strength and an adequate stiffness for structural uses. On the other side, as negative aspects, concrete is not eternal and is brittle. Long-term performances of concrete are of widespread importance both for new constructions and existing structures. The brittle behavior means a very low tensile strength and lack of ductility. To overcame this drawback, one of main strategies is the addition of fibers, as will be discussed in the following. Concerning concrete durability, cementitious materials porosity is the key parameter: governing porosity and thus permeability is possible to produce a more durable material.

Porosity, however, is an intrinsic property of the cementitious materials and, despite the efforts to reduce and control this parameter, it is not possible to completely prevent voids formation. Generally voids are classified considering their size in: gel pores, capillary pores, macro-voids (entrapped and entrained air) and cracks (Table I.1). Porosity greatly influences not only durability properties but also mechanical strength (Neville, 1995). The presence of accessible pores and the presence of interconnected galleries represents an easy way for the penetration of several agents: water, chlorides, sulfates, carbon dioxide, etc., that determine the increase of decay rate and deterioration of cementitious materials.

Table I.1 *Pores classification, dimension and influenced properties*

Type of pore		Size	Influenced properties
Gel pores		1-10 nm	Shrinkage, creep
Capillary pores		0.01-10 μm	Permeability, strength and shrinkage
Macro-voids	Entrained air	0.06-1 mm	Permeability, strength
	Entrapped air	1-5 mm	
Micro-cracks		50-200 μm	Permeability, strength
Macro-cracks		mm order	Permeability, strength

I.2 Durability of cementitious materials

Durability of cementitious materials is defined as its ability to resist weathering action, chemical attack, abrasion, or any other process of deterioration. Durable concrete will retain its original form, quality, and serviceability when exposed to its environment (ACI 201.2R-01).

As previously discussed, porosity is the main aspect that should be considered in the evaluation of cementitious materials durability. In the following paragraphs transport mechanisms and degradation phenomena will be discussed.

I.2.1 Transport mechanisms in cementitious materials

Generally, deterioration agents could be present in the environment where the structure is built but they can be already present in the structure, due to a lack of controls on raw materials, for example. Thus, deterioration occurs because attacking agents are able to penetrate throughout the concrete (i.e. concrete should be permeable) and move inside pores due to pressure, concentration, moisture and temperature gradients. The mechanisms and the causes of mass transports can be summarized in:

- *Permeability*: the transport is determined by a pressure gradient;
- *Diffusion*: a concentration gradient causes the movement;
- *Sorption*: generated by the forces of surface adhesion, depending on the affinity of a liquid, water in particular, with the surfaces of a solid (i.e. concrete).

Thus, cementitious materials durability, is governed by transport properties that are influenced and controlled by porosity (number, type, size and distribution of the pores) and cement paste/aggregates interfacial transition zone (ITZ).

As seen, depending on the driving force and the nature of the transported matter (gas, liquid or ion), different transport processes are recognizable as permeability, diffusion and sorption.

I.2.1.1 Permeability

Permeability is a measure of the ability of a porous material to allow fluids to pass through it. In particular, the driving force derives from the action of a pressure differential. Permeability is clearly dependent not only on the porosity but also on the level of connection of the pores. Darcy's law states that the steady-state rate of flow is directly proportional to the hydraulic gradient (eq. I.1), i.e.:

$$v = \frac{Q}{A} = -K\left(\frac{dh}{dL}\right) \tag{I.1}$$

where ν is the apparent velocity of flow, Q is the flow rate, A is the cross-sectional area of flow, dh is the head loss over a flow path of length dL, K is called the coefficient of permeability (Basheer et al., 2001).

Darcy's law has been generalized to apply to any fluid flowing in any direction through a porous material, so long as the conditions of flow are viscous. The law can be expressed by the equation:

$$v = \frac{Q}{A} = -\left(\frac{k}{\mu}\right)\left(\frac{dp}{dL}\right) \tag{I.2}$$

where dP is the pressure loss over the flow path dL, μ is the viscosity of the fluid, k is referred to the intrinsic permeability of the porous medium. Intrinsic permeability, measured in m^2, depends only on the characteristics of the porous medium and is independent of those fluid characteristics which govern the flow, i.e. viscosity μ, expressing the shear resistance of the fluid (Basheer et al., 2001).

I.2.1.2 Diffusion

When the matter is transported from one part of a system to another due to a concentration gradient, it refers to the diffusion process. The macroscopic movement occurs as a result of small random molecular motions, which take place over small distances. The progress of diffusion is much faster in gases than in liquids, being the slowest in solids (Basheer et al., 2001). The permeant, i.e. the molecules that are in movement, flow from high concentration to low concentration across the interface: flux is a measure of diffusion and represents the flow rate per unit area at which mass moves. Fick's first law of diffusion, eq. I.3, states that the rate of transfer of mass through unit area of a section, J, is proportional to the concentration gradient $\delta c/\delta x$ and the diffusion coefficient:

$$J = -D\frac{\delta c}{\delta x} \tag{I.3}$$

For non-steady state conditions, the concentration c at the location x changes with time, and the balance equation generally referred to as Fick's second law of diffusion (eq. I.4) describes the change in a unit volume with time:

$$\frac{\delta c}{\delta t} = D\frac{\delta^2 c}{\delta x^2} \quad \text{(I.4)}$$

In this equation, D may be constant or a function of different variables, such as time, temperature, concentration, location, etc. For a constant D, the solution of the above equation for the boundary condition of $c = c_{(0,t)}$ and the initial condition of $c = 0$ for $x > 0$ and $t = 0$, is given by eq. I.5:

$$C = c_0\left(1 - erf\left(\frac{x}{2\sqrt{Dt}}\right)\right) \quad \text{(I.5)}$$

where *erf* is the standard error function. A factor to consider while dealing with the diffusion process is the chemical reactions taking place between the penetrating substances and concrete. For example, the diffusion of chloride ions into the concrete is accompanied by reaction such as physical and chemical binding at the hydration products. The reaction reduces the concentration of movable chloride ion at any particular site and, hence, the tendency for inward diffusion is further reduced. In experiments, which do not explicitly consider binding, erroneous estimates are made using the diffusion equation (eq.I.4) (Basheer et al., 2001).

I.2.1.3 Sorption

Sorptivity, represents the capacity of a medium to absorb (or desorb) liquid by capillarity. Absorption is a process in which atoms, molecules or ions enter in a material (that could be in gas, liquid or solid form) and the capillary action is the ability of a liquid to flow in pore spaces initially filled with a fluid, due to interfacial pressure differences. In particular, the affinity between a liquid with a solid (in our case water and concrete, respectively), generates adhesive forces due to surface tension, generating a depression that determines water capillary rise. Depression can be determined using Laplace equation:

$$P_{cap} = \frac{2\sigma\cos\vartheta}{r} \quad \text{(I.6)}$$

where P_{cap} is the depression in the capillary pores, σ is the superficial tension of the water ($7.2\cdot10^{-2}$ N/m a 25°C), θ is the contact angle between the liquid and the pore surfaces and r is the radius of the pore. Considering some boundary conditions (laminar and unidirectional flow) and integrating the resulting equation in the direction of pore, is possible to determine the water absorbed per unit surface, due to the capillary rise (I.7).

In particular, the water absorbed by surface unit at time t_i and the square root of the time are correlated by the sorptivity (or coefficient of capillary sorptivity):

$$\boldsymbol{I_{t_i} = S\sqrt{t}} \tag{I.7}$$

Basheer et al. (2001), report a modified equation in which is considered also the initial disturbance (due to the surface finish probably):

$$\boldsymbol{I_{t_i} = S\sqrt{t}}+\mathrm{C} \tag{I.8}$$

where *C* is the initial disturbance.

I.2.2 Degradation of cementitious materials

As stated before, the degradation of cementitious materials can be due either to external factors deriving from the environment or by internal agents, i.e. already present within the material. Causes of degradation can be classified in three categories: physical, chemical and mechanical (Neville, 1995). Physical causes of deterioration include the effects of temperature: exposure to high temperature or of the differences in thermal expansion of aggregate and of the hardened cement paste but also freeze/thawing cycles. The chemical causes of deterioration include the alkali-silica and alkali-carbonate reactions, the action of aggressive ions, such as chlorides, sulfates, or of carbon dioxide, as well as many natural liquids and gases or industrial pollutants. Mechanical damage is caused by impact, abrasion, erosion or cavitation.

It should be observed that the physical and chemical processes of deterioration can act in a synergistic manner, for example the associated action of de-icing salts and freeze/thawing deterioration. Thus, concrete degradation is rarely due to one isolated cause.

The most important causes that determine the decrease of cementitious materials durability, will be briefly discussed in the following paragraphs.

I.2.2.1 Physical causes of deterioration

I.2.2.1.1 Freeze/thaw cycles

In cold climates, it is impossible to avoid the exposure of concrete to alternating freezing and thawing cycles. Freezing of water results in an increase in volume of approximately 9%, thus the water held in the capillary pores expands. Repeated cycles of freezing and thawing have a cumulative effect and when the dilating pressure in the concrete exceeds its tensile strength, damage occurs. Concrete deterioration starts from the exposed

surface and proceeds through its depth. Each cycle of freezing causes a migration of water to locations where it can freeze. These locations include fine cracks which become enlarged by the pressure of the ice and remain enlarged during thawing when they become filled with water. Subsequent freezing repeats the development of pressure and its consequences. As the larger voids in concrete, arising from incomplete compaction, are usually air-filled and, therefore, not appreciably subject to the action of frost. While the resistance of concrete to freezing and thawing depends on its various properties (e.g. strength of the hardened cement paste, extensibility, and creep), the main factors are the degree of saturation and the pore system of the hardened cement paste (Neville, 1995).

I.2.2.1.2 High temperatures

The effect of high temperature on reinforced concrete is disruptive. Steel bars can resist up to 500 °C while concrete compressive strength decreases dramatically between 300 and 800 °C, in particular after 650 °C (Ma et al., 2015). The protective action exerted by the concrete cover is of widespread importance because delays the heat transfer: higher the cover higher is the time necessary for the steel bars to reach the collapse temperature. Moreover, the temperature increase determines also an increase of steel bars volume, generating tensions that can lead to the cover spalling. Attention must be paid during the fire extinguishing operations at water temperature and lime formation.

I.2.2.1.3 Shrinkage and cracking

Shrinkage of cementitious materials is one of the most important durability related issues because can determine the occurrence of cracking phenomena. Shrinkage of concrete takes place in two distinct stages: early and later ages. As early stages, the first 24 h can be considered while setting and hardening are occurring. Thus, later ages refer to 24 h and over (i.e. long term). In these two distinct periods, several types of shrinkage can be identified (Figure I.1): plastic, drying, autogenous, thermal and carbonation.

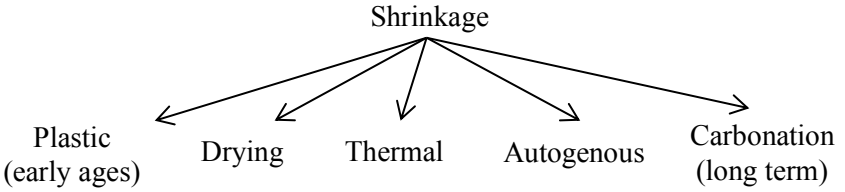

Figure I.1 *Diagram of shrinkage types and age*

In the fresh state of concrete, when is not fully rigid, water movements in the porous structure cause contractions. Moreover, during the hydration reactions of cement, volume changes occur and the volumetric contraction is about 1% of the absolute volume of the dry cement (Neville, 1995). Finally, in the plastic stage, water can also be lost by evaporation from the surface of concrete. All the aforementioned phenomena contribute to the *plastic shrinkage* until the concrete is in the plastic state. The key parameter is the amount of water lost from the surface that is influenced both by temperature and relative humidity of the environment but also by wind speed. If the amount of water lost per unit area exceeds the amount of water brought to the surface by bleeding and is large, surface cracking can occur. This is known as plastic shrinkage cracking: a correct curing after casting, i.e. a rate of evaporation of water lower than 1 kg/m^2 per hour, eliminates plastic cracking. Plastic shrinkage is greater the greater the cement content of the mix and the lower the w/c ratio (Neville, 1995).

Once that setting has taken place, volume changes can still occur. Expansion occurs if water is continuously supplied, continuing hydration, while shrinkage occurs if no moisture movement is permitted. The water present in the capillary pores is consumed to continue the hydration of unhydrated cement: this phenomenon is more pronounced for very low w/c ratios. This process is called *autogenous shrinkage* and is restrained by the rigid skeleton of the already hydrated cement paste and also by the aggregate particles. As self-desiccation is greater at lower water/cement ratios, autogenous shrinkage could be expected to increase but this may not occur because of the more rigid structure of the hydrated cement paste at low w/c ratios (Neville, 1995).

While autogenous shrinkage of cement paste and concrete is defined as the macroscopic volume change occurring with no moisture transferred to the exterior surrounding environment, *drying shrinkage* results from a loss of water from the concrete. High w/c ratios correspond to more unbound water and thus higher drying shrinkage but the change in volume of drying concrete is not equal to the volume of water removed. The loss of free water, which takes place first, causes little or no shrinkage. As drying continues, adsorbed water is removed and the change in the volume of unrestrained hydrated cement paste at that stage is equal approximately to the loss of a water layer one molecule thick from the surface of all gel particles. Since the thickness of a water molecule is about 1 % of the gel particle size, a linear change in dimensions of cement paste on complete drying would be expected to be of the order of $10\,000 \times 10^{-6}$; values up to 4000×10^{-6} have actually been observed (Neville, 1995).

Carbonation shrinkage is a long-term shrinkage that occurs when there is a high CO_2 concentration in the air around the concrete (the process of carbonation is discussed in the following, § 1.2.2.2.1). However, it should be noted that, because carbon dioxide is fixed by the hydrated cement paste, the

mass of the latter increases. Consequently, the mass of concrete also increases. When concrete dries and carbonates simultaneously, the increase in mass on carbonation may at some stage give the misleading impression that the drying process has reached the stage of constant mass, i.e. equilibrium (Neville, 1995).

Carbonation shrinkage is probably caused by the dissolving of crystals of $Ca(OH)_2$ while under a compressive stress (imposed by the drying shrinkage) and depositing of $CaCO_3$ in spaces free from stress; the compressibility of the hydrated cement paste is thus temporarily increased. Carbonation increases the shrinkage at intermediate humidities, but not at 100 % or 25 %. In the latter case, there is insufficient water in the pores within the cement paste for CO_2 to form carbonic acid (H_2CO_3). On the other hand, when the pores are full of water, the diffusion of CO_2 into the paste is very slow; it is also possible that the diffusion of calcium ions from the paste leads to precipitation of $CaCO_3$ with a consequent obstruction of surface pores.

I.2.2.2 Chemical causes of deterioration

I.2.2.2.1 Aggression by Carbon Dioxide

One of the most important chemical aggression, for cement based materials, is that deriving from carbon dioxide (CO_2). Two different deterioration phenomena can occur: carbonation and leaching.

Carbonation is the reaction of calcium hydroxide, $Ca(OH)_2$, with atmospheric carbon dioxide and the consequent production of calcium carbonate:

$$CO_2 + Ca(OH)_2 \longrightarrow CaCO_3 + H_2O$$

This reaction is favored by the presence of moisture, and is faster if there is the presence of sodium ions or potassium ions (i.e. alkali). CO_2 diffuses into the air contained in the pores of the concrete, as a result of a difference in concentration of CO_2 (driving force) between the interior mortar and the outside environment. The reaction reduces the pH of the pores solution (generally around 13), causing problems in the case of reinforced concrete frames where passivation is no longer assured. Passivity is ensured by the presence of a thin iron oxide film on the surface of the metal. It should be noticed that carbonation is greatly influenced by the concrete moisture: the most dangerous relative humidity range is between 50-80%. If pores are dry or saturated, carbonation cannot occurs. Therefore, CO2 diffusion is very fast if pores contain only air and quite slow is moisture is present. In conclusion, carbonation is dangerous particularly for reinforced concrete structures.

Leaching is the dissolution of various minerals present in the cement based materials due to a mechanical action of the water flow. This phenomenon is more pronounced when water is more acid due to carbon dioxide or pollutants present in the environment (acid rain).

I.2.2.2.2 Sulfate attack

Another important chemical cause of deterioration is sulfate attack. When salts are present in solution they can react with hydrated cement paste producing expansive compounds. In soil or groundwater is not rare to found sulfates of sodium, potassium, magnesium and calcium. An example of sulfate attack can be the reaction of sodium sulfate with calcium hydroxide that produces gypsum (calcium sulfate dihydrate). Gypsum can attack calcium aluminate hydrate to form ettringite, i.e. calcium sulfoaluminate ($3CaO{\cdot}Al_2O_3{\cdot}3CaSO_4{\cdot}32H_2O$). The formation of ettringite is followed by an increase of volume that leads to delamination, swelling and cracking. In particular conditions (low temperature and high relative humidity) an even more dangerous compound can be produced, i.e. thaumasite.

The reactions with sulfate magnesium are less common but more disruptive.

I.2.2.2.3 Alkali-aggregates reaction

Alkali-silica reaction occurs between the active silica constituents of the aggregates and the alkalis present in the cement (Na_2O and K_2O). The reactive forms of silica are opal (amorphous), chalcedony (cryptocrystalline fibrous) and tridymite (crystalline) (Neville, 1995). The alkaline hydroxides present in the pore water, derived from the alkalis, attack the siliceous minerals in the aggregates producing an alkali-silicate gel. This compound can attract water by absorption or by osmosis, increasing its volume. Since the gel is confined by the surrounding hydrated cement paste, thus hardened, internal pressures are generate resulting in expansion, cracking and disruption of the cement paste (pop-out and spalling).

The alkali–silica reaction occurs only in the presence of water. The minimum relative humidity in the interior of concrete for the reaction to proceed is about 85% at 20 °C. At higher temperatures, the reaction can take place at a somewhat lower relative humidity. Because water is essential for the alkali–silica reaction to continue, drying out the concrete and prevention of future contact with water is an effective action to stop the reaction. However, the alkali–silica reaction is very slow, and its consequences may not manifest themselves until after many years (Neville, 1995).

I.2.2.2.4 Chlorides

Chlorides, particularly calcium chloride ($CaCl_2$) and sodium chloride (NaCl) have two detrimental actions on concrete structures. Chlorides can leach calcium hydroxide leading to a loss of strength, but they can also attack the steel reinforcement present in reinforced concrete, promoting corrosion. In fact, the presence of chlorides in the pore solution can reduce the passivation of the alkaline cement paste pore solution. There is a threshold concentration of the chloride ions which must be exceeded before corrosion occurs. The corrosion due to chloride ingress progresses at a much higher rate than that due to carbonation and it can be both generalized and localized (i.e. pitting). General corrosion may have more total loss in iron, but pitting corrosion causes more loss in cross-sectional area and hence is more dangerous (Basheer et al., 2001). Several transport mechanism can participate: if capillary pores are relatively dry, absorption dominates and when they are relatively saturated, diffusion becomes the dominant transport process.

I.2.2.3 Mechanical causes of deterioration

I.2.2.3.1 Abrasion

Abrasion damage occurs when the surface of concrete is unable to resist wear caused by rubbing and friction. This phenomenon is common for vehicular traffic surfaces. Moreover, it can occurs also in hydraulic structures, such as dams, spillways, and tunnels. A minor influence have the particles transported by the wind. As the outer paste of concrete wears, the fine and coarse aggregate are exposed, increasing the rate of deterioration.

I.2.2.3.2 Impacts

As concrete is a brittle material, if the intensity of the impact is high, degradation occurs, reducing concrete strength.

I.2.2.3.3 Erosion

Erosion, is a particular type of wear due to the wind, water or ice, that produces the removal of material from the surface of structures. It depends from the speed, the amount of hard dust in the fluid (i.e. wind or water) and the quality of concrete.

I.2.2.3.4 Cavitation

Cavitation occurs where there is the presence of water in movement (speed > 12 m/s). The high speed of the water and the presence of an irregular surface produce a turbulence flow that creates bubbles (or cavities) in the water flow with a local drop of pressure that wear the surface.

I.3 Sustainability and waste management

I.3.1 Generalities

The idea of a sustainable development can be traced back in the centuries since XVIII century when raised up the problem of the forest management in Europe, but only in 1980 appeared the term sustainable development when the International Union for the Conservation of the Nature published a document for the world conservation strategy (IUCN, 1980). Finally, in 1987 a clear definition of the sustainable development was present in the Brundtland Report (Brundtland et al., Our Common Future, 1987):

> *"Sustainable development is the development that meets the needs of the present without compromising the ability of future generations to meet their own needs".*

Sustainable development should take into account several fields and aspects: economic growth, social equality and environmental protection (Figure I.2).

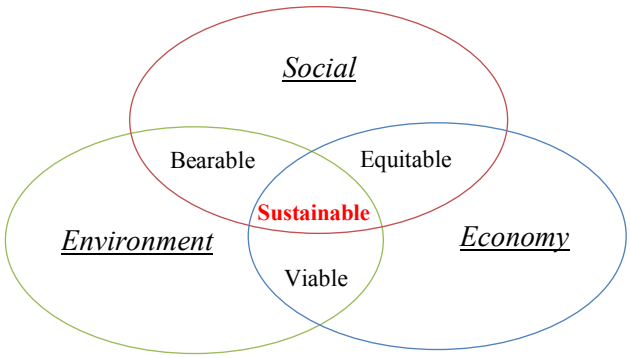

Figure I.2 *The three dimensions of the sustainable development*

After the Brundtland Report, the actions, the initiatives and also the goals, were defined in the "Agenda 21" in 1992 (United Nations, 1992). This first report was followed by other publications, as a result of several events organized by the United Nations in 1997, 2002 and 2012.

Seen the desire of a sustainable development, this theme will be discussed more deeply in the following paragraphs, focusing the attention on the topics of interest of the present thesis. In particular, attention will be paid to the issues deriving from the cement industry and plastic disposal/recovery, presenting the life cycle assessment (LCA) methodology as a viable instrument to take into account sustainability related aspects.

One of the most important concerns associated to the construction and plastic industries is the waste management (Sharma and Bansal, 2016;

Butera et al., 2015; Horvath, 2004; Turk et al., 2015, Rigamonti et al., 2014). Recycling, recovering energy from waste materials and reducing the consumption of raw resources are viable strategies to make economy more sustainable and competitive. During last years, the concept of circular economy has grown and established itself as an opportunity to make World's economy cleaner and more competitive (Figure I.3).

Figure I.3 *Difference between traditional linear economy and innovative circular economy (Henry, 2016)*

In the European legislation, the idea of circular economy was firstly introduced in the Manifesto for a Resource Efficient Europe (European Commission. Brussels, December 2012) and recently confirmed in a communication from the commission to the European parliament were the attention is focused not only on the waste but also on the full product cycle, i.e. from the invention and manufacturing of a product (European Commission. Brussels, December 2015).

The current EU waste policy establish a concept known as the waste hierarchy (Figure I.4) were, ideally, waste should be prevented, and what cannot be prevented should be reduced, reused, recycled or recovered as much as possible, with landfilling being the least favored option (Directive 2008/98/EC).

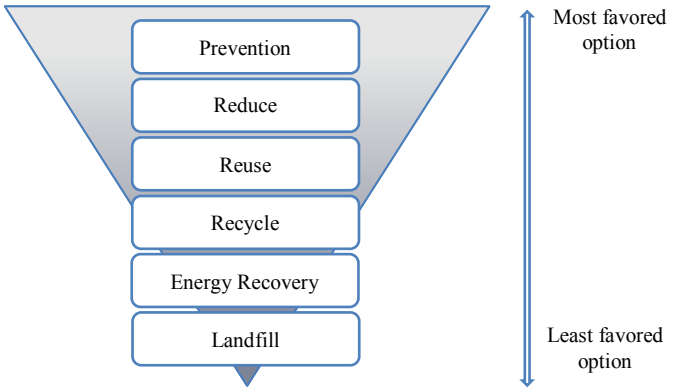

Figure I.4 *The waste hierarchy: from the most favored option to the least one (from the top to the down, respectively)*

The Waste Framework Directive (Directive 2008/98/EC, November 2008) defines the so called *end-of-waste materials*, i.e. when waste ceases to be waste and becomes a secondary raw material. In particular, waste shall cease to be waste when it has undergone a recovery, including recycling, operation and complies with specific criteria to be developed in line with certain legal conditions (article 6, Directive 2008/98/EC, November 2008).
The European Commission (EC) prepared some proposals for end-of-waste criteria for specific waste streams, according to the legal conditions and following the Joint Research Centre (JRC) methodology guidelines. So far, the criteria have been laid down for:

- Iron, steel and aluminum scrap (Council Regulation N° 333/2011);
- Glass cullet (Council Regulation N° 1179/2012);
- Copper scrap (Council Regulation N° 715/2013);
- Waste paper (Technical proposal April 2011; rejected by the European Parliament in December 2013).

Regarding the waste plastics, after two workshops (November 2011 and May 2012) a final report concerning end-of-waste criteria for plastics was published in October 2014. The scope of the document and the proposals of end-of-waste criteria included in it refer to waste plastic for conversion, i.e. waste plastic that is reprocessed into a ready input for re-melting in the production of plastic articles and products (Report EUR 26843 EN, Villanueva and Eder, 2014). Plastic conversion is understood as the transformation of plastic materials by application of processes involving pressure, heat and/or chemistry, into finished or semi-finished plastic products for the industry and end-users. The process normally involves sorting, size reduction operations to shred, flake or regrind, cleaning (including or not washing), agglomeration, melt-filtering, and final shaping into granular (pellet) or powder form, although some of the mentioned steps may be omitted. Once recyclate is in a suitable form and is of the required standard, it can be converted into a finished article (Report EUR 26843 EN, Villanueva and Eder, 2014). Further discussion on the issues related to waste plastics will be discussed in the following (§ I.3.3).

Finally, cementitious materials deterioration makes structures unsafe (social concern), maintenance and thus raw materials consumption are necessary (economical and environmental concerns, respectively), leading to sustainability related issues. As previously discussed, durability of cementitious materials is very important and several deterioration phenomena are possible (§ I.2.2). It is only from 70s that durability of cementitious materials started to be investigated and discussed in literature, reaching more than 1200 publications only in 2015 (Figure I.5). The durability and the sustainability of construction materials are strictly correlated since the cement industry is one of most important polluters and, more in general, the construction field poses some problems concerning the topic of sustainability as will be discussed in the following.

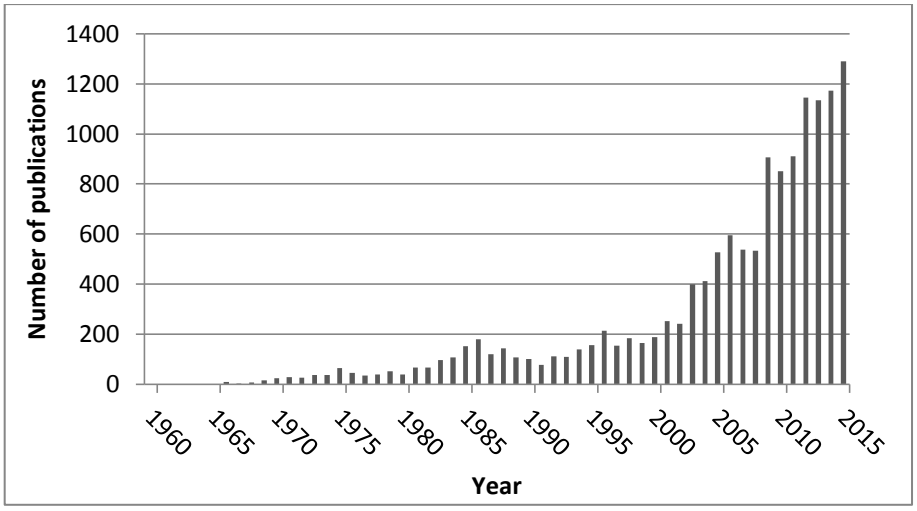

Figure I.5 *Number of publications about concrete durability (source Scopus, 06/10/2016)*

I.3.2 Environmental effects of the cement industry

Sustainability is the intersection of different fields (Figure I.2): social, environmental and economical. The construction sector takes into account all the aforementioned fields because involves numerous manufacturing sectors (principally building materials), systems (heating, ventilation and air conditioning) and people (engineers, customers etc.). Among all the materials, crushed rock, gravel, sand, water and cement (i.e. the main constituents of the traditional concrete) are the most used as concrete is the most widely used construction material in the world, with annual consumption estimated at between 20 and 30 billion tons (Sabnis, 2015). It is worth to mention that exists an important difference, in terms of sustainability, between concrete and cement: the former can be considered an ecofriendly material while cement production generates about 5-7% of worldwide CO_2 emissions, about 1 ton of CO_2 emitted per ton of cement produced (Sabnis, 2015; Meyer, 2009). Moreover, the production of ordinary Portland cement (OPC) is also very energy intensive: each ton of OPC produced requires 60-130 kg of fuel oil (or equivalent) and about 110 kWh of electricity (Imbabi et al., 2012). Finally, the large amount of required water to produce concrete is a further environmental issue. On the contrary, considering not only the environmental impact during the manufacturing process but also during the entire life cycle of the product, concrete is highly durable and energy efficient if well designed and cast. Furthermore, construction and demolition wastes (CDWs) have shown promising results in substitution of natural aggregates in pavements (Ossa et al., 2016), geotechnical applications (Cardoso et al., 2016) and concrete-filled steel

tubes (Chen et al., 2016). Therefore, is possible to use concrete, but with as little OPC quantity as possible. This means an improvement in the use of recycled materials in place of natural resources but also in the use of supplementary cementitious materials, especially those that are by-products of industrial processes. Meyer (2009), summarized the use of recycled materials in concrete, focusing the attention on silica fume, fly ash, ground granulated blast furnace slag, as supplementary cementitious materials, i.e. that is possible to use in place of the OPC; CDWs, post-consumer glass and recycled plastic, as natural aggregates replacement. Moreover, Aprianti (2017) reviewed also the agricultural wastes that have been investigated as supplementary cementitious materials: rice husk ash, palm oil fuel ash, bagasse ash, wood waste ash, bamboo leaf ash and corn cob ash.

In recent years, particularly attention has been paid also to the reuse of waste water (mostly deriving from ready-mixed concrete plants) for trucks washing or concrete production (Audo at al., 2016; Schoon et al., 2015).

Finally, as in other fields, also in the construction sector, researchers are trying to take advantages from the use of nanoparticles. The use of nanoparticles modifies not only mechanical and durability properties, but is also able to introduce new functionalities: photocatalytic action, anti-microbial activity, anti-fogging, self-sensing and self-cleaning (Shah et al., 2015; Jayapalan et al., 2013). The improvement of concrete durability (i.e. the reduction of maintenance operations and costs) represent an improvement of concrete sustainability, mitigating the negative effects of the cement industry.

I.3.3 The problem of plastics

The plastic is the most common material of the 21th century and in 2013 plastics world production (Figure I.6) reached the three hundred megaton (Plastics-The facts, 2015). Thanks to its advantageous properties (versatility, lightweight, low cost and ease to process) the use of plastics seems to be essential in our life. However, plastic production and disposal present several environmental issues. One of the disadvantages resides on the speed with which these materials immediately became waste. In Europe (EU28+NO/CH) in 2014, 25.8 million tons of post-consumer plastics waste ended up in the waste upstream: 69.2% was recovered through recycling and energy recovery processes while 30.8% still went to landfill (Plastics-The facts, 2015). The only key to reduce environmental issues caused by waste disposal and use of non-renewable resources is recycling. According to the waste hierarchy (Figure I.4) and the waste framework directive previously mentioned (Directive 2008/98/EC, November 2008), in the EU member states, not less than 30% of plastic waste should be reused or recycled. Moreover, the directive clearly states that by 2020, all solid waste streams (including plastics) should be redirect towards thermal and/or mechanical

treatment and energy recovery reducing the percentage of solid waste being landfilled to a minimal.

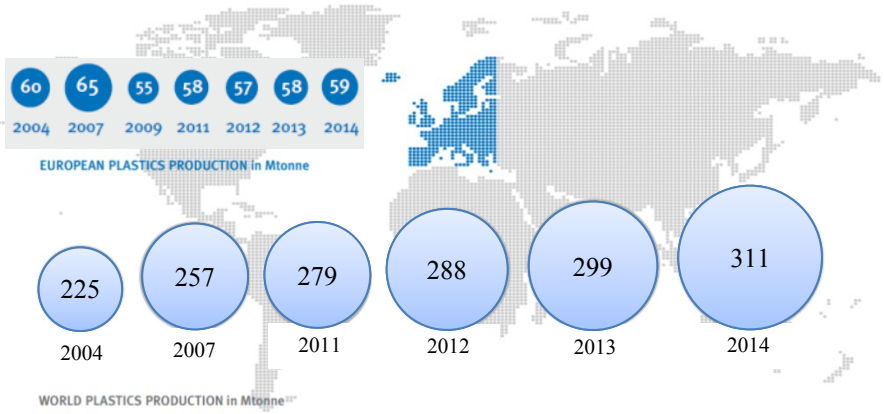

Figure I.6 *Plastics production in the World and Europe (EU28+NO/CH), source: Plastics-The facts 2015*

Four different categories of plastics waste recycling can be defined (Figure I.7): re-extrusion (primary recycling), mechanical (secondary recycling), chemical (tertiary recycling) and energy recovery (quaternary recycling). Each method provides a unique set of advantages that make it particularly beneficial for specific locations, applications or requirements. Primary mechanical recycling is the direct reuse of uncontaminated discarded polymer into a new product without loss of properties. In most cases, primary mechanical recycling is conducted by the manufacturer itself for post-industrial waste. In principle, also post-consumer waste can be subjected to primary recycling; however, in this case, a number of additional processes are necessary that significantly increase the costs of recyclates. Before reintegration of a used material into a new product, it normally requires grinding (i.e. shredding, crushing, or milling). These processes make the material more homogeneous and easier to blend with additives and other polymers for further processing. Therefore, only thermoplastic polymers, such as PP, PE, PET and PVC, can normally be mechanically recycled. The best-known methods of this type of processing of mechanical recyclates are injection molding, extrusion, rotational molding and heat pressing (Ignatyev et al., 2014). Secondary mechanical recycling (i.e. secondary or material recycling) involves physical treatment, whilst chemical recycling (i.e. tertiary encompassing feedstock recycling) produces feedstock chemicals for the chemical industry, and energy recovery involves complete or partial oxidation of the material, producing heat, power and/or gaseous fuels, oils and chars besides by-products that must be disposed of, such as ash (Al-Salem et al., 2010).

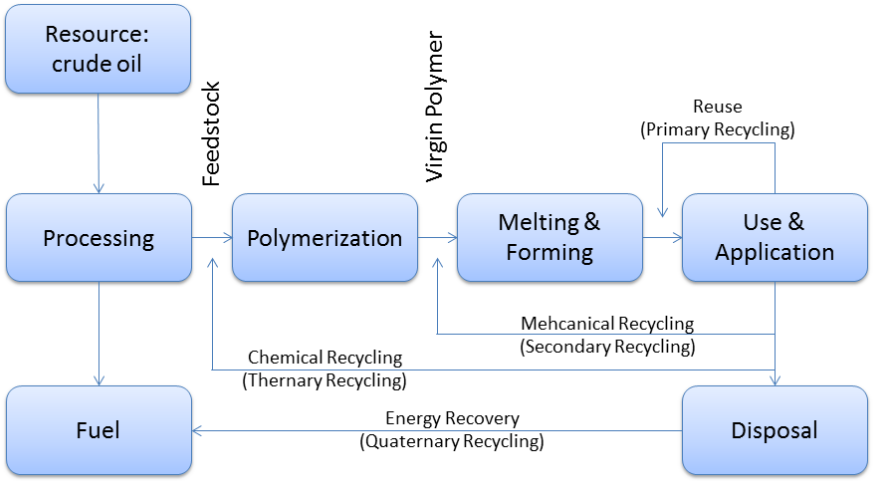

Figure I.7 *Treatment methods related to polymers lifecycle (readapted from Ignatyev et al., 2014; Al-Salem et al., 2010)*

The pre-treatment and sorting operations for plastics waste enable this valuable resource to be diverted from landfill and to deliver recyclate of the required market-driven qualities. A wide range of technologies are currently used for waste pre-treatment and sorting. These range from manual dismantling and picking to automated processes such as shredding, sieving, air or liquid density separation, magnetic separation and highly sophisticated spectrophotometric sorting technologies, e.g. UV/VIS, NIR, Laser, etc. Modern sorting plants are often complex infrastructures applying several of these technologies that have been adapted to specific waste streams in order to reach an optimal output and cost performance (PlasticsEurope). Plastic waste sorting allows the recovery of large volumes of polymeric fractions but while rigid plastics are easy to separate and recycle, more difficulties are found for flexible films which represent a great part of plastic waste. Moreover, the presence of different plastic types, which are not easy to separate and often are also immiscible at micro-scale produces materials with very poor properties (Bertin and Robin, 2002; Shanks et al., 2000; Dintcheva et al., 2001).

Recently, a possibility for the effective increase of polymeric blends properties is the addition of suitable additives (commercial compatibilizers are graft or block copolymers), to improve the interfacial adhesion and the dispersion of the mixture components. However, traditional block and graft copolymers are specific, relatively expensive to engineer, and very difficult to produce for polymeric mixtures with more than two components. Another viable solution is the use of nanoclay that act as nucleating agents for in-situ graft formation (Garofalo et al., 2015).

I.3.4 Life Cycle Assessment (LCA)

The International Organization for Standardization (ISO) adopted an environmental management standard in the 1990s as part of its 14000 standards series, with the 14040 series (EN ISO 14040 and EN ISO 14044, 2006) focusing on establishing methodologies for life cycle assessment (Singh et al., 2011). ISO 14040 defines life cycle as the ‘‘consecutive and interlinked stages of a product system, from raw material acquisition or generation from natural resources until its final disposal’’ (EN ISO 14040, 2006). Moreover, the life cycle assessment (LCA) is the compilation and evaluation of the inputs, outputs and the potential environmental impacts of a product system throughout its life cycle (EN ISO 14040, 2006). LCA is a valid tool to learn about the environmental effects of a certain product, work, process etc. Regarding at the building and construction field, LCA determines the environmental effects deriving from the construction of a given structure, its service life, reuse, demolition and waste management. In addition, some important aspects must be necessarily considered: restoration, maintenance and repair actions of the structure. LCA methodology should also take into account preventive maintenance programs which will require an effort and commitment by future generations (Mora, 2007). One of most important aspect of the LCA is the possibility to take into account materials (or, more in general, products) end-of-life. The possibility of materials reuse, recycle, recover, etc., is the principal idea of sustainability, strictly linked to the effects on the environment, i.e. the irreversibility of an action. Remaining in the field of constructions, LCA is a systematic analysis of not only the direct but also the indirect environmental effects of construction materials. Direct effects relate to the energy and material use in the materials production stage, whereas indirect effects reveal the contributions of the supply chains (Mora, 2007). ISO standard define a four stage iterative framework for performing LCA analyses. The four steps are: goal and scope definition, inventory analysis, life-cycle impact assessment (LCIA) and interpretation (Figure I.8).

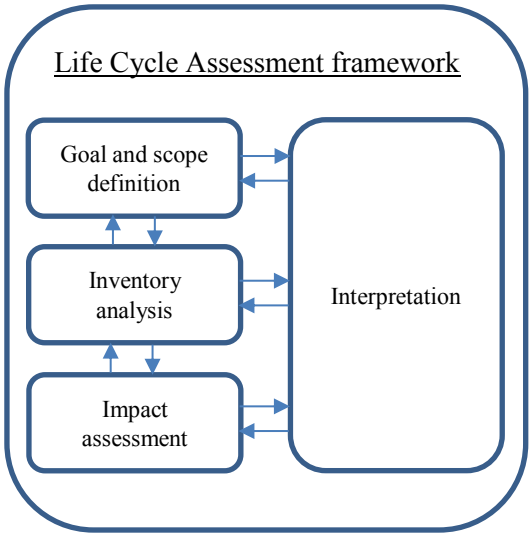

Figure I.8 *Phases of LCA according to ISO 14040*

The first step includes identification of the purpose and boundary of the study, establishing the functional unit of analysis, and defining the key processes, material and energy flows for analysis. Inventory analysis involves collection of data and the analysis of material and energy flows for each stage of the product life cycle. According to the standard, LCIA is the phase of LCA aimed at understanding and evaluating the magnitude and significance of the potential environmental impacts for a product system throughout the life cycle of the product (EN ISO 14040, 2006). The last step includes interpretation of the environmental impact results, either to assist environmentally preferable product and process selection, or to provide recommendations for system improvements (Singh et al., 2011).

The most significant problems with LCA studies have been the issues with boundary definition, data acquisition, data quality, uncertainty, and interpretation of results. Various assessments of the same material may yield radically different results because of varied assumptions about scope and data sources (Mora, 2007). Such decisions may compromise research objectivity and the reliability of results but is difficult to give scientific criteria for exclusion of certain processes and inputs. The above LCA methodology recommended by ISO standards is referred to as a process-based LCA. Another method is the economic input-output LCA (EIO-LCA) that has been used as a way to address some of aforementioned issues (Singh et al., 2011). The EIO-LCA method employs a geographical region, typically a national economy, as the boundary of analysis and incorporates economy-wide interdependencies by using input-output matrices. It uses publicly available and regularly compiled data on industry sector-level inputs, energy use, and emissions. However, EIO-LCA methods

suffer from another set of limitations, including the high level of aggregation of disparate products in industry and commodity sectors in the national input-output tables, and dependence on sector-level monetary flows which may distort physical input-output technology relationships. High levels of aggregation in EIO-LCA models make them unsuitable for LCAs of products that are atypical outputs of industry sectors, or for comparative LCAs of products within the same industry sector. Hybrid methods that combine EIO-LCA and process-based LCA have been developed to maximize the advantages of both approaches (Singh et al., 2011).

Considering the field of constructions, several LCAs have been carried out to investigate sustainability of different materials, in particular cementitious materials containing waste or end-of-waste materials. The use of waste materials in the concrete sector, is a viable way to reduce the environmental footprint of conventional concrete. As seen previously (§ I.3.2), different end-of-waste materials can be used (construction and demolition waste, .industrial wastes etc.). However, the prerequisite for their use as a substitute for natural materials is their environmental acceptability and their technical adequacy (Turk et al., 2015). Attention must be paid at the boundary conditions, functional units, exclusion criteria etc., otherwise LCAs interpretation could be incorrect. For example, Knoeri et al. (2013) analyzed the life cycle impacts of 12 recycled concrete (RC) mixtures and compared them with those of corresponding conventional concretes (CC). While previous studies showed equal or even higher environmental impacts of RC compared to CC, this study demonstrated that RC reduces the environmental impacts to about 70 % of the CC impacts if co-products from the recycling process are not excluded from the scope. This was mainly attributed to the benefits obtained from the recovered scrap iron (from the steel reinforcement), as well as to the avoidance of the need to transport construction and demolition waste to a landfill site, and to the avoided impacts of such disposal (Knoeri et al., 2013). Another example is the investigation of Turk et al. (2015). Authors reported about environmental impacts of several “green concretes”, i.e. concretes containing industrial waste products (fly ash, foundry sand and electric arc furnace, EAF S, slag) and waste concrete showing significant reduction of environmental impacts. The main reason for the significant improvement in their environmental friendliness lies in the greater credit related to the avoided impacts, such as the prevention or reduction of landfilling (i.e. the landfilling of both the waste concrete and the alternative material is avoided, which results in a relatively high credit) (Turk et al., 2015). Recently, Napolano et al. (2016), investigated environmental impacts of the production of different types of lightweight concretes comparing the use of natural lightweight aggregates (i.e. natural clay) and recycled wastes (i.e. muds deriving from industrial processes). Considering a functional unit of $1m^3$ of lightweight concrete, it can be pointed out that the concrete with natural lightweight aggregates,

presents a larger impact than all of the mixes containing recycled aggregates, in all the damage and impact categories. Furthermore, the environmental impact of natural lightweight aggregates in the concrete production accounts for around 55% of the total environmental burden, whereas the environmental impact of recycled lightweight aggregates is almost 15% of total environmental burden in lightweight concrete production. These results were confirmed also when a CO_2 rule was applied as allocation approach (Napolano et al., 2016).

As previously discussed, also the plastic sector poses issues and concerns in the field of sustainability (I.3.3). To this extent, several studies investigated the reduction of environmental effects when plastic wastes were used in the sector of constructions. For example, Intini and Kühtz (2011) investigated the energy savings and the environmental benefits of the use of PET bottles postconsumer to manufacture products for buildings thermal insulation. Another example is the study to assess the environmental impact of four alternative scenarios for reinforcing concrete footpath using also recycled fibers carried out by Yin et al. (2016). In particular, the four options considered were: a) steel reinforcing mesh (SRM), b) virgin polypropylene (PP) fibers, c) recycling industrial PP waste and d) recycling domestic PP waste. Significant environmental benefits were assed in terms of CO_2, water and oil equivalent savings. However, domestic recycled PP fibers require more water for the washing processes (Yin et al., 2016).

Finally, it is important to consider not only the materials production and end-of-life sustainability, but all the project should be sustainable. To this extent, the idea of a marketable green certification systems was developed leading to several certifications. One of the most important is the Leadership in Energy and Environmental Design (LEED) rating systems, developed by the United States Green Building Council (USGBC, 2008). The LEED rating systems provide guidance for implementing sustainable design and construction strategies and award green building certification for having utilized such strategies (Singh et al., 2011). Some recent reviews about green buildings have been carried out by several authors (Zuo and Zhao, 2014; Robichaud and Anantatmula, 2011).

I.4 Fiber reinforced cementitious materials (FRC)

As discussed in the previous paragraphs, cementitious materials have some drawbacks: are brittle materials, have some durability related issues and negative environmental effects. In this paragraph, the use of fibers into cementitious materials will be presented as a viable solution to partially or fully overcome the aforementioned drawbacks. Moreover, the use of plastic wastes to produce synthetic fibers is a sustainable way to recycle, according to the theory of circular economy.

I.4.1 Generalities

Brittle materials are reinforced since ancient times using fibers, resulting in a composite material. The last decades have seen an increasing use of fibers both in concrete and in mortar. The low tensile strength which characterizes cementitious materials can be improved by adding short randomly distributed fibers which can also reduce plastic shrinkage cracking. Fibers increase the early tensile strength and hinder, by mechanical bridging, the growth of initial cracks. For such applications short and thin fibers, even with low strength, may fulfill the requirements. The parameters that affect fibers efficiency are fibers mechanical properties, volume fraction and aspect ratio (i.e. shape and dimensions). Moreover, fiber/matrix interactions are of fundamental importance for the composite performances. The role of interfacial bond between fibers and the cementitious matrix has been widely investigated with several kind of fibers. Generally polymeric fibers have a smooth surface resulting in a weak bond and a poor adhesion with the cementitious matrix. Consequently, to improve the composite properties is necessary to develop fibers with special features able to increase the interfacial bond (Kakooei et al., 2012; Aly et al., 2008; Banthia and Gupta, 2006; Kim et al., 2010; Shannag et al., 1997; Naaman, 2003).

The key mechanical properties for a successful cementitious composite were summarized by Naaman (Figure I.9):

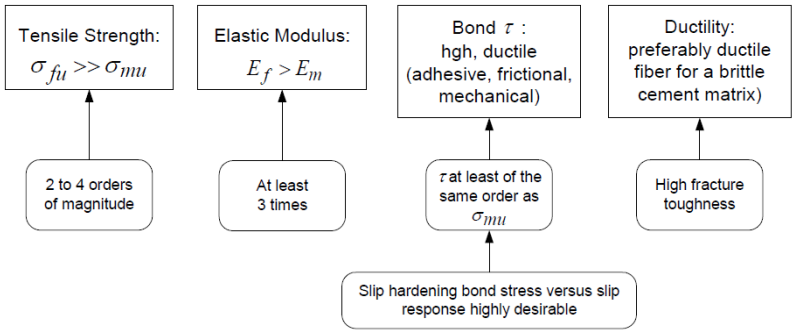

Figure I.9 *Desirebale fiber versus matrix properties (Naaman, 2003)*

Different fibers (glass, steel, carbon, aramid, nylon, polyethylene and polypropylene) have been used according to the aim of the composite. High strength fibers are generally used for structural purposes (toughness increase) while low modulus synthetic fibers are used to avoid shrinkage cracking, concrete spalling and improve impact resistance (Fraternali et al., 2011; Coppola et al., 2014a; Coppola et al., 2014b). Fibers are chosen not only for their mechanical properties, but also for their cost and effectiveness. Some common fibers and their typical properties are reported in Table I.2.

Table I.2 *Typical properties of fibers (Bentur and Mindess, 2006)*

Fiber	Diameter (μm)	Specific gravity	Modulus of elasticity (GPa)	Tensile strength (GPa)	Elongation at break (%)
Steel	5-500	7.84	200	0.5-2.0	0.5-3.5
Glass	9-15	2.6	70-80	2-4	2-3.5
Abestos					
Crocidolite	0.02-0.4	3.4	196	3.5	2.0-3.0
Chrysolite	0.02-0.4	2.6	164	3.1	2.0-3.0
Polypropylene	20-400	0.9-0.95	3.5-10	0.45-0.76	15-25
Aramid (Kevlar)	10-12	1.44	63-120	2.3-3.5	2-4.5
Carbon (High strength)	8-9	1.6-1.7	230-380	2.5-4.0	0.5-1.5
Nylon	23-400	1.14	4.1-5.2	0.75-1.0	16.0-20.0
Cellulose	-	1.2	10	0.3-0.5	-
Acrylic	18	1.18	14-19.5	0.4-1.0	3
Polyethylene	25-1000	0.92-0.96	5	0.08-0.60	3-100
Wood fiber	-	1.5	71.0	0.9	-
Sisal	10-50	1.5	-	0.8	3.0
Cement matrix (for comparison)	-	1.5-2.5	10-45	0.003-0.007	0.02

Fibers addition significantly modifies the behaviour of the composite. In particular, if a high volume fraction of high modulus fibers is added, a strain hardening behaviour is achieved (Figure I.10). For example, in thin sheet components, in which conventional reinforcing bars cannot be used, and in which the fibers therefore constitute the primary reinforcement, the fibers volume fraction is very high (typically > 5%). In these applications fibers are able to increase both the strength and the toughness (i.e. strain hardening) of the composite, and can be classified as high performance FRC (Bentur and Mindess, 2006). On the contrary, a low volume fraction of normal modulus fibers leads to a strain softening behaviour (Figure I.10). In these applications, fibers are often referred to as secondary reinforcement. In this case fibers provide post-cracking ductility, but the stresses are smaller than the first crack stress, that is a strain softening material. In both cases, the brittle failure of traditional cementitious materials is avoided (Figure I.10).

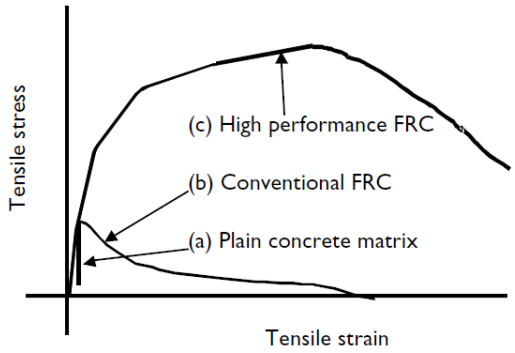

Figure I.10 *Typical stress-strain curves for conventional and high performance FRC (Bentur and Mindess, 2006)*

More recently, much work has been done in the fibers optimization: new fiber types and geometries have been developed but also surface treatments to improve fiber/matrix interactions. In this way, fibers can be tailored to be applied for specific applications for which conventional cementitious systems are not suitable. At the same time, new production technologies have evolved as new fibers have been developed. For example, exists a strong contradiction between the fiber geometry required to allow easy handling of the fresh FRC (i.e. good workability) and that required for maximum efficiency in the hardened composite. Longer fibers of smaller diameter will be more efficient in the hardened FRC, but will make the fresh FRC more difficult to handle (Bentur and Mindess, 2006). To overcome this difficulty, there are a number of possible alternatives:

1. modification of the fiber geometry, to increase bonding without an increase in length (e.g. hooked fibers, deformed fibers or fibrillated networks);
2. chemically treating the fiber surface to improve its dispersion in the fresh matrix;
3. modifying the rheological properties of the matrix, through the use of chemical admixtures (mainly high range water reducers) and mineral admixtures (e.g. silica fume and fly ash) as well as optimization of the matrix particle size distribution;
4. using special production techniques to ensure that a sufficiently large volume of fibers can be dispersed in the mix.

In the following paragraphs, some of the aforementioned alternatives will be discussed more deeply. In addition, a focus on synthetic and non-synthetic fibers mostly used in FRC will be presented. It should be considered that in recent years also fibers hybridization is widely studied in literature (Abbas and Khan, 2016). Finally, emphasis will be given to the use of synthetic fibers to reduce plastic shrinkage cracking.

I.4.2 Synthetic Fibers

Synthetic (polymer) fibers are widely used for the reinforcement of cementitious materials. Many synthetic fibers are present in commerce (particularly polyolefin fibers) and a lot of synthetic fibers have been studied in literature. As shown in Table I.2, strength and modulus of elasticity vary significantly among these class of fibers. Moreover, as reported in Figure I.9, to increase the strength of the composites, fibers must have a modulus of elasticity greater than that of the matrix. However, for cementitious materials, for which the modulus of elasticity ranges from about 15 to 40 GPa, this condition is difficult to meet with most synthetic fibers (Bentur and Mindess, 2006).

Plastic fibers can be in the form of micro fibers or macro fibers. The micro plastic fibers refer to the plastic fibers whose diameter ranges from 5 to 100 μm and length is 5–30 mm. These micro fibers can effectively control plastic shrinkage cracking, as will be later discussed, however, they normally do not have evident effects on the properties of hardened concrete (Yin et al., 2015). It is noteworthy that some micro plastic fibers, such as nylon fibers, can provide good thermal energy storage to concrete (Ozger et al., 2013), effectively control shrinkage of concrete (Song et al., 2005) and also significantly improve tensile strength and toughness of concrete (Spadea et al., 2015). The macro plastic fibers normally have a length of 30–60 mm and cross section of 0.6–1 mm^2 (Yin et al., 2015a). The macro plastic fibers are able to control not only plastic shrinkage but also drying shrinkage (i.e. the shrinkage that occurs in the hardened concrete). Another significant benefit is the post-cracking performance provided by the macro plastic fibers. Therefore, when concrete breaks, the common large single cracks can be substituted by dense micro-cracks due to the presence of fiber reinforcement.

It is possible to divide synthetic fibers according their elastic modulus, among low modulus fibers we can find: polypropylene (PP), polyethylene (PE), acrylic (PAN), nylon, polyester (PET). On the contrary, high modulus synthetic fibers are: carbon fibers, aramid fibers (Kevlar), polyvinyl alcohol (PVA). From the first group, PP fibers are the most used thanks to easy of production, good mechanical properties (in comparison with PE) and good resistivity in alkaline environment (compared to PET) (Yin et al., 2015). As high modulus synthetic fibers, PVA fibers have been widely investigated thanks to the good affinity with the cementitious matrix, low cost (compared to carbon and Kevlar fibers) and high elastic modulus (Thong et al., 2016).

Moreover, seen the desire to reuse and recycle plastic wastes, in literature, many authors investigated the possibility to produce synthetic fibers from waste materials. Li et al. (2004) investigated the use of waste tire for fibers production. Authors found that longer fibers tend to entangle and suggested 50 mm as maximum length. In addition, increasing the stiffness of the waste tire fibers can increase the strength and stiffness of the rubberized

concrete. Therefore, using truck tire fibers is better than using car tire fibers and fibers with steel belt wires are better than fibers without steel belt wires (Li et al., 2004). Yin et al. (2015b), explored the feasibility of using an improved melt spinning and hot drawing process to produce virgin and recycled PP fibers of high mechanical properties in an industrial scale. Virgin PP fibers of high tensile strength and high Young modulus (457 MPa and 7526 MPa, respectively) were produced by the melt spinning and hot drawing process under factory conditions. However, the recycled PP fiber produced by the same method showed significantly lower tensile strength but comparable Young modulus (342 MPa and 7115 MPa, respectively). One of the most investigated recycled matrix for synthetic fibers was polyethylene terephthalate (PET). Ochi et al. (2007), developed a method to produce recycled PET fiber to be used as reinforcing in concrete. Authors investigated also the concern of alkali resistance and it was found that there was no problem when used in normal concrete. Moreover, the measured wetting tension of PET (40 mN/m) was lower than that of PVA (45 mN/m) but higher than that of PP (35 mN/m). Finally, an increase of bending strength and toughness index was achieved at increasing fibers volume fraction (Ochi et al., 2007). Also Kim et al. (2008) investigated the use of recycled PET but focused the attention on the mechanical modification of fibers surface to improve fiber/matrix interactions. As stated before and as will be in the following discussed, one of the main concern in the use of synthetic fibers is their low wettability resulting in a weak adhesion with the cementitious matrix. Recently, also the use of recycled HDPE was investigated for fibers production (Pešic´et al., 2016). Authors found that HDPE fibers improved concrete durability thanks to a reduction of concrete water permeability and of plastic shrinkage cracks width, compared to the equivalent plain concrete (Pešic´et al., 2016).

I.4.3 Non-Synthetic Fibers

Non-synthetic fibers is a wide class containing fibers of different nature: steel, glass and natural (Alizade et al., 2016; Bentur and Mindess, 2006; Pacheco-Torgal and Jalali, 2011). Among all the natural fibers, researchers focused the attention on the use of basalt, bamboo, hemp, jute, sisal, coconut, bagasse and sugar cane fibers. All the three aforementioned fibers have some durability problems: the steel fibers can be exposed to corrosion; the glass fibers have some issues with the alkalinity of the cementitious matrix and the natural fibers may undergone to degradation.

As stated before, hybrid fiber-reinforced concretes, i.e. containing two or more different types of fibers are attracting an increasing interest among researchers, thanks to the ability to select fibers according the properties that is necessary to improve or confer to the concrete (Afroughsabet and Ozbakkaloglu, 2015; Abbas and Khan, 2016).

I.4.4 Fiber/matrix interactions

I.4.4.1 Stress transfer, bond and pull-out

The effectiveness of fibers reinforcing action depends to a large extent on the fiber/matrix interactions. Three types of interactions are particularly important (Bentur and Mindess, 2006):

1. physical and chemical adhesion;
2. friction;
3. mechanical anchorage induced by deformations on the fiber surface (e.g. crimps, hooks, twisted, deformed fibers).

The adhesional and frictional bonding between a fiber and cementitious matrix are relatively weak. They have however significant contribution and practical significance in the case of composites having high surface area fibers and advanced cementitious matrices which are characterized by an extremely refined microstructure and very low porosity (i.e. very low water/binder ratios). In conventional fiber reinforced concretes, where the matrix water/binder ratio is 0.40 and above, and the fibers are of a diameter in the range of 0.1 mm or bigger, efficient reinforcement cannot be induced by adhesional and frictional bonding, and mechanical anchoring is required. For this purpose a variety of fiber shapes have been developed and are used commercially, as will be discussed in the following.

The schematic diagram in Figure I.11 shows the different failure modes associated with the fiber reinforced concrete (Zollo, 1997; Yin et al., 2015). Fiber rupture (1), pull-out (2) and debonding of fiber from matrix (4) can effectively absorb and dissipate energy to stabilise crack propagation within concrete. Fiber bridging the cracks (3) reduces stress intensity at the crack tip. In addition, the fiber bridging can decrease crack width, which prevents water and contaminants from entering the concrete matrix to corrode reinforcing steel and degrade concrete. Fiber in the matrix (5) prevents the propagation of a crack tip. Consequently, minor cracks will be distributed in other locations of the matrix (6). Although every individual fiber makes a small contribution, the overall effect of reinforcement is cumulative. Therefore, fibers can effectively control and arrest crack growth, hence preventing plastic and dry shrinkage cracks, retaining integrity of concrete and altering the intrinsically brittle concrete matrix into a tougher material with enhanced crack resistance and ductility (Yin et al., 2015).

Thus, in all the mechanisms, the key parameter is fiber/matrix bond that is generally quantified by pull-out tests. In the past, direct and indirect experimental methods were developed to quantify the fiber/matrix bond of FRC (Abbas and Khan, 2016). As stated, the frictional bond governs fiber/matrix interactions while physical/chemical bond plays a minor role. The study of these interactions is extremely sophisticated because of the presence of nonlinear interactions: interfacial debonding, plastic material

deformations, mechanical bond deformations, and frictional sliding (Abbas and Khan, 2016).

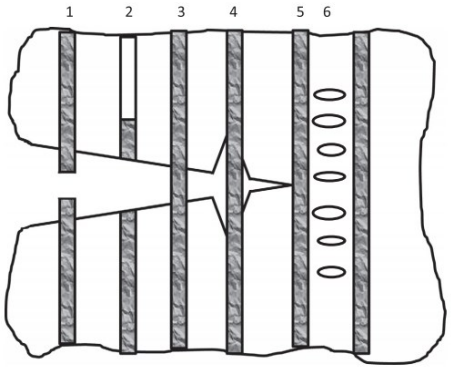

Figure I.11 *Failure mechanisms in fiber reinforced concrete (Zollo, 1997; Yin et al., 2015)*

To determine the fiber/matrix bond behavior, uniaxial tensile tests are carried out, according the simple pull-out geometry and stresses distribution shown in Figure I.12. This simple test allows the determination of the pull-out load and the corresponding fiber slippage during the test. This test can provide important information on the fiber/matrix bond of FRC because it simulates the debonding and pull-out of fibers, i.e. the mechanisms 2 and 4 of Figure I.11 (Abbas and Khan, 2016). It should be noticed that because of the nonlinearities associated with the fiber/matrix shear stress distribution along the fiber length, particularly for deformed fibbers, some assumption and hypothesis are necessary. Anyway, fiber pull-out test is a valid solution to assess the efficiency of fibers surface treatments.

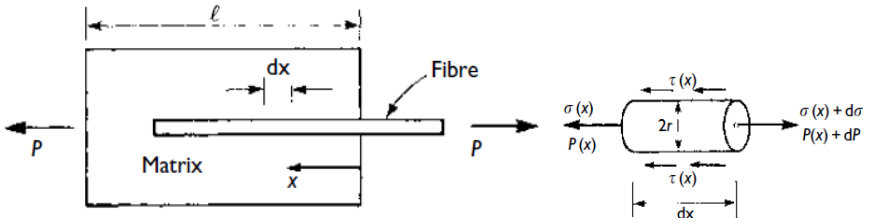

Figure I.12 *Pull-out geometry to simulate fiber/matrix interactions (Bentur and Mindess, 2006)*

Pull-out tests report pull-out load vs. fiber slippage, thus constitutive relations (which are at the basis of the analytical models applied to interpret these curves) are necessary to provide interfacial shear stress vs. pull-out displacement. Generally, the pull-out behavior of straight fibers is classified into two modes of fracture: elastic physical/chemical adhesion between the fiber and the matrix; frictional sliding. As reported in Figure I.13a, different behaviors are recognizable during straight fibers pull-out: from slip softening

to slip hardening. Moreover, many of the models assume a constant frictional interfacial shear behavior (Figure I.13b).

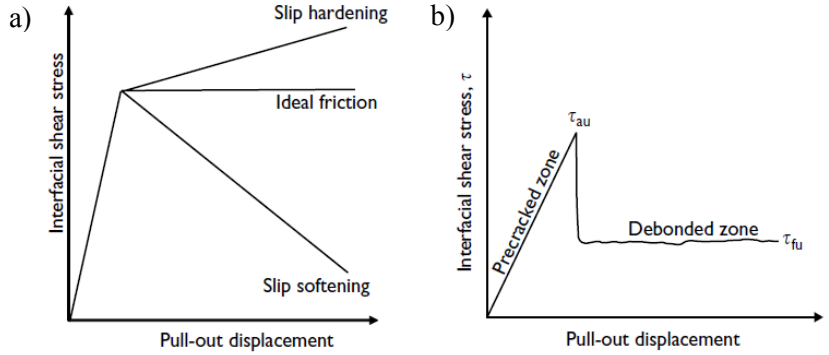

Figure I.13 *Ideal interfacial shear stress–slip curves: (a) range of behaviors demonstrating slip softening to slip hardening; (b) ideal presentation of a sharp transition from elastic stress transfer to a constant frictional stress transfer (Bentur and Mindess, 2006)*

However, fibers pull-out behavior depends on fibers geometry and affinity with the cementitious matrix. In fact, for deformed fibers, more complex models are necessary and also fibers properties should be considered. In particular, it can be assumed that the anchoring mechanisms involve two processes: the energy is dissipated as the fiber undergoes to plastic deformation while being pulled out and/or the stressing and cracking of the matrix near the fiber. In the case of deformed fibers, the sphere of influence of the fiber is wider than that of a straight fiber. Thus, when using deformed fibers, are important in controlling the bonding not only fiber properties but also matrix bulk properties (Bentur and Mindess, 2006).

In brittle matrix composites, as cementitious materials, two different cases should be considered for the stress-transfer: the pre-cracking stage and the post-cracking stage. Before any cracking has taken place, elastic stress transfer is the dominant mechanism, and the longitudinal displacements of the fiber and matrix at the interface are geometrically compatible. The stress developed at the interface is a shear stress which is required to distribute the external load between the fibers and matrix (since they differ in their elastic moduli), so that the strains of these two components at the interface remain the same. This elastic shear transfer is the major mechanism to be considered for predicting the limit of proportionality and the first crack stress of the composite. The elastic shear stress distribution along the fiber/matrix interface is non-uniform. At more advanced stages of loading, debonding across the interface usually takes place and the process controlling stress transfer becomes one of frictional slip. In this case relative displacements between the fiber and the matrix take place. The frictional stress developed is a shear stress, which is assumed in many models to be uniformly

distributed along the fiber/matrix interface. This process is of greatest importance in the post-cracking zone, in which the fibers bridge across cracks. Properties such as the ultimate strength and strain of the composite are controlled by this mode of stress transfer. The transition from elastic stress transfer to frictional stress transfer occurs when the interfacial shear stresses due to loading exceed the fiber/matrix shear strength. This will be referred to as the adhesional shear bond strength, τ_{au}. As this stress is exceeded, fiber/matrix debonding is initiated and frictional shear stress will act across the interface in the debonded zone. The maximum frictional shear stress (i.e. the frictional shear strength) that can be supported across the interface will be called τ_{fu}. The values of τ_{fu} and τ_{au} are not necessarily the same. The value of τ_{fu} is very sensitive to normal stresses and strains; in most analytical treatments it is assumed to be constant over the entire pull-out range, implying the ideal interfacial shear stress–displacement curve shown in Figure I.13b. However, in practice, τ_{fu} may be reduced at advanced stages of loading (slip softening) or increased (slip hardening), depending on the nature of the interaction and the damage developed across the interface during the slip process. The transition from elastic stress transfer prior to debonding, to frictional stress transfer after debonding, is a gradual process, during which both types of mechanisms are effective. Debonding may even take place prior to the first cracking of the matrix, and thus, the combined effect of these two mechanisms may influence the shape of the stress–strain curve prior to matrix cracking. The occurrence of such a sequence of events depends upon the fiber/matrix adhesional shear bond strength and on the tensile strength of the matrix. If the latter is high, one may expect debonding to occur prior to matrix cracking, when the elastic shear stress exceeds the adhesional shear bond strength (Bentur and Mindess, 2006).

Summarizing, three different step are necessary in the modelling of fibers pull-out (Abbas and Khan, 2016):

1. assume an elastic fiber/matrix bond until the initiation of the first crack;
2. assume a notably simple post-cracking model;
3. estimate the stress distribution along the fiber/matrix interface, using semi-empirical methods.

It is important to highlight that many of the analytical models developed for smooth, straight fibers may not be applicable quantitatively (or even qualitatively) to complex shaped fibers.

As stated, most of the available models consider a constant fiber/matrix interfacial bond but more complex models are reported in literature, considering also a variable stress distribution along the fiber/matrix interface, in particular in the post-cracking stage (Abbas and Khan, 2016). In fact, the initiation of the initiation of the first crack changes the role of the fiber/matrix interfacial bond. Before the first crack begins, the ultimate shearing stress over the fiber surface is located at its edges (Figure I.14a).

However, after the first crack, the ultimate shearing stress is located at approximatively at the mid-length of the fiber (Figure I.14b).

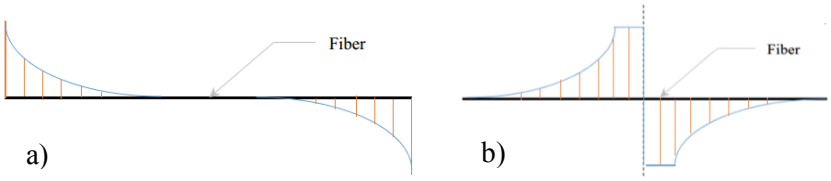

Figure I.14 *Nonlinear distribution of shearing stress over the fiber surface: (a) at pre-cracking stage, (b) at post-cracking stage (Abbas and Khan, 2016)*

After this brief theoretical modeling introduction, few words are necessary concerning physical modeling. Fiber/matrix interfacial interactions have been investigated using direct and indirect methods. Direct methods are based on pull-out tests of single fiber or group of fibers. In indirect methods, the fiber/matrix interfacial bond is quantified from a mechanical property of a type of FRC, generally flexural strength. A comprehensive review on pull-out methods has been carried out by Abbas and Khan (2016). As highlighted by the authors, despite the great efforts to develop an ideal pull-out test method, none of the used setups satisfies all the technical requirements for a perfect physical simulation of the fiber/matrix interactions.

I.4.4.2 The issue of the adhesion

The composite behaviour is greatly affected by the fiber/matrix bond and the effectiveness of fibers bridging across cracks strictly depends on it. The improvement of the fiber/matrix interactions can prevent the fiber/matrix debonding under load.

However, synthetic fibers, particularly polypropylene (PP) fibers, are chemically inert into a cementitious matrix. On the one hand, due to chemical inertness, PP fibers are durable in the alkaline environment of a cementitious composite, but on the other hand their poor wettability implies a weak fiber/matrix bond. Moreover, polymeric fibers have a smooth surface, resulting in a poor adhesion. To improve the adhesion and/or the interactions between fibers and the cementitious matrix several technics have been investigated: fibers mechanical deformation, surface chemical treatments but also interfacial transition zone (ITZ) densification. In the first case the aim is to increase the surface area of contact using crimped, twisted, fibrillated or embossed fibers (Kim et al., 2008; Chan and Li, 1997; Wu and Li, 1999; Rottstegge and al., 2006; Coppola et al., 2015). In the second one, an increase of fiber/matrix chemical affinity was obtained. In the latter, a densification of the interface transition zone between fibers and matrix is achieved adding silica fume or other fillers to the mix. The effects of these modifications on the composite are generally evaluated by fiber pullout tests (Shannag et al., 1997; Kim et al., 2008; Singh et al., 2004).

Cementitious composites are characterized by an interfacial transition zone (ITZ) in the vicinity of the reinforcing inclusion, in which the microstructure of the paste matrix is considerably different from that of the bulk paste, away from the interface. The nature and size of this transition zone depends on the type of fiber and the production technology; in some instances it can change considerably with time (Bentur and Mindess, 2006).

Generally, the matrix in the vicinity of the fibre is much more porous than the bulk paste matrix, and this is reflected in the development of the microstructure as hydration advances: the initially water-filled transition zone does not develop the dense microstructure typical of the bulk matrix, and it contains a considerable volume of CH crystals, which tend to deposit in large cavities. Intensive mixing can result in the densification of the ITZ, by reducing bleeding and forcing a better packing of the cement particles at the fiber surface. The special microstructure has two consequences:

1. a porous and weak interface which will cause an overall reduction in bonding;
2. a weak interface which is not at the fibre surface, but rather in the porous layer of the ITZ, somewhat away from the fibre surface.

The first characteristic directly affects the bond and the pull-out resistance, whereas the second one will have an indirect effect by influencing the mode of debonding when cracks develop in the matrix and propagate towards the fiber (Bentur and Mindess, 2006).

In the following paragraphs, several technics used to improve fiber/matrix interactions are reported and discussed.

I.4.4.3 Mechanical modification of fiber surface

Fibers physical modification consists in changing the shape of the fibers that can be twisted, crimped, hooked and fibrillated (Lanzoni et al., 2012; Kim et al., 2008). Fibers mechanical deformation increases fiber/matrix contact area improving friction and thus pull-out resistance, delaying fiber/matrix debonding under load (Borg et al. 2016). Naaman (2003) developed twisted steel fibers, known as “Torex”, able to enhance FRC ductility. Singh et al. (2004), proposed a mechanical indentation for polypropylene fibers, reporting a sharp increase in the fiber/matrix bond (up to 300 %), avoiding fibers tensile failure.

I.4.4.4 Fiber surface chemical modification

More recently, fibers chemical treatments, oxygen plasma, graft copolymerization of acrylic acid (Pei et al., 2004), alkaline hydrolysis (Lopez-Buendia et al., 2013; Machovič et al., 2013) and nano-silica deposition (Yang et al., 2013) are attracting growing research interest. Fibers chemical treatments allow chemical interactions between fiber surface and cement paste (Coppola et al., 2015).

I.4.4.5 Densification of the interfacial transition zone (ITZ)

The interfacial transition zone (ITZ) densification and the physical modification of fibers surface were demonstrated particularly effective. The ITZ densification, especially around fibers, is commonly obtained using low w/c ratios and nanosized additives such as silica fume. It is largely demonstrated, in fact, that nanoparticles are effective in reducing the porosity of cementitious materials (Chang et al., 2007; Pacheco-Torgal and Jalali, 2011). ITZ densification provides a more uniform and continuous interphase between the two components (i.e. the polymeric fibers and the cementitious matrix).

I.4.5 Use of synthetic fibers to reduce plastic shrinkage cracking

American Concrete Institute (ACI) defines the plastic shrinkage as the shrinkage that takes place before cement paste, mortar, grout, or concrete sets (Uno, 1998). Plastic shrinkage cracking is caused by the volumetric contraction of the cement paste which is accelerated by moisture loss after casting via evaporation. The presence of superficial cracks represents not only an aesthetic issue but also a serious problem regarding durability of construction materials. Plastic shrinkage cracking occurs at early age, before set and prior that mortar (or concrete) has a sufficient tensile strength. Generally, if the moisture evaporation rate exceeds 0.5-1 kg/m^2/h, it causes negative capillary pressure inside the concrete, resulting in internal strain (Uno, 1998; Banthia and Gupta, 2006; Yin et al., 2015a). Although synthetic fibers are not able to control moisture evaporation, at low volume fractions are generally used to control plastic shrinkage cracking. To this extent, different fibers have been investigated by researchers: PP (Banthia and Gupta, 2006), PE and PET (Borg et al. 2016, Kim et al., 2008), in particular. During last years, seen the need to increase recycled materials usage, several authors investigated the possibility of using recycled polymeric fibers from post consumers materials (Kim et al., 2008; Pešić et al., 2016, Borg et al. 2016). Generally, longer fibers are more efficient than shorter fibers in controlling plastic shrinkage cracking.

The main parameters that influence the extent of mortar shrinkage are temperature and relative humidity of the environment. A simple formula was proposed by Uno (1998) to determine the evaporation rate:

$$\boldsymbol{E = 5[(T_c + 18)^{2.5} - r(T_a + 18)^{2.5}] \cdot (V + 4) \cdot 10^{-6}} \qquad \text{(I.9)}$$

where E is the evaporation rate (kg/m^2/h), T_c is the concrete (water surface) temperature (°C), T_a the air temperature (°C), r the relative humidity and V the wind velocity (km/h).

I.5 Lightweight aggregates

I.5.1 Generalities

Lightweight aggregates have been successfully used for over two millennia and gained a renewed interest during last fifteen years (Figure I.15). Using lightweight aggregates to produce a lightweight concrete leads not only to weight reduction, but also to improved thermal properties, fire resistance, durability enhancement and architectural expression (thinner slabs, longer spans, expressive roof design, taller buildings etc.).

Reducing structures dead load is possible to decrease columns and/or beams cross section but also walls and foundations. Moreover, since the earthquake loads that act on structures and buildings are proportional to their mass, is possible to reduce the risk of earthquake damages to structures (Hassanpour et al., 2012; Libre et al., 2011).

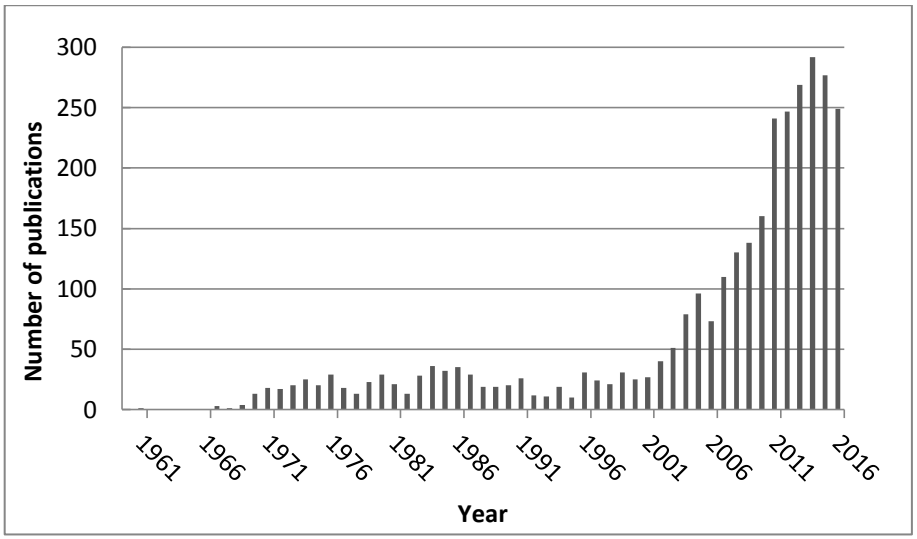

Figure I.15 *Number of publications about lightweight aggregate (source Scopus, 25/10/2016)*

As stated before, the first known use of lightweight concrete dates back over 2000 years. The most notable example is the Pantheon, finished in 27 B.C. (another well-known example is the Coliseum, 75-80 A.D.), that incorporates concrete varying in density from the bottom to the top of the dome. For the Pantheon, the Romans varied the concrete weight by decreasing the thickness of the dome as the height increases and changed the aggregate weight within the concrete three different times (Figure I.16). The aggregate in the concrete changes from broken bricks at the base of the dome

to bricks and tuff in a small midsection and ends with tufo giallo and scoria for the top portion (Lancaster, 2005; Ries and Holm, 2004).

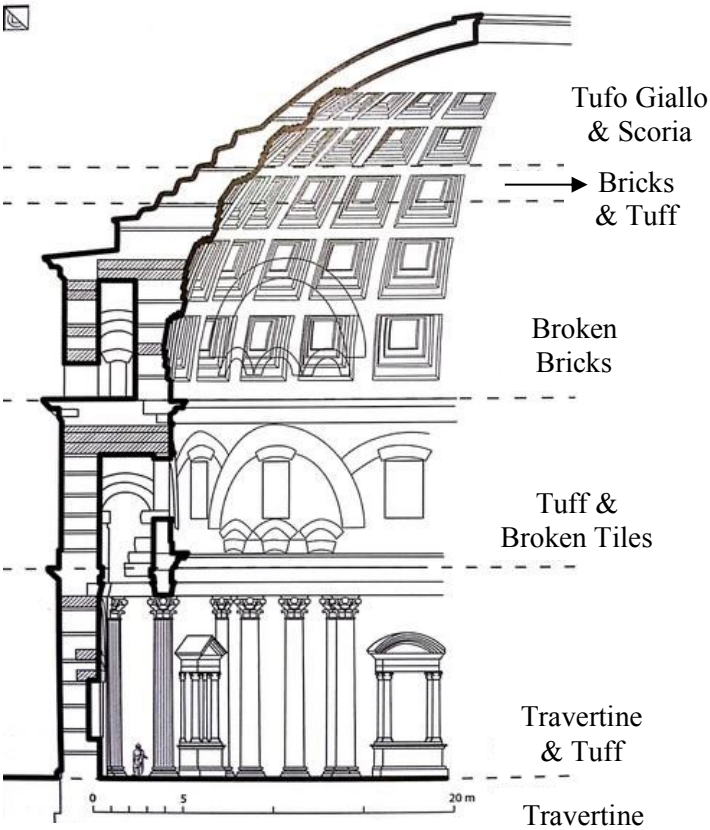

Figure I.16 *Section of the Pantheon showing the different concrete aggregates (Lancaster, 2005)*

Lightweight concretes are mainly divided in two categories: structural lightweight concrete and non-structural lightweight concrete (mainly for insulating properties or non-structural elements). Commonly, the reduction of the unit weight of concretes is reached by substituting natural aggregates with lightweight ones. Generally, lightweight aggregates are classified according their nature (artificial or natural aggregates). In the following paragraphs a description of the different lightweight aggregates is reported, focusing the attention on plastic aggregates. Finally, the advantages and the issues deriving from the use of lightweight aggregates are discussed.

I.5.2 Lightweight aggregates classification

I.5.2.1 Plastic aggregates

As previously discussed, plastic is a lightweight, low cost and easy produced material. These unique properties promoted the use of plastics, making plastic one of the most used materials in the world. Thanks to plastic low specific weight, adding plastic aggregates to concrete, its specific weight decreases. Moreover, also mechanical (mainly flexural and compressive strength) and physical properties (thermal conductivity, water vapor permeability, water absorption et.) change, as will be later discussed. The main drawbacks are the influence on concrete (or mortar) workability, the reduction of compressive strength and the low adhesion between plastic aggregates and cement paste.

As plastic is one of the most used materials, a high quantity of plastic wastes have to be managed. Many authors investigated the possibility to produce plastic aggregates from plastic wastes, particularly in the last ten years (Figure I.17).

Plastic aggregates of different shape (pellets, flakes etc.) and typology (expanded and non-expanded) have been studied. A brief literature review is presented in the following.

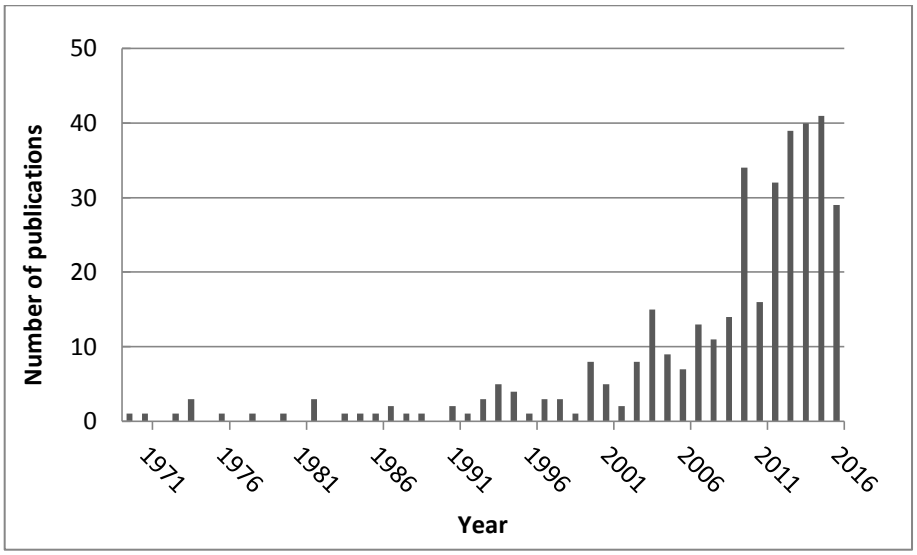

Figure I.17 *Number of publications about plastic waste aggregate (source Scopus, 25/10/2016)*

I.5.2.1.1 Expanded plastic aggregates

Several authors studied the use of expanded plastics as aggregates replacement revealing some issues: i.e. aggregates proportioning, deformability, water absorption and buoyancy. On the contrary, foams porous surface enables water and cement paste penetration resulting in a better aggregates/paste adhesion. The most investigated foamed plastic aggregates were polyurethane and polystyrene.

Gutierrez-Gonzalez et al. (2012) investigated the use of polyurethane (PU) foam wastes deriving both from automobile and construction industry. Authors reported a decrease of consistency at increasing plastic foam percentage and a sharp decrease of density (up to 65 % for a plaster/polymer ratio of 1/4). Moreover, they found that the adherence force decreases proportional to the percentage of polyurethane foam but all the samples were broken due to cohesion (i.e. cohesive failure). The failure occurred at the interface between plaster and polyurethane where high porosity and low homogeneity were found. The authors found also a sharp decrease of thermal conductivity (up to 66 %, compared to the reference material, i.e., without foam plastic wastes). Mounanga et al. (2008) reported the same issues in proportioning polyurethane foam waste focusing the attention on the difficulties in the estimation of the PUR foam density, which is greatly influenced by both the high compressibility and absorption of the lightweight aggregates. Also in this case an important reduction of both thermal conductivity and density was obtained but also of mechanical resistance. In addition, authors measured a drying shrinkage 4-5 times more important compared to the control specimen.

Madandoust et al. (2011) investigated the use of expanded polystyrene (EPS) in the production of self-compacting lightweight concrete, focusing the attention on fresh properties. In this case, thanks to the hydrophobic nature of EPS aggregates and the lower internal friction (due to the spherical shape of artificial aggregates compared to angular natural aggregates) at increasing EPS percentage a minor dosage of high range water reducer was necessary, to obtain the same slump flow. On the contrary, the segregation tendency of EPS aggregates can be reduced by using nano-SiO_2. As expected, the use of EPS aggregates reduced compressive strength. Kan and Demirboğa (2009a and b) tried to overcame the issues deriving from the high compressibility and thus low mechanical properties of EPS using a thermal treatment. In this way EPS shrinks, increasing density and increasing its compressive strength. However, a decrease of concrete strength was measured at increasing lightweight aggregates content. Babu and Babu (2003) improved lightweight concrete (containing EPS beads) strength adding silica fume. Silica fume and EPS shape increased flow values without adding superplasticizer. Moreover, good durability properties (waster absorption and chloride diffusion) were also obtained.

Other foamed rubber were investigated by Corinaldesi et al. (2011). These authors investigated the use of different waste rubber particles in mortar: styrene butadiene rubber (SBR) or polyurethane (PU) waste particles or scraps coming from wasted rubber-shoe outsoles. In all cases a lighter mortar was achieved, with a higher unit weight decrease for mortars containing PU particles. Moreover, authors found that the contemporary addition of limestone powder and superplasticizer can mitigate the detrimental effect of rubber particles on compressive strength. Also flexural tests reported a decrease of flexural strength but less sharp for mortars containing PU particles. By SEM pictures, authors investigated the ITZ between rubber particles and cement paste, evidencing a good adhesion in the case of PU particles and a weak bond for SBR particles.

Finally, Tittarelli et al. (2016), demonstrated also that using recycled EPS instead of virgin EPS was possible to obtain an economical saving over than 25 %.

I.5.2.1.2 Dense plastic aggregates

As previously stated, in cementitious materials, not only expanded aggregates but also dense plastic aggregates have been investigated. In particular, most of the works in literature are carried out considering polyethylene terephthalate (PET), high density polyethylene (HDPE) and other rigid plastics for aggregate production.

Ferreira et al. (2012) investigated the use of different typologies of waste PET aggregates. In particular, two lamellar aggregates and one cylindrical particle were investigated. Authors found that plastic waste aggregates addition decreases compressive strength, splitting tensile strength and modulus of elasticity, regardless of the type of artificial aggregates. Ferreira et al. (2012) investigated also different curing regimes and w/c ratios. Waste PET lightweight aggregates were produced also by Choi et al. (2009) and used both in mortar and concrete. In this case, waste PET aggregates were sand coated to improve aggregates/cement paste adhesion.

A mixture of PET and polyolefin for the production of plastic aggregates was investigated by Liguori et al. (2014). Authors reported a chemical interaction between plastic aggregates and cement paste probably due to the exothermic nature of the hydration reaction and the alkalinity of the cementitious environment. Moreover, composite systems showed a higher decomposition temperature, compared to the neat components and the scarce sensitivity to flashover (that is the ignition of exposed combustible material in an area near a fire). Also Iucolano et al. (2013) investigated a mixture of PET and polyolefin producing a plastic sand whose particle size and morphology appears extremely heterogeneous. As a result of this heterogeneity combined to the poor chemical compatibility with the cementitious matrix, an increase of porosity was measured. To improve plastic particles/cementitious matrix interactions, Li et al. (2004)

investigated the effect of chemical and mechanical treatments of particles surface. In particular, two methods were investigated: immersion of the particles in a saturated solution of NaOH and formation of a hole in the particles. However, both treatments (chemical and physical) lead only to partial improvements.

Wang and Meyer (2012) investigated the use of high impact polystyrene (HIPS) as aggregates in a cement mortar. Authors obtained a decrease of compressive strength and splitting tensile strength but also of thermal conductivity and water vapor permeability. Generally, using plastic aggregates, an improvement of water vapor permeability is achieved.

I.5.2.2 Non-plastic lightweight aggregates

Traditional non-plastic lightweight aggregates are pumice and scoria, that are naturally occurring lightweight aggregates mined from volcanic deposits. Lightweight aggregates can also be produced in manufacturing plants by thermal treatments from raw materials (shales, clays, fly ashes or blast-furnace slags). Generally, raw materials are introduced in a rotary kiln process heated at more than 1000 °C (Ries and Holm, 2004). During the heating process a cellular pore system is created due to the gases formed causing the expansion.

Other typical lightweight aggregates are tuff stone (Al-Zboon and Al-Zou'by, 2016; Cai et al., 2016, Bogas and Gomes, 2015), vermiculite (Rashad, 2016), cork (Hernandez-Olivares at al., 1999; Nóvoa et al., 2004; Panesar and Shindman, 2012).

I.5.3 Advantages and issues deriving from the use of plastic LWAs

In this paragraph, a brief summary on the advantages and issues deriving from the use of plastic lightweight aggregates (LWAs) in cementitious materials will be presented.

Considering the issues, a decrease both of workability and mechanical properties should be taken into account. Moreover, one of the main drawbacks in the use of plastic aggregates is the low wettability of artificial aggregates, due to their hydrophobicity, and thus the poor ITZ with the cementitious matrix. In addition, the presence of free water around plastic aggregates causes not only a more porous ITZ but also the reduction of the hydration products around artificial aggregates. ITZ microstructure has a great influence on diffusive transport into cementitious matrix: a denser ITZ corresponds to a better water and gases barrier. In the fresh state, particular attention must be paid to buoyancy, segregation and compaction.

On the other side, using plastic aggregates is possible to produce lighter and sustainable concrete with promising properties in terms of fracture mechanism (toughness increase), thermal conductivity and water vapor

permeability. More recently, some authors investigated also the residual properties of concrete containing plastic aggregates after high temperatures or fire exposure.

I.5.4 Use of porous aggregates for the internal curing

Internal curing refers to the possibility of supply an internal water source for cementitious materials that promotes cement hydration and reduces internal desiccation. Moreover, the internal curing can reduce the effects related to the autogenous shrinkage, characteristics of low w/c ratio mixtures. Internal curing can be provided by adding saturated lightweight aggregates (LWAs) or superabsorbent polymers (SAP) to the concrete. According to Jensen and Hansen (2001), SAPs offer more advantages because can be used as a dry concrete admixture and avoid the presence of large amount of mechanically poor aggregate particles.

The key parameter is the ease with which the water can be released from the internal curing reservoirs upon necessity. This phenomenon mainly depends on the pore size, the gradient of internal humidity and capillary pressure. Moreover, also the cementitious matrix structure is influent since the released water moves towards low humidity areas.

As reported by several authors in literature (Golias et al., 2012; Bentz et al., 2005; Castro et al., 2011), the mass of LWAs required to provide enough internal curing water to compensate the chemical shrinkage of the mixture, as a function of the degree of saturation, is:

$$\boldsymbol{M_{LWA}} = \frac{\boldsymbol{C_f \times CS \times \alpha_{max}}}{\boldsymbol{S \times \phi_{LWA}}} \qquad \text{(I.10)}$$

where M_{LWA} (kg/m^3) is the mass of LWA (in a dry state) that needs to be water filled to provide water to fill in the voids created by chemical shrinkage, C_f (kg/m^3) is the cement content of the mixture, CS (g of water per g of cement) is the chemical shrinkage of the cement, α_{max} (unit less) is the expected maximum degree of hydration (0-1), S (unit less) is the expected maximum degree of saturation of the LWA and Φ_{LWA} (kg of water/kg of dry LWA) is the absorption capacity of the LWA.

Castro et al. (2011) investigated the time dependent absorption and desorption of lightweight aggregates, useful in the mixture proportioning (according to eq. I.10). Kong et al. (2009), demonstrated that pre-wetting LWA was possible to improve concrete durability, since the reduction of the ITZ permeability thanks to the promoted hydration by internal curing. Golias et al. (2012) investigated different degree of saturation of lightweight aggregates, reporting that also with oven-dry LWAs was possible to obtain internal curing advantages if mixing water is adjusted.

I.6 Aim of the work and thesis structure

This Ph.D. study focuses the attention on the possibility to improve the interactions between polymeric fibers (or aggregates) and cementitious materials. In particular, as widely reported in literature, one of the main drawbacks in the use of synthetic fibers and artificial plastic aggregates is their low chemical affinity with cement paste. To this extent, the production of fibers and aggregates with very rough and porous surface was achieved by making use of an extrusion-foaming process on a laboratory scale. Such engineered fibers demonstrated to be able to offer interlocking positions for the cementitious matrix. Moreover, some chemical treatments (alkaline hydrolysis and sol-gel deposition of nano-silica) were performed on smooth fibers, to improve chemical adhesion with the cement paste. Besides the results obtained with virgin polymers, foamed fibers and aggregates were produced starting from an end-of-waste material. This allow to take into account the sustainability issues related to the use of cementitious mortars and the necessity of reducing the consumption of raw materials. Indeed, by using end-of-waste materials in cementitious composites makes possible to reduce the amount of plastic wastes that goes to landfill and to increase the final product sustainability. At the same time, the addition of foamed fibers (i.e. fibers with high fiber/matrix interactions) allows to improve mortar durability. Moreover, the substitution of natural aggregates with plastic particles into cementitious mortars allows not only the reduction of the unit weight and the thermal conductivity, but also improves water vapor permeability.

The thesis is structured in five chapters:

- In the *first chapter* a state of the art is presented and particular attention is paid at the durability issues of cementitious materials. Strictly related are the concept of sustainability and waste management: the theory of circular economy and the life cycle assessment (LCA) are discussed. Finally, the advantages and disadvantages deriving from the use of fibers and lightweight aggregates (LWAs) in cementitious materials are reviewed;

- In the *second chapter* materials and methods used for the experimental part are described. Moreover, also some principles of the foam extrusion process are reported, to better understand the processes of nucleation, bubble growth and foam stabilization;

- In the *third chapter* the results of the investigations on chemically modified fibers are reported. In particular, fibers characterization and their use into a cementitious mortar are discussed, focusing the attention on the benefits obtained in terms of fiber/matrix interactions by pull-out tests and ITZ investigations;

- In the *fourth chapter* the optimization of the foam extrusion process, to obtain rough fibers, is presented. Once fibers with adequate diameter and surface texture were obtained, it was possible to use them into a cementitious mortar. Fiber reinforced mortar rheological, mechanical and durability properties were investigated. In particular, attention was paid to fiber/matrix interactions and the influence of the improved adhesion on fiber reinforced mortar properties;

- In the *fifth chapter* the characterization and use of lightweight plastic aggregates into a cementitious mortar are discussed. Rheological, mechanical and physical properties of the produced lightweight mortar were investigated. In particular, specific weight, thermal conductivity and water vapor permeability were studied, since such properties are of interest for a plaster or rendering mortar. Finally, some preliminary results on the use of foamed aggregates (with a porous structure) as water reservoir for internal curing are presented.

This Ph.D. work is the result of a joint Ph.D. between University of Salerno (Italy) and University of Liège (Belgium).

Chapter II
Experimental: materials and methods

II.1 Polymeric materials

In this study, two different polymeric materials were used to produce synthetic fibers and artificial aggregates. In particular, chemical treatments were performed on polypropylene fibers (§ Chapter III) while foamed fibers were produced using both polypropylene and end-of-waste materials (§ Chapter IV). In the end, also artificial aggregates were produced starting from end-of-waste materials (§ Chapter V). In the following, the main characteristics of the different polymeric materials are discussed.

II.1.1 Virgin polymer

A commercial polypropylene (MOPLEN V79S, Montell Polyolefins) with melt flow index of 2.1 g/10 min (230 °C, 2.16 kg) and density of 0.91 g/cm^3 was used to produce different type of fibers.

II.1.2 End-of-waste polymer

The end-of waste polymer used to produce fibers and aggregates comes from post-consumer flexible packaging and was supplied in densified pellets. It was a polyolefin blend containing polypropylene (PP) and polyethylene (PE). As previously stated, particular attention should be paid to processing a polymeric blend as a result of the different melting temperature of each component. In particular, DSC analysis carried on recycled material showed three different melting peaks, as reported in Figure II.1. The first sharp melting peak (126°C) is representative of polyethylene (PE) while the second one (162°C) of polypropylene (PP). Moreover, the presence of a shoulder (109°C) in the shape of the peak may be associated to the presence of heterogeneous crystalline phases.

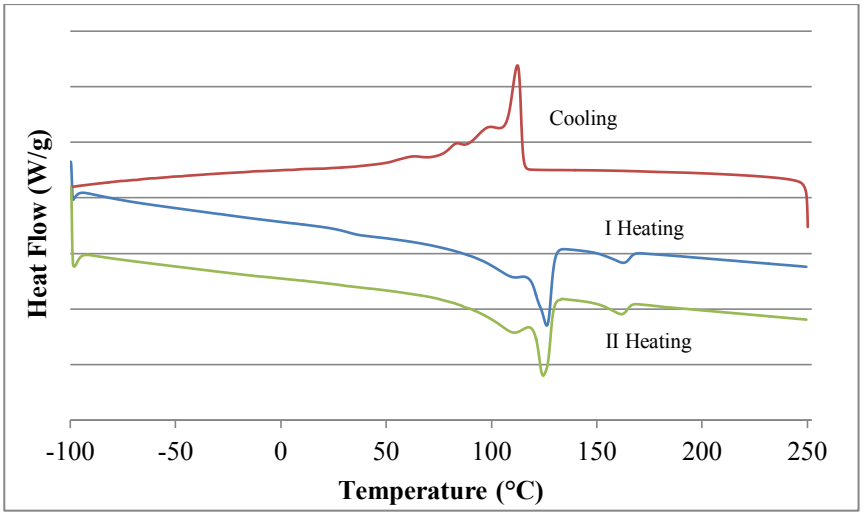

Figure II.1 *DSC thermograms of end-of-waste polymer pellets*

As will be discussed in the experimental part (§ …), an heterogeneous dispersion of PP droplets in the continuous PE matrix can be found (Figure IV.10). PE/PP incompatibility has been widely proved and explained in literature (Bertin and Robin, 2002; Shanks et al., 2000; Dintcheva et al., 2001) and represents the main reason for the unsatisfactory mechanical properties of these recycled mixed plastics.

II.2 Foam extrusion

II.2.1 Principle

A foam can be simply defined as a substance in which a gaseous void is surrounded by a much denser continuum matrix that can be in liquid or solid phase (Lee and Park, 2014). Foams exist in nature (cellulosic wood, marine organisms etc.) or can be produced synthetically. According to Lee and Park (2004), foamed plastics can be classified in different ways (Table II.1):

Table II.1 *Foam classification (Lee and Park, 2014)*

Category	Terminology	Range
Density	High, medium, and low	> 0.5, 0.2-0.5, < 0.2 (specific gravity)
Dimension	Board, thick and thin sheet	> 2 cm, 1-2 cm, < 1 cm
Structure	Open and closed cell	50% open cell as the borderline
Cell size	Nano, microcellular, foam	< 1µm, 1-100 µm, > 100 µm
Nature	Flexible and rigid	N/A

In particular, regarding the foam extrusion process of thermoplastic polymers, two main strategies are viable: thermal activation foaming (using chemical blowing agents) and gas dissolution foaming (by physical blowing agents). The former is dependent on chemical reaction and the latter involves physical variation in polymer states. In both methodologies, the same three steps: gas implementation, gas expansion and foam stabilization, are involved (Lee and Ramesh, 2004). Thermoplastic foams are generally produced by a process based on the phase separation that occurs within a polymer/gas solution and thus the key parameter is the gas solubility in the molten polymer. Equations of state (EOSs) are viable solutions to model gas solubility and different theories have been proposed (Lee et al., 2007; Lee and Park, 2014): Flory-Huggins, Sanchez-Lacombe and Simha–Somcynsky.

It is worth to mention that during the foaming process of thermoplastic polymers, state changes occurs, as reported in Figure II.2. The raw plastic material is first heated and pressurized (state A) then a blowing agent (both chemical and physical) is added (state B). The foam structure is developed by lowering the pressure (state C), and finally, a foam product is yielded by cooling the polymer matrix (state D) (Lee et al., 2007).

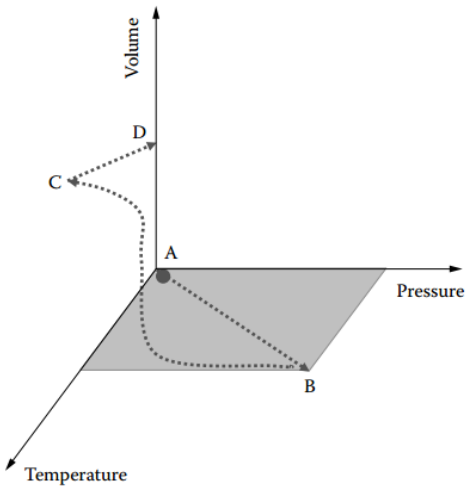

Figure II.2 *P-T-V change of foam extrusion from A to D; A: low V, low P, low T., B: low V, high P, high T, C: high V, low P, high T, D: high V, low P low T (Lee et al., 2007)*

As stated before, after gas solubilization, bubble formation (or nucleation), bubble growth and structure stabilization occur. Bubble nucleation can occurs in two different process: homogeneous nucleation and heterogeneous nucleation, respectively. The first takes place if the bubbles are generated from a single homogeneous phase containing no impurity or dirt. In reality, most of the commercial resins contain additives inside for several purposes, thus this process is quite rare. On the contrary,

heterogeneous nucleation occurs if tiny particles are present in the liquid, and if they assist in the formation of cells, since the nucleation took place at the solid/liquid interface.

II.2.1.1 Homogeneous nucleation

In the classical theory of nucleation, the nucleation rate is governed by the rate at which invisible gas clusters are energized by effective diffusion as a result of supersaturation to exceed the critical radius (Lee and Park, 2014). Homogeneous nucleation occurs when a sufficient number of dissolved gas molecules form clusters for a long enough time to make a critical bubble radius to cross over the resistance path as shown in Figure II.3 (Lee and Ramesh, 2004).

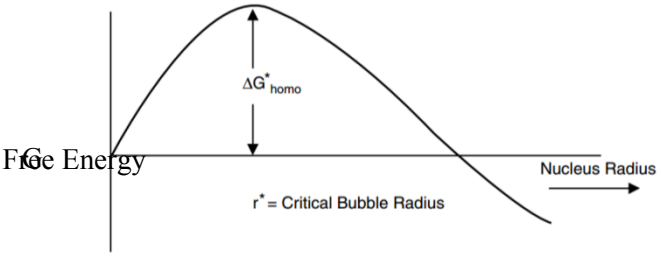

Figure II.3 *Homogeneous bubble nucleation (Lee and Ramesh, 2004)*

Thus, initially a molten polymer is saturated with gas at a certain pressure. After, reducing the pressure, the nucleation of tiny bubbles occurs due to the thermodynamic instability. Formation of bubbles involves the creation of new surfaces with certain volumes. Bubbles formation (in a liquid or in a solid) requires an increase in the free energy of the system, used to create new surfaces. Moreover, the birth of a gas bubble in a polymer through a reversible thermodynamic process has an excess free energy associated with it. It should be distinguished two phases: a metastable region and the equilibrium (Lee and Park, 2014).

Mathematically, in the metastable region, the total work for the surface area generation, size expansion and evaporation can be expressed as:

$$\Delta G = -V_b\left(P_g - P_l\right) + A\sigma + n(\mu_g - \mu_l) \qquad \text{(II.1)}$$

where σ, A, V, P and μ denote the surface tension of the liquid (the polymer in this case), bubble surface area and volume, pressure and gas molecules chemical potential (of the liquid, l, and the gas, g), respectively. Thus, lowering the surface tension by using surfactants will assist in the formation of bubbles. Nucleating agents such as talc, diatomaceous earth, and silica are more effective because they offer voids at the interface (Lee and Ramesh, 2004).

At the equilibrium, the chemical potentials μ_g and μ_l are equal. Moreover, assuming that the embryos are spherical in size as the spherical shape contains the minimum surface area (or surface energy), eq. II.1 can be rewritten as:

$$\Delta G = -\frac{4}{3}\pi r^3 \Delta P + 4\pi r^2 \sigma \quad \text{(II.2)}$$

where r is the bubble radius; ΔP is the pressure drop (e.g., die pressure drop in extrusion foaming); and σ is the surface tension of the polymer matrix. The maximum value of ΔG, denoted as ΔG*, occurs at a critical size r*, or when there is a critical number of gas molecules in the embryo, and represents the free energy of formation of the critical nucleus (Figure II.3). It is worth to mention that in polymeric systems, non-spherical geometries might be encountered. But the assumption of the spherical shape of the nucleus is reasonable, because offers the minimum resistance for nucleation for a given volume. The activation free energy for homogeneous nucleation of a critical nucleus is derived as:

$$\Delta G^*_{homo} = \frac{16\pi\sigma^3}{3\Delta P^2} \quad \text{(II.3)}$$

where σ is the surface tension of the polymer and $\Delta P = P_{sat} - P_s$ is the supersaturated pressure. From eq. II.3 is clear that when the degree of supersaturation is increased, both critical radius and critical free energy decrease. Physically this means that a greater amount of gas in the polymer makes it easier for bubbles to form. Similarly, the higher the pressure drop, the higher the nucleation rate of bubbles. (Lee and Ramesh, 2004). Since a polymer always contains residual catalyst or unreacted monomers or contaminants, from the thermodynamic perspective, it is hardly possible to justify homogeneous nucleation in polymeric melt foaming. However, when the pressure gradient and the surface tension dominate, it is not surprising to find good agreement with homogeneous predictions (Lee and Park, 2014).

II.2.1.2 Heterogeneous nucleation

In the practice, heterogeneous nucleation is the common type of nucleation found in polymer systems containing additives. The efficiency of producing bubbles depends on several factors, such as the type and shape of nucleating particles and interfacial tensions of solid and solid–gas interface. The primary benefit comes from the interface, which acts like a catalyst for nucleation. The presence of tiny particles and cavities reduces the activation energy required to achieve a stable nucleus. Figure II.4 shows the reduction of Gibbs free energy associated with the heterogeneous nucleation process.

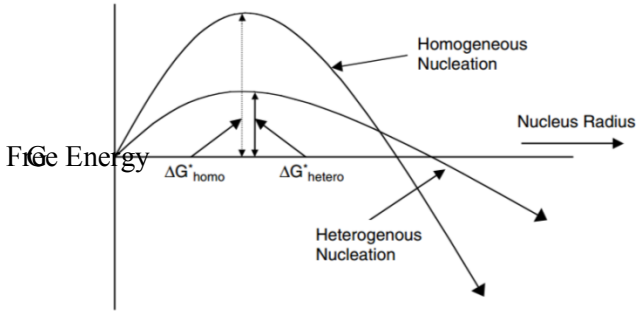

Figure II.4 *Heterogeneous bubble nucleation: $\Delta G^*_{hetero} < \Delta G^*_{homo}$ (Lee and Ramesh, 2004)*

Blander and Katz proposed a simple heterogeneous nucleation model for liquids in 1975:

$$\Delta G = \sigma_{lg} A_{lg} - \Delta P V_b + A_{sg}(\sigma_{sg} - \sigma_{sl}) + n(\mu_g - \mu_l) \qquad \text{(II.4)}$$

The subscripts lg, sg and sl represent liquid-gas, solid-gas and solid-liquid interfaces, respectively. The thermodynamics of heterogeneous nucleation and its mathematical analysis are given in Uhlmann and Chalmers (1965). The heterogeneity factor can be used to correct the activation energy term derived for homogenous nucleation:

$$\Delta G^*_{hetero} = \Delta G^*_{homo} f(\theta) \qquad \text{(II.5)}$$

Because of the presence of solid surface, a chemical equilibrium between gas and melt is not useful for bubble formation. Its interfacial phenomenon is depicted in Figure II.5.

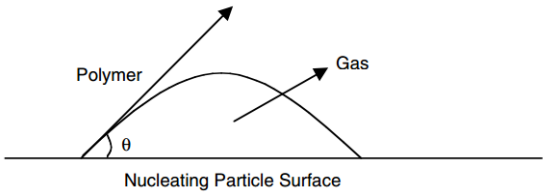

Figure II.5 *Schematic of nucleating particle interaction with gas and polymer (Lee and Ramesh, 2004)*

Considering the configuration of Figure II.5, Uhlmann and Chalmers (1965) derived and expression for $f(\theta)$:

$$f(\theta) = \frac{(2+cos\theta)(1-cos\theta)^2}{4} \qquad \text{(II.6)}$$

Combining equations II.6, II.5 and II.3 is possible to express the activation energy for heterogeneous nucleation as:

$$\Delta G^*_{hetero} = \frac{16\pi\sigma^3}{3\Delta P^2} f(\theta) \qquad \text{(II.7)}$$

where θ is the wetting angle, $f(\theta)$ is the heterogeneity factor, and σ represents the interfacial tensions of a polymer–gas bubble (Lee and Ramesh, 2004).

II.2.1.3 Bubble growth

After cell nucleation, the bubbles grow due to the diffusion of excess gas in the polymer. The viscosity of the polymer, the gas concentration, the foaming temperature, and the amount of nucleating agent and its nature are some of the variables that control the foam growth process (Lee and Ramesh, 2004). The bubble growth is essentially the main mechanism to dissipate the super-saturation state that is inherent to the polymeric foaming phenomena. In fact, the degree of super-saturation appears to be the main driving force in most bubble growth. Moreover, diffusion and expansion are interrelated during bubble growth: diffusion causes influx to bubble, and expansion tends to reduce gas concentration in the bubble for diffusion (Lee et al., 2007).

However, in reality, bubble expansion takes place in a finite polymeric medium, and possibly in a different thermal environment. When foam exits into room temperature the natural cooling will solidify the surface to cause extra resistance for growth. In addition, gas molecules close to the boundary or surface can diffuse to the surface and escape from the surface, rather than into the cell as illustrated in Figure II.6.

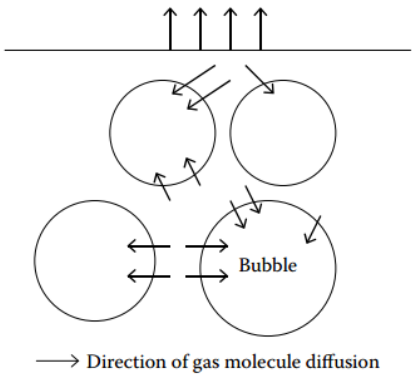

Figure II.6 *Gas molecules diffusion and surface escape in cell growth (Lee et al., 2007)*

II.2.1.4 Foam stabilization

As stated previously, the foaming process in unstable in nature. Both nucleation and growth dissipate energy to re-establish the equilibrium. To keep the foamed product stable, cooling is necessary to freeze the cellular structure. During solidification, material strength increases and due to the viscosity reduction, expansion slows down. Moreover, gas molecules close to the skin of the foam tend to diffuse and escape from the surface, as previously described (Figure II.6). As soon as cooling begins, the replacement of the blowing gas contained in the foam cells with the surrounding gas (i.e., air) begins. It is driven by the concentration gradient existing between the inside and the outside of the foamed product (Lee et al., 2007).

II.2.2 Procedure

To produce foamed fibers and aggregates a foam extrusion process was performed, using a commercial chemical blowing agent (CBA): Hrydrocerol CF, Clariant. This agent was dry blended with polymer pellets and then extruded by a single screw extruder (Brabender Do-Corder E330 L = 400 mm and L/D = 20). Above 150 °C, the CBA starts to decompose, a gas is produced and bubbles appear at the outlet of the die, due to the pressure gradient. As reported in literature (Sauceau et al., 2011), this operation does not give good control of porosity and products often exhibit non-uniform cellular structures. Moreover, CBA decomposition temperature is a key parameter because should match with polymer matrix melting temperature. If decomposition temperature is too low, gas could be generated prematurely, thus leading to gas loss and/or premature generation of cells. Conversely, if the decomposition temperature is too high, the CBAs might not be activated completely, which might result in non-uniform cell structure and/or limited foam expansion (Lee and Park, 2014).

Another issue derives from the difficulties generally reported in literature about the foaming of polypropylene (PP). In particular, as reported by Yu et al. (2013), PP has a high crystallinity and low melt viscosity. The issue derives from the non-dissolvability of the gas in the crystallites and the non-uniformity of the polymer-gas solution. Thus, processing parameters (temperatures profile, screw speed rotation, take-up speed, capillary die diameter) were optimized, in order to achieve the desired characteristics. In the next paragraph (§ II.3), fibers production is analyzed more in detail.

As stated before, bubble growth takes place outside the forming die and involves extensional (or elongational) flow. As the bubbles grow during foaming, bubbles walls are stretched in the flow direction (similarly to what occurs during film blowing). Thus, it is possible to conclude that foam morphology and consequently foam properties, are governed by the extensional rheology.

II.3 Fibers production

As stated before, fibers were produced using a single screw extruder. Processing parameters and fibers nomenclature are reported in Table II.2. The optimization of the foamed fibers extrusion process was necessary in order to achieve the desired surface roughness. To this extent, different foaming agent contents (0.5, 1, 2 and 5 wt.%) were investigated. Moreover, also temperatures profile and screw speed rotations were modified during the optimization. The three temperatures correspond to the different zones of the extruder from the hopper to the die. Finally, in order to obtain a smaller diameter, also capillary die was modified. Some of the produced fibers are reported in Figure II.7-8.

Concerning the end-of-waste material, pellets were oven dried for 12 h at 70 °C before the extrusion.

Table II.2 *Fibers nomenclature and extrusion parameters*

Name	Capillary die (mm)	Temperature profile (°C)	Screw speed (rpm)	Foaming agent (wt.%)	Take-up speed (m/min)
PP[1]	2	180-220-180	24	-	30
PP[2]	0.5	190-220-200	1	-	9.5
PP+0.5FA	2	180-210-180	30	0.5	30
PP+1FA	2	180-220-180	24	1	16
PP+2FA	2	180-220-180	16	2	12
PP+5FA	0.5	190-220-200	3	5	5.5
Recycled	0.5	165-230-195	1	-	1.5
Recycled+2FA	0.5	165-230-195	1	2	1

[1] Used for chemical treatments (Chapter III);
[2] Used as non-foamed fibers for comparison (Chapter IV).

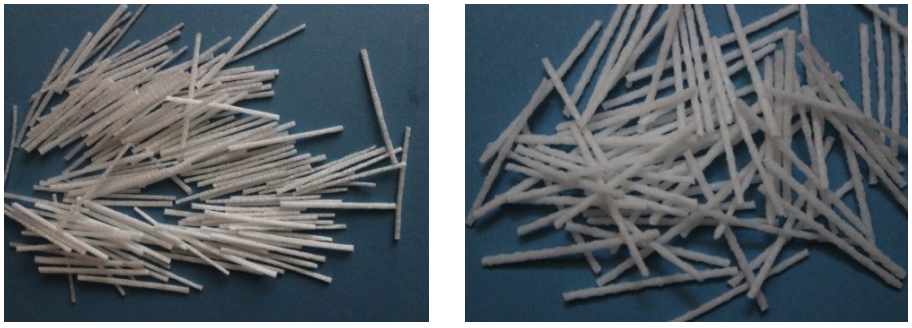

Figure II.7 *a) PP+1FA and b) PP+2FA foamed fibers*

Figure II.8 *a) PP fibers and b) Recycled+2FA foamed fibers*

II.4 Fibers chemical surface treatments

Chemical treatments were performed on PP fibers (Table II.2) in order to investigate the influence of such treatments on fiber/matrix interactions

II.4.1 Alkaline hydrolysis

A solution with 40 g of NaOH (Sigma-Aldrich) and 100 g of distilled water was prepared. Fibers were maintained in the solution at 95 °C for 2 h and then left for 12 h at room temperature. Elapsed this time, fibers were washed with distilled water (till any alkalinity trace was removed) and dried at room temperature.

II.4.2 Sol-gel deposition of nano-silica

The sol-gel process involves the synthesis of colloidal suspension of solid particles (sol) in a liquid (gel). The chemical reaction can be divided in two following steps: a precursor reacts with water producing an hydroxyl ion (hydrolysis) then hydrolysed molecules can link together in a condensation reaction, liberating water or alcohol. As this reaction goes on, large molecules containing silicon are created by a process of polymerization. Metal alkolxides are popular precursors and the most used is tetraethyl orthosilicate (TEOS) which chemical formula is $Si(OC_2H_5)_4$. The chemicals used for the sol-gel reaction were: TEOS (99 %, Sigma-Aldrich), ammonium hydroxide solution (28 % NH_3 in H_2O, Sigma-Aldrich), absolute ethanol (Jt Baker) and distilled water. According to the procedure used by Yang et al. (2013) fibers were dipped in a mixture of absolute ethanol (200 g), deionized water (20 g) and ammonia water (30 g). Fibers and the mixture were maintained for 10 min at 60 °C and then TEOS (40 g) was gradually added into solution. After 1 h of continuous magnetic stirring, fibers were filtered and dried at room temperature.

II.5 Fibers characterization

II.5.1 Physical and morphological properties

Fibers diameter was evaluated by an optical microscope (Zeiss Axioskop 40): the measure is the average of at least three measurements. In the case of fibers with a surface roughness, pictures were taken also by a digital camera and then the profile was plotted to define a roughness coefficient (§ IV.1.1). Fibers density was measured by means of a gas pycnometer, using helium as gas. The average value of five measurements for each sample was taken as fiber density. Porosity of the cross section and surface roughness were determined by SEM (SEM, LEO model 420) images analysis.

II.5.2 Mechanical properties

Mechanical properties of fibers were determined by tensile tests, according to ASTM C 1557-03. The tests were carried out at two cross-head speeds using a universal testing machine with a load cell of 1 kN (SANS CMT 6000). For each sample ten fibers were tested at a lower cross-head speed (4 mm/min) for determining elastic modulus (E) while other ten fibers were tested at a higher cross-head speed (40 mm/min) to evaluate tensile strength and strain at failure (σ_b and ε_b). Gauge length was always 40 mm.

II.6 Fiber reinforced mortar preparation

All the investigated mortars were prepared according the procedure described in EN 196-1. Mortars constituents are described in the following.

Fibers length, volume fraction and mortars nomenclature are reported in each chapter for ease of reference.

II.6.1 Mortar constituents: sand, cement and water

Two different sands were used for mortars preparation (both with particle size 0/2mm): a calcareous sand and a quartz sand. In particular, the former was used to produce mortars with chemically modified fibers while the latter was used both for mortars containing foamed fibers and lightweight mortars (for lightweight mortars preparation see § II.9). Aggregates/cement ratio was always 3.

The cements used were CEM II/A-LL 42.5 R and CEM I 42.5 N. The first was used for mortars containing chemically modified fibers while the second for mortar reinforced with foamed fibers and lightweight mortars.

A w/c ratio of 0.50 was used for all the fiber reinforced mortars, using always tap water at room temperature.

II.7 Fiber reinforced mortar characterization

II.7.1 Rheological properties

Characterization of cementitious materials properties at fresh state is of widespread importance, in order to evaluate workability issues deriving from the investigated mixture composition. The quality of fresh concrete is determined by the ease and homogeneity with which it can be mixed, transported, compacted and finished (Ramachandran and Beaudoin, 2000). Moreover, according to Neville (1995), workability can be defined as the amount of internal work necessary to produce full compaction. Obviously, a key parameter that affects cementitious materials workability is the amount of water in mixture. But, it is widely known the negative influence of an excess of water (porosity, mechanical properties, durability, segregation, bleeding etc.). Workability may also be modified by the addition of admixtures (plasticizers and air entraining agents) or fine particles (Westerholm et al., 2008; Nehdi et al., 1998; Ferraris et al., 2001). Other parameters that affect workability are: aggregates size, grading, shape and surface roughness; proportion between cement paste and aggregates. Consistency (or fluidity) describes the ease with which a substance flows but a concrete having the same consistency may, however, have different workability characteristics (Ramachandran and Beaudoin, 2000).

Several standards or methodologies describe how to determine some parameters (in most of them consistency) describing the mixture workability but none is capable of measuring this property directly. The most extensively used test is the slump test. This method is described by EN 1015-3 (for mortar) and by EN 12350-2 (for concrete). Slump, of course, is a rheological measurement, but slump only describes a part of the behavior and is an empirical measure; it cannot be compared with other rheological measures. Other measures of cementitious materials workability exist, but they are less common principally due to the necessity of expensive rheometers.

The fresh cementitious materials properties can be assimilated to the flow behavior of concentrated suspensions. Basic principles of rheology are discussed in the following paragraph

II.7.1.1 Principle

The study of flow behavior is called rheology and is generally applied to fluid materials (or materials that exhibit a time-dependent response to the stress). Flow is typically measured using shear and the shear parameters of stress (τ) and strain rate ($\dot{\gamma}$) are calculated from measurements of torque and flow rate.

The apparent viscosity (μ) is defined as:

$$\mu = \frac{\tau}{\dot{\gamma}} \tag{II.7}$$

It is important to always specify at which viscosity we are referring to (i.e. apparent viscosity, plastic viscosity, differential viscosity etc.).

Several models have been proposed for flow behavior description (Figure II.9). The simplest and ideal behavior is the Newtonian one, with a linear relationship between stress and strain rate (starting from zero, i.e., at zero stress corresponds zero strain rate). In other cases, flow initiates only above some level of stress (called yield stress, τ_0); these materials are called Bingham fluids and have a plastic behavior with a linear relationship between stress and strain. Another common behavior is pseudo-plastic (or shear thinning), in which viscosity decreases as strain rate increases. Finally, there is the shear thickening (or dilatant) behavior, found particularly for self-compacting concrete (Feys et al., 2008). For self-compacting concrete (SCC) some thickenings are necessary to avoid aggregates segregation.

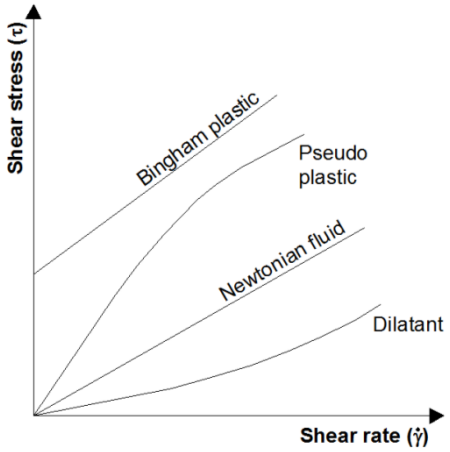

Figure II.9 *Different rheological behaviors*

Also from the slump test is evident that cementitious materials are able to stand unsupported without flowing under their own weight, thus exists a limit of stress above which the flow starts. As discussed previously, the simplest model that take into account this behavior is the Bingham one:

$$\tau = \tau_0 + \mu \cdot \dot{\gamma} \tag{II.8}$$

The yield stress is a consequence of the interparticle forces: links between particles are broken by the shearing, thus the measured yield stress depends upon time and previous shear history (Banfill, 2006)

The constitutive relationship for the pseudo-plastic behavior is the power low equation:

$$\tau = K \cdot \dot{\gamma}^n \tag{II.9}$$

where K is the consistency and n the power index, which represents the deviation from Newtonian behavior (n is less than unity for shear thinning systems and higher than the unity for shear thickening materials). A combination of the power law (eq. II.9) and the Bingham model (eq. II.8) is the Herschel- Bulkley law:

$$\tau = \tau_0 + K \cdot \dot{\gamma}^n \tag{II.10}$$

More complex laws have been proposed and reviewed by Banfill (2006). Moreover, cementitious materials exhibit also a time-dependent behavior: at a constant stress level, a progressive and reversible decrease in viscosity is achieved. Materials with the as described behavior are called thixotropic fluids.

A more detailed analysis is necessary for fiber reinforced cementitious materials. It is widely proven that fibers addition decreases cementitious materials workability. This influence is strictly correlated to fibers aspect ratio, r, and volume fraction, ϕ_f:

$$r = \frac{L_f}{D_f} \tag{II.11}$$

where L_f and D_f are fibers length and diameter, respectively. Moreover, due to their elongated shape, fibers effect depends on the position and the orientation within a structure relative to principal stresses. Fibers are needlelike particles that increase the resistance to flow and contribute to the formation of an internal structure of aggregate grains and fibers (Grünewald, 2012), as shown in Figure II.10.

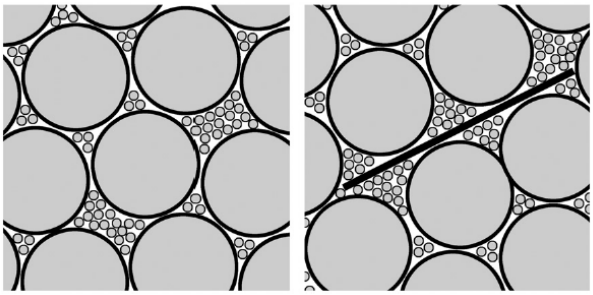

Figure II.10 *Effect of a fiber on the packing of gravel and sand mixtures (Martinie et al., 2010)*

According to Grünewald, the effect of fibers on workability is mainly due to four reasons:

1) The shape of the fibers is more elongated than the shape of the aggregates; the surface area at the same volume is larger;
2) Stiff fibers change the structure of the granular skeleton, whereas flexible fibers fill the space between them. Stiff fibers push apart particles that are relatively large compared to the fiber length, which increases the porosity of the granular skeleton;
3) The surface characteristics of fiber differ from that of cement and aggregates, i.e. plastic fibers might be hydrophilic or hydrophobic;
4) Fibers can be deformed (i.e. have hooked ends, be crimped or waveshaped) to improve the anchorage between them and the surrounding matrix.

The phenomenon described at the point two, and illustrated in Figure II.10, is very important, because the packing density is reduced with fiber addition in a slightly larger way with coarse aggregate than with sand, because the sand is able to pack tightly around the fiber, whereas coarse aggregates are pushed apart by the fiber's presence (Martinie et al., 2010).

Plastic fibers mainly affect the rheological behavior of the cement paste (due to their deformability and ability to form entangled structures) while steel fibers affect the yield stress of concrete.

In this thesis, two investigations were carried out: flow table tests and rheological measurements using a rheometer (RheoCAD 200), in order to study low and high shear rates, respectively.

II.7.1.2 Flow table test

Fresh mortar workability was determined by flow table test, according to EN 1015-3. The diameter of the spread mortar was measured in two perpendicular directions using a caliper and then consistency was calculated considering the ratio with the initial diameter (100 mm). Three tests were carried out for each composition. Flow table tests were performed on fiber reinforced mortars (with both foamed and non-foamed fibers) and lightweight mortars containing artificial plastic aggregates.

II.7.1.3 Rheometer RheoCAD

The main shear test was performed using a RheoCAD 200 (CAD Instrumentations), reported in Figure II.11a. The rheometer is computer controlled: the torque is measured at imposed rotational speed. The shear is given by an anchor-like shaped stirrer (Figure II.11b) while an outer stirrer (hook-like shaped) is necessary for the homogenization of the mixture before and after a measurement. Homogenization of the mortar may become necessary as the applied momentum, i.e. the centrifugal force, may lead to (partial) segregation of the mixture. The rotational speed profile used for

rheological tests is reported in Figure II.12. Careful calibration of the system allows to transfer the relation between torque and rotation rate to plastic viscosity and yield stress:

$$T = g + N \cdot h \qquad \text{(II.12)}$$

where T is the torque (Nm), N is the rotation rate (rpm), g is the relative yield stress (Nm) and h is the relative plastic viscosity (Nm/rpm).

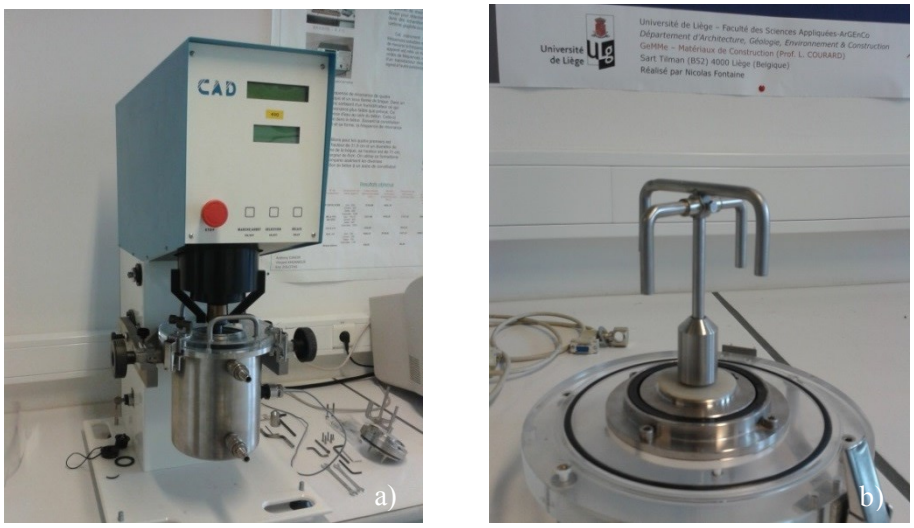

Figure II.11 *a) RheoCAD 200 and b) anchor-like stirrer*

The rotational speed profile used for rheological tests (Figure II.12) contains three different zones, in order to achieve several requirements (Corcella et al., 2004):

1) Minimize the effects of mortar preparation and loading in the rheometer (all the mortars were prepared according EN 196-1, but after mixing mortar was transferred into the rheometer) removing the initial history;
2) Acquisition of the data necessary for the construction of the flow curves (torque vs. rotational speed), in the descending part of the triangle;
3) Evaluate the thixotropic behavior of the mortar.

The results obtained can be then analyzed and discussed using the models previously described, in particular Bingham (eq. II.8) and Hershel-Bulkley (eq. II.10).

RheoCAD was used to determine the rheological behavior of mortars containing both foamed and non-foamed fibers.

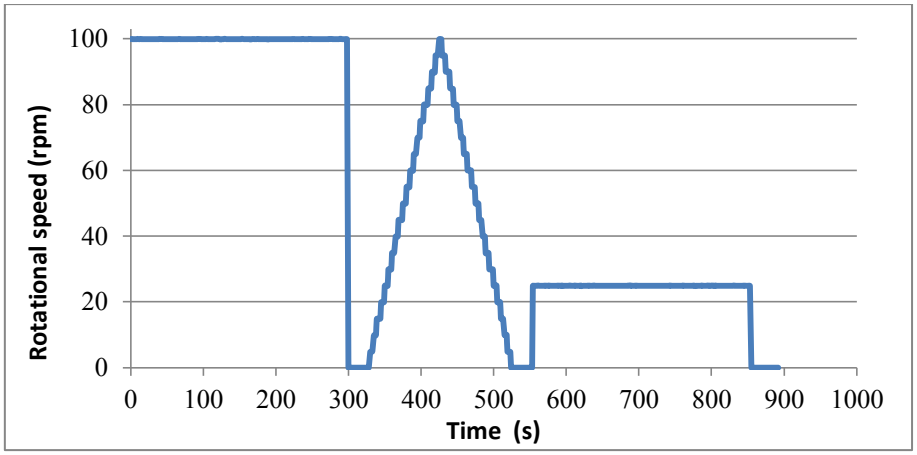

Figure II.12 *Rotational speed profile used for rheological tests*

II.7.2 Mechanical properties

Mortars mechanical properties were determined according to EN 196-1. Specimens of 40 mm x 40 mm x 160 mm were casted in steel molds and compacted by a jolting table; three specimens for each composition were tested after 28 days of wet curing.

II.7.2.1 Flexural strength

Mortar flexural strength was determined by three-point bending test (Figure II.13). Flexural strength was obtained by the following equation:

$$R_f = \frac{1.5 \cdot F_f \cdot L}{B^3} \qquad \text{(II.13)}$$

where F_f is the maximum applied load, L is the distance between the 2 supports and B is the side of the square section of the specimen (40 mm).

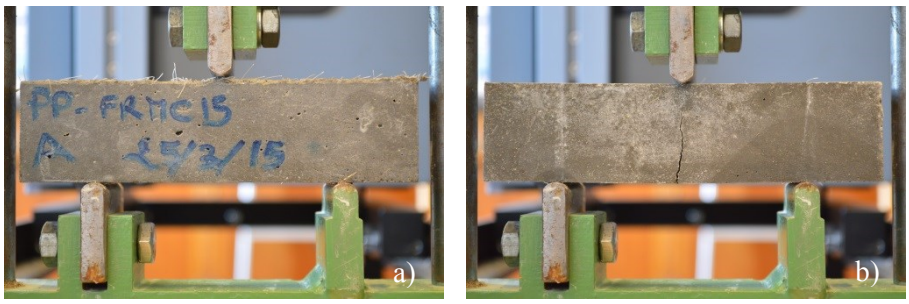

Figure II.13 *Mortar specimen before (a) and after (b) the test to determine flexural strength*

II.7.2.2 Compressive strength

Compression tests were performed on the half prisms resulting from flexural tests (Figure II.14). Compressive strength was determined by equation:

$$R_c = \frac{F_c}{A} \tag{II.14}$$

where F_c is the maximum applied load and A is the specimen section (1600 mm^2).

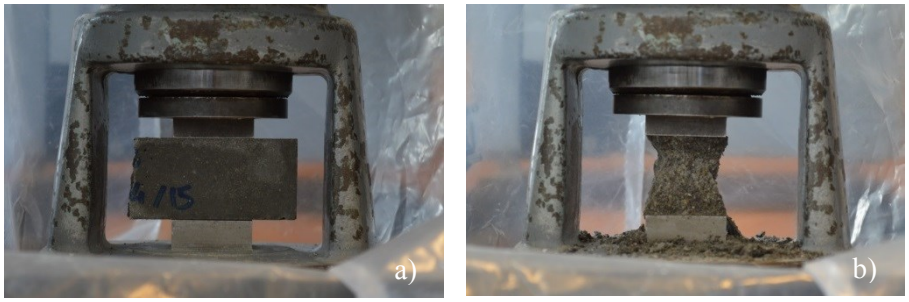

Figure II.14 *a) mortar specimen before and b) after compression test*

II.7.3 Durability properties

As stated in the previous chapter, cementitious materials are inevitably porous materials and porosity allows the access of several dangerous agents for mortar/concrete durability. In the following, the methods used to investigate durability properties are described.

II.7.3.1 Water absorption

Mortar water absorption was determined both via capillary water absorption tests and total immersion tests. The tests were carried out on the same specimens (before tested for the determination of the capillary rise and then for total immersion) after 28 days of wet curing. Three prismatic samples (75 mm x 75 mm x 150 mm) were investigated for each mixture.

II.7.3.1.1 Capillary water absorption

Capillary water absorption tests were performed according to EN 1015-18. After 28 days of wet curing, samples were dried at 40°C until constant mass was achieved, named M_0. Also the mass of saturated specimen was measured and named M_s. Then, specimens were immerged in water and the mass was evaluated at several times: 1, 10, 15, 30 and 60 min; 2, 4, 6, 24, 48

and 72 h. Determining the amount of absorbed water, ΔM, was possible to calculate the absorbed water per unit surface (A) at time t_i, i_{ti}, and the capillary water absorption coefficient, S_{ti}:

$$i_{ti} = \frac{\Delta M}{A} \quad \text{(II.15)}$$

$$S_{ti} = \frac{i_{ti}}{\sqrt{t_i}} \quad \text{(II.16)}$$

II.7.3.1.2 Total immersion absorption

With this test is possible to calculate porosity open to water starting from the total amount of water absorbed after total immersion of the sample.

$$Ab = \frac{M_S - M_0}{M_0} \cdot 100 \quad \text{(II.17)}$$

$$P = \frac{\Delta M}{V} \cdot 100 \quad \text{(II.18)}$$

where M_s is the saturated mass, M_0 the oven-dry mass and V is the volume of the sample. It should be noticed that this is the porosity open to water and that ΔM represents the volume occupied by the water (considering that 1 g of water have a volume of 1 cm^3 because water density is 1 g/cm^3).

II.7.3.2 Sulfate attack

Cementitious materials exposed to sulfate solutions can exhibit signs of deterioration due to the formation of gypsum, ettringite and thaumasite (or a mixture of these compounds) (§ I.2.2). The samples were immersed in a saturated solution of sodium sulphate ($NaSO_4$) and oven-dried (110 °C), according to ASTM C88-05. The evaluation of sulphate attack was made by measuring the samples weight variation along a total of ten cycles. Moreover, in order to evaluate also visually the degradation at the end of each cycle, pictures of the samples were taken. Three prismatic samples (75 mm x 75 mm x 150 mm) were investigated for each mixture. The solution was prepared with 215 g of anhydrous $NaSO_4$ per liter of water.

II.7.4 Physical properties

Fiber reinforced mortar physical properties were investigated in order to study the influence of the different fiber/matrix interactions. In particular, fiber/matrix bond was evaluated by pull-out tests and SEM investigations. Moreover, the influence of fibers addition and their bond with the cement paste on plastic shrinkage cracking was evaluated by a modified Kraai's method (Kraai, 1985).

II.7.4.1 Fiber/matrix bond investigation

II.7.4.1.1 Pull-out test

As stated in the previous chapter single fiber pull-out tests are not regulated by national or international standards (except the Japanese JCI SF-8), but common procedures exist in literature (Abbas and Khan, 2016). In particular, the test configuration used in this study consists of a single fiber embedded in a 50 mm cubic mortar specimen. Three fiber embedment lengths were investigated (10, 20 and 30 mm). Tests were performed with a universal testing machine (Instron 4301) equipped with a 1 kN load cell at a constant displacement rate of 1 mm/min. Five samples for each fiber were investigated. Pullout load versus displacement curves were obtained and the pullout strength, τ_{max}, was determined with the following equation:

$$\tau_{max} = \frac{P_{max}}{(2 \cdot \pi \cdot r) \cdot l} \tag{II.19}$$

where P_{max} is the pull-out peak load; l is the embedded fiber length and (2πr) is the fiber circumference.

II.7.4.1.2 ITZ investigation

Fiber/matrix interfacial transition zone (ITZ) was investigated by SEM observations on the fracture surface of specimens cured for 28 days in water. Attention was paid to the presence of hydration products on the fiber surface and the matrix adhesion onto fibers.

II.7.4.2 Shrinkage cracking test

Restrained plastic shrinkage cracking tests were performed according to a literature consolidated methodology firstly proposed by Kraai (Kraai, 1985) and then adapted by several researchers. Slabs of 50x50x5 cm restrained by angular steel profile were used. After casting, specimens were taken for 8 hours in a climatic chamber with a fixed wind speed. Weight, temperature and relative humidity were monitored and the rate of water evaporation was

determined by measuring the loss in weight of the mortar slabs before crack pattern evaluation. The crack pattern of each specimen was observed and photographs were taken every hour.

II.8 Foamed aggregates production

Lightweight aggregates (LWAs) manufacturing consisted of three following steps: foam extrusion process, strands grinding and aggregates sieving. The foam extrusion process was performed as described before for fibers production (§ II.2.2 and II.3). Pellets and chemical foaming agent (Hydrocerol CF) at 2wt.% were dry blended and then extruded by a single screw extruder (BRABENDER DO-CORDER E330, L/D = 20 with a D_{screw} = 20 mm, capillary die of 0.5 mm) operating at the following temperature profile: 165°C-230°C-170°C, varying screw speed rotation to obtain foamed strands with different diameters. Filaments were collected by a winder and then grinded by a pelletizer. In the last step aggregates were sieved according to EN 933-1 and separated in four different particle size grades: 2-1.4 mm, 1.4-1.0 mm, 1.0-0.50 mm and 0.50-0.18 mm. The four aggregates were mixed in order to reproduce, almost completely, the standard EN 196-1 sand particle size distribution (Figure II.15). Aggregates grading, i.e. particle size distribution, is of wide importance for mortar density, porosity, aggregates distribution and also mechanical properties (He et al., 2015). LWAs particle distribution (Figure II.15) was almost the same of quartz sand grading curve but with less fine sand.

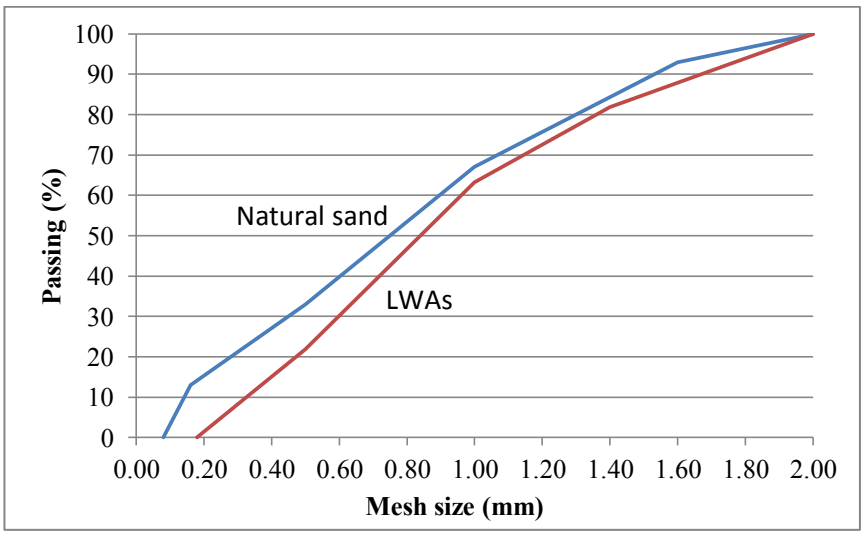

Figure II.15 *Aggregates particle size distribution (LWAs = LightWeight Aggregates)*

As reported in Table II.3, LWAs are coarser, i.e. the presence of coarse aggregates is higher, as evident also by the higher modulus of fineness. In this study, the use of fine artificial aggregates was excluded for the difficulty in producing a such small particle size with the described procedure.

Table II.3 *Natural and artificial sand cumulative passing*

Mesh opening (mm)	Cumulative passing (%)	
	Natural sand	LWAs
2.00	100	100
1.60	93	-
1.40	-	82
1.00	67	63
0.50	33	22
0.18	-	0
0.16	13	-
0.08	0	-
Modulus of fineness	2.94	3.33

II.9 Lightweight mortar production and characterization

II.9.1 Mix design

All the mortar samples were prepared in accordance with the procedure described in EN 196-1. Nomenclature and composition of the studied mixtures are reported in Table V.2. LWAs were used both in saturated and unsaturated conditions and three w/c ratios were investigated (0.30, 0.45 and 0.50, respectively). Saturated LWAs were soaked in part of the mixing water for 24 hours under vacuum. Four natural quartz sand volume replacement were investigated (5, 10, 25 and 50%) comparing lightweight mortars (LWMs) with control specimens, i.e. without LWAs. In some compositions was also used a superplasticizer (Dynamon SX, Mapei) at two different wt.% respect the used cement (0.5 and 4.5 %).

For the compositions used for the investigation on the use of LWAs as water reservoir for internal curing, additional water was added at the mixing water, then aggregates were saturated under vacuum for 24 h, as previously described. In particular, considering an average porosity of 8 % for LWAs, the amount of water necessary to saturate aggregates pores was calculated for the different natural sand volume fraction replacements.

II.9.2 Rheological properties

Lightweight mortars consistency was evaluated after flow table test as previously described (§ II.7.1.2) according EN 1015-3.

II.9.3 Mechanical properties

Flexural and compressive strength were measured in accordance to what previously exposed concerning fiber reinforced mortars (§ II.7.2).

II.9.4 Physical properties

II.9.4.1 Aggregates distribution

Natural and lightweight aggregates interaction with cement paste and distribution in the cross section were investigated by SEM analysis. Pictures were taken both on polished and fractured surfaces.

II.9.4.2 Oven-dry density

The oven-dry density, ρ_d, of hardened mortars was determined on specimens dried at 105°C until constant mass, according to EN 12390-7. Three specimens for each composition were tested.

II.9.4.3 Thermal conductivity

Thermal properties of building materials, in particular thermal conductivity, are important for the realization of eco-efficient building with a lower energy demand. Thermal conductivity can be measured both in steady state and transient conditions but with a different accuracy (Dubois and Lebeau, 2015). The most used method is the so-called "guarded hot plate technique" (GHP), defined in the ISO 8302 and specified in European standards EN 12664 and EN 12667. Its principle is to reproduce the uniform, unidirectional and constant thermal flux density existing through an infinite homogeneous slab-shaped specimen caught between two infinite isothermal planes (Dubois and Lebeau, 2015).

The device used in this research was provided by Prof. F. Lebeau. A specimen is sandwiched between an electrically-heated hot plate maintained at temperature T_h and a cold plate maintained at a lower temperature T_c. The heat dissipated by the Joule effect in the hot plate would travel to the cold plate through the sample, but also backwards and laterally on the edges of the hot plate. Back and lateral guard zones are then necessary to neutralize these leaks.

Thermal conductivity can be thus determined with the one-dimensional Fourier equation:

$$\lambda = \frac{F \cdot s}{A(T_h - T_c)} \quad \text{(II.20)}$$

where F (W) is the heat flow-rate that in an ideal unidirectional condition would traverse the specimen through an area A (m^2) called measurement area; s (m) is the thickness of the specimen. It's important to notice that the thermal flux F is equal to the electric power injected in the heater plate only if the instrument is perfect (Dubois and Lebeau, 2015).

The difference of temperature generates a heat flow from the hot plate to the cold one (in accordance with the first principle of thermodynamics). When the thermal equilibrium is achieved, the instrument is able to determine the thermal conductivity (λ) of the sample.

Thermal conductivity measurements were carried out on mortar specimens of size equal to 30x30x5 cm^3 (Figure II.16a), manufactured in wooden molds. After 28 days of water curing specimens were conditioned (25 °C and 50 % RH) until constant mass before testing.

The slab square-shaped specimen is placed between a hot plate assembly and an upper cold plate assembly, mounted horizontally on a support frame (Figure II.16b). A rail system allows to displace the cold plate assembly vertically, to adjust the GHP to the thickness of the sample. On its lateral faces, the sample is surrounded by insulation panels.

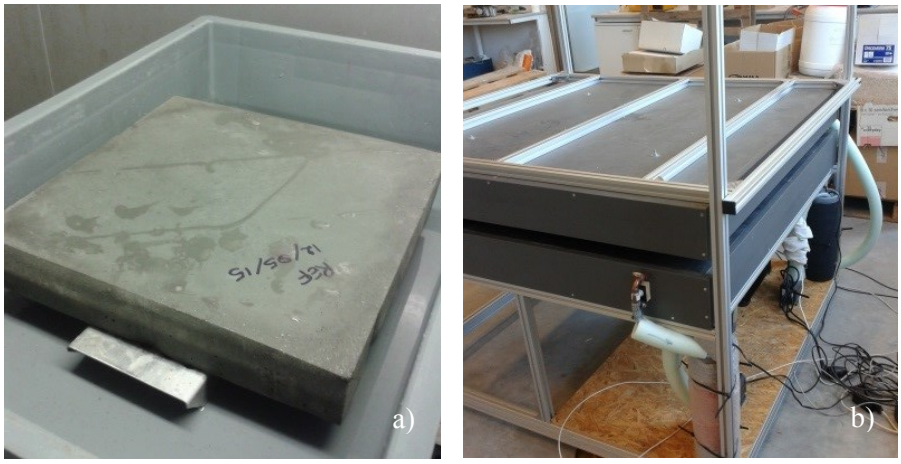

Figure II.16 *a) slab-shaped specimen (30 x 30 x 5 cm^3) and b) GHP apparatus*

II.9.4.4 Autogenous and total shrinkage

Autogenous and free total shrinkage tests were performed in order to evaluate the effectiveness of foamed plastic aggregates as reservoir for internal curing water. Three prisms (40 mm x 40 mm x 160 mm) were tested for each composition and test (i.e. fixed the composition, three were used for the evaluation of the autogenous shrinkage and three for the total shrinkage). Specimens were provided of metal plugs at the extremities, according to EN 12617-4. Samples for autogenous shrinkage were wrapped in aluminum foil and covered with epoxy resin. All the samples were stored in a climatic chamber at constant temperature and relative humidity (20 °C and 50%, respectively). Length variations were measured each day for the first month and once a week for the remaining time, using a digital comparator. Dimensional variations were controlled for 120 days (4 months) approximatively.

II.9.4.5 Water vapor permeability

Water vapor permeability of lightweight mortar samples was determined according EN 1015-19 that defines a test method to determine water vapor permeability in steady-state conditions. Four flat cylindrical specimens (diameter of 75 mm and thickness of about 20 mm), conditioned at relative humidity of 50 % and 20 °C, were prepared for each lightweight mortar and sealed on glass containers, in which a saturated solution of KNO_3 was contained (Figure II.17). This solution, at 20°C, provides a relative humidity of 93.2%: the gradient of water vapor pressure between the lower part of the sample (RH = 93.2%) and the environment in which samples are stored (RH = 50 %) causes a water vapor flow through the mortar sample

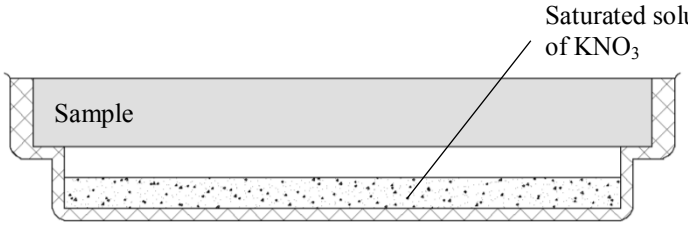

Figure II.17 *Water vapor permeability test, sample set-up*

Water vapor transmission rate (WVT) per surface unit represents the amount of water vapor flowing during the time through the sample surface and can be determined according eq. II.1:

$$WVT = \frac{\Delta G}{\Delta t \cdot A} \qquad \text{(II.21)}$$

where ΔG (kg) is the mass variation, Δt (s) is time interval and A (m^2) is the sample area.

Moreover, water vapor permeability (W_{vp}) can be calculated cosidering also a unit gradient of water vapor tension and sample thickness, according eq. II.2:

$$W_{vp} = \frac{s}{\frac{\Delta p}{WVT} - R_A} \quad \text{(II.22)}$$

where s is the sample thickness (m), Δp is the gradient of water vapor tension between saturated solution and samples storing chamber (Pa) and R_A is the resistance to water vapor diffusion in the air between the sample and the KNO_3 saturated solution ($0.048 \cdot 10^9$ Pa m^2 s/kg, for 10 mm of interspace). Finally, water vapor resistance factor (μ) is measured in comparison to the properties of air (eq. II.3):

$$\mu = \frac{\delta_A}{W_{vp}} \quad \text{(II.23)}$$

where δ_A is air permeability ($1.94 \cdot 10^{-10}$ kg/Pa m s) in test conditions (20 °C and 50% RH).

Chapter III
Chemically modified fibers: characterization and use into a cementitious mortar

III.1 Fibers characterization

Fibers surface chemical modification could affect not only the interaction between fibers and the cementitious matrix, but also fibers physical and mechanical properties. To this extent, before the use of chemically modified fibers, their properties were investigated.

III.1.1 Fibers physical and mechanical properties

As reported in Table III.1, chemical treatments were not influent on fibers radius while the sol-gel deposition slightly affects fibers density. For PP T2 a negligible increase of density, ρ, (from 0.91 to 0.93 g/cm^3) is recognizable.

Table III.1 *Nomenclature, density (ρ) and radius (r) of fibers (Coppola et al. 2015)*

Fiber	Chemical treatment	ρ (g/cm^3)	r (mm)
PP	-	0.91	0.38
PP T1	Alkalyne hydrolysis	0.91	0.38
PP T2	Sol-Gel process	0.93	0.38

It is important to verify that chemical treatments have no negative influence on fibers mechanical properties, before to use chemically treated fibers as reinforcing phase into a cementitious composite. As reported in Table III.2, tensile strength of fibers was not affected by chemical treatments

while a low decrease of strain at failure (about 15 %) for PP T1 fibers was recognizable. The slight decrease of ductility is due to material removal from PP T1 fibers surface during alkaline hydrolysis (Figure III.1). A small increase of elastic modulus (about 15 %) was measured for both chemically treated fibers, probably due to an increase of crystallinity resulting from fibers exposure to high temperatures during chemical treatments.

Thus, it is possible to assess that chemical treatments have no significant influence on fibers mechanical properties.

Table III.2 *Fiber mechanical properties: modulus (E), stress at break (σ_b), elongation at break (ε_b) (Coppola et al. 2015)*

Fiber	E (MPa)	σ_b (MPa)	ε_b (%)
PP	895	39	1345
PP T1	1036	45	1173
PP T2	1082	37	1330

III.1.2 Fibers morphology

Fiber surface texture and its chemical affinity with the cement paste are the key parameters to have a good fiber/cementitious matrix bond. Figure III.1a shows the smooth surface of a non-treated PP fiber while Figure III.1b reports the effects of the alkaline hydrolysis. The high aggressiveness of this treatment results in the subtraction of fiber surface portions (Figure III.1b). The presence of superficial cavities leads to an improvement of the fiber/matrix interactions, thanks to the offered interlocking positions for the cement paste. Whit regard to the sol-gel treatment, Figure III.2a shows the distribution of nano-silica particles, which appear as a powder and is well recognizable also at naked eye, on the fiber surface; at higher magnification (Figure III.2b) the spherical shape and low diameter dispersion (with a mean value of 300 nm) of particles is evident.

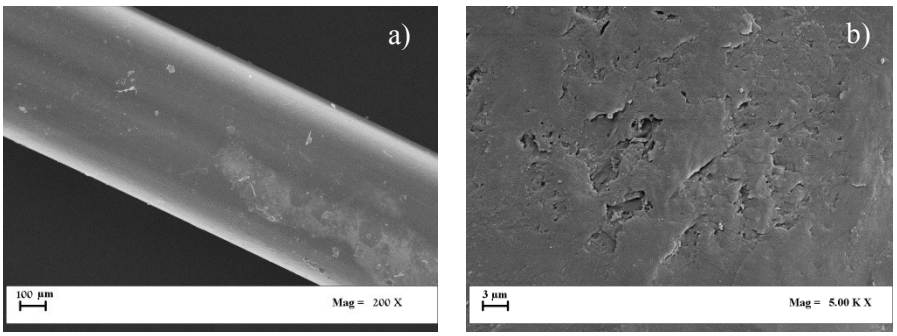

Figure III.1 *SEM micrographs of a) PP fiber and b) PP T1 fiber surface (Coppola et al. 2015)*

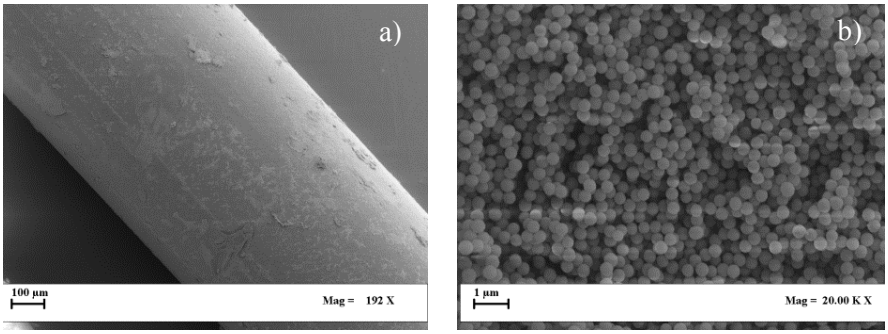

Figure III.2 *a) PP T2 fiber and b) nano-silica particles on fiber surface (Coppola et al. 2015)*

FTIR spectroscopy was performed on PP and PP T2 fibers and the obtained infrared spectra are reported in Figure III.3. The three main absorption peaks characteristic of silica groups appear at 1096 cm^{-1} (asymmetric vibration of Si-O), 948 cm^{-1} (asymmetric vibration of Si-OH) and 808 cm^{-1} (symmetric vibration of Si-O) (Innocenzi et al., 2003; Edrissi et al. 2011).

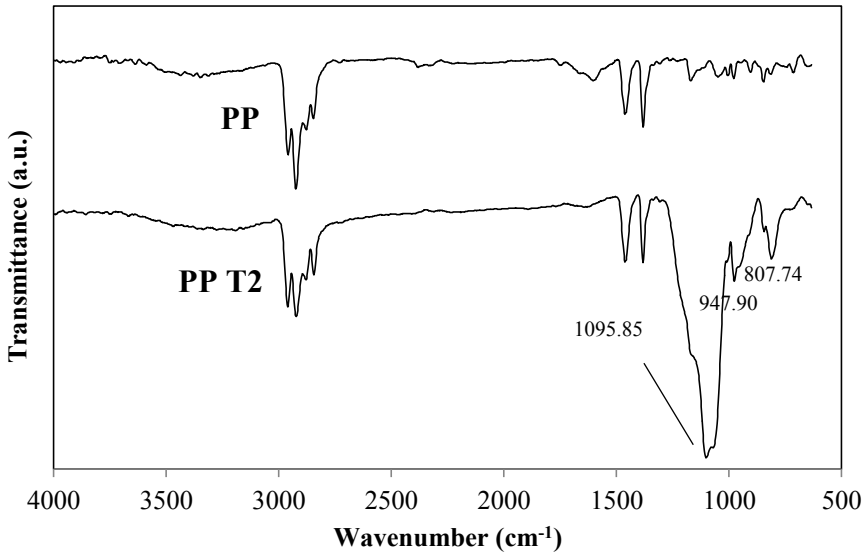

Figure III.3 *Infrared spectra of PP and PP T2 fiber in the 600-400 cm^{-1} wavelength range (Coppola et al. 2015)*

III.2 Fiber reinforced mortar characterization

III.2.1 Mechanical properties

In order to investigate the effects of fiber length (l_f), volume fraction (V_f) and chemical treatment on fiber reinforced mortars flexural strength, the different mortar samples were submitted to flexural tests. The nomenclature and composition of the investigated systems are reported in Table III.3, together with the values of the flexural strength R_f. The same R_f values are also reported in graph in Figure III.4, to better compare the flexural behaviour of the mixtures.

Table III.3 *Mixture nomenclature, composition and flexural strength (R_f) (Coppola et al. 2015)*

Mixture	Fiber	Fiber Length (mm)	V_f (%)	R_f (MPa)
Reference	-	-	-	7.09 ± 0.33
PP-FRMA15	PP	15	0.50	8.36 ± 0.70
PP-FRMB15			1.00	8.57 ± 0.86
PP-FRMA30		30	0.50	9.04 ± 0.16
PP-FRMB30			1.00	9.17 ± 0.08
PPT1-FRMA15	PP T1	15	0.50	7.69 ± 0.33
PPT1-FRMB15			1.00	9.45 ± 0.42
PPT1-FRMA30		30	0.50	9.52 ± 0.46
PPT1-FRMB30			1.00	9.56 ± 0.29
PPT2-FRMA15	PP T2	15	0.50	9.88 ± 0.24
PPT2-FRMB15			1.00	9.20 ± 0.54
PPT2-FRMA30		30	0.50	9.09 ± 0.70
PPT2-FRMB30			1.00	9.74 ± 0.77

As shown in Figure III.4, a general increase of flexural strength (R_f) over the reference sample was achieved. As expected, at increasing fiber volume fraction higher flexural strengths were obtained. On the contrary, fiber length was not particularly influent. As mentioned before, fiber chemical treatments improve fiber/matrix adhesion resulting in an increase of flexural strength for mix containing treated fibers compared to mix containing untreated fibers. Moreover, slight higher values of flexural strength were reported for mortars containing PP T2 fibers respect mixtures with PP T1 fibers. Thus, the presence of nano-silica particles on fibers surface strengthens fiber/matrix bond resulting in a better transmission of stresses between matrix and fibers.

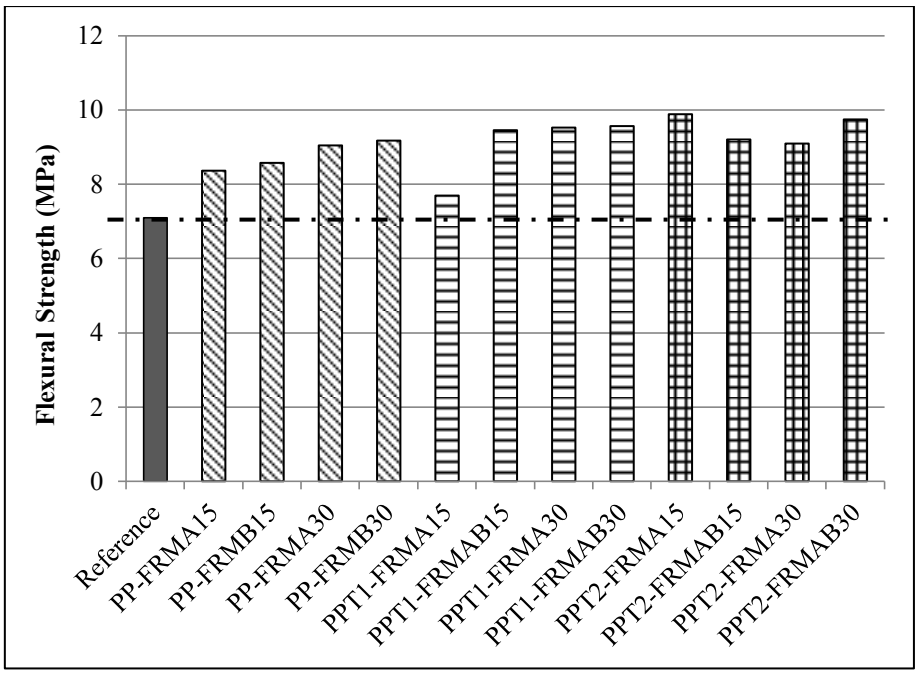

Figure III.4 *Comparison of fiber reinforced mortars flexural strengths (Coppola et al. 2015)*

III.2.2 Fiber/matrix interactions

III.2.2.1 Single fiber pull-out

Pull-out tests confirmed the weak interactions between untreated polypropylene fibers and the cementitious matrix: Figure III.5 shows the complete debonding of a smooth polypropylene fiber during the test. Figures III.6-8 report load vs. displacement curves recorded during pullout tests considering the three investigated embedded lengths: 10, 20 and 30 mm, respectively. The mechanism of fiber pullout consists in two different steps: first, fiber debonding and then fiber slipping. Thus, after the initial linear load/displacement relationship up to a peak load value (clearly recognizable in Figures III.6-8), two potential behaviours are possible: slip-softening and slip-hardening. In the first case, the complete fiber pullout takes places and friction influence is quite negligible; in the second case, after fiber debonding, the slipping resistance contribution is high.

In this case, at increasing fiber embedded length an increase of friction was achieved, resulting in a slip-hardening behavior, particularly evident for the embedment length of 20 and 30 mm. The slip-hardening behavior corresponds to an increase of pullout energy, i.e. the energy absorbed during pullout, that is the area under pullout curve.

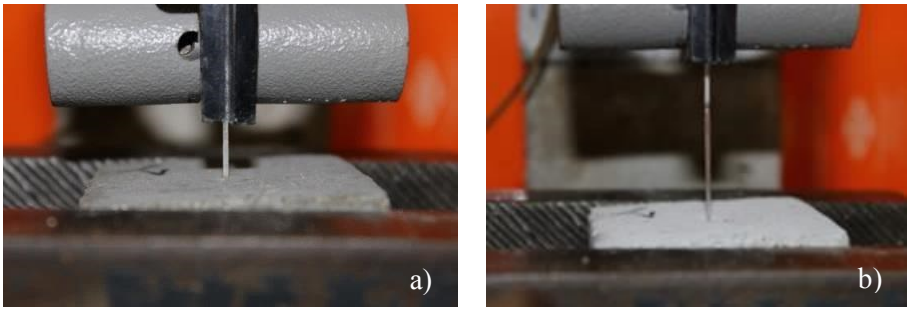

Figure III.5 *Pull-out setup and PP fiber debonding during the test (Coppola et al. 2015)*

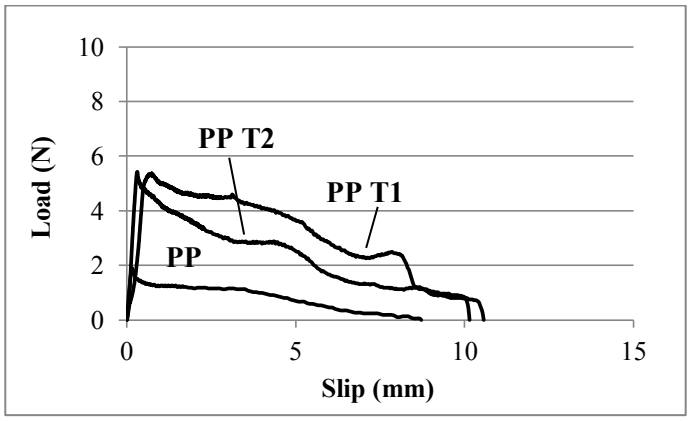

Figure III.6 *Pull-out curves for PP, PP T1 and PP T2 (embedment length 10 mm) (Coppola et al. 2015)*

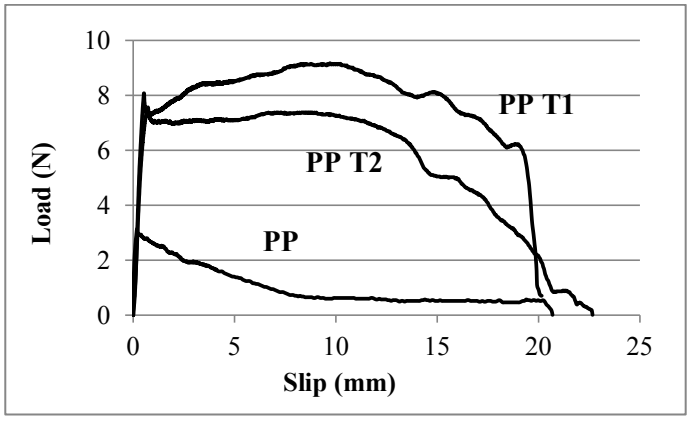

Figure III.7 *Pull-out curves for PP, PP T1 and PP T2 (embedment length 20 mm) (Coppola et al. 2015)*

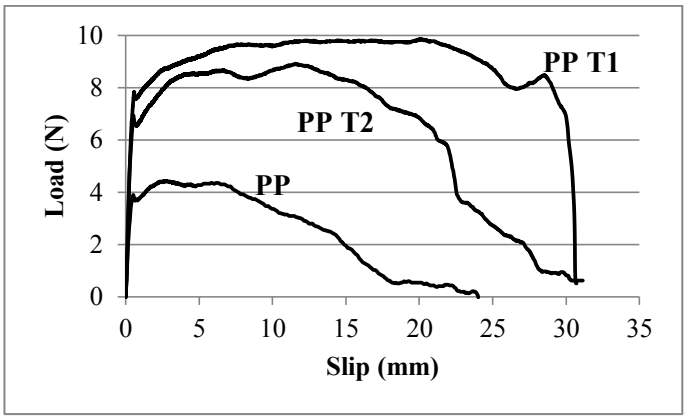

Figure III.8 *Pull-out curves for PP, PP T1 and PP T2 (embedment length 30 mm) (Coppola et al. 2015)*

The mean values of the pull-out peak load (F_{max}), i.e. the load after elastic behavior, obtained from the pull-out test, are reported in Table III.4. Both T1 and T2 lead to an increase of F_{max}, having slight higher values for fibers treated by alkaline hydrolysis. PP fibers show a slip-softening mode in the case of 10 and 20 mm while a slip-hardening behavior is recognizable in the case of 30 mm embedment length, thanks to the higher fiber abrasion during pull-out.

Table III.4 *Maximum pullout load varying fibers and embedded length (Coppola et al. 2015)*

Mix	Embedded length (mm)	F_{max} (N)
PP	10	1.92 ± 0.15
	20	3.57 ± 0.39
	30	3.93 ± 0.75
PP T1	10	5.34 ± 0.08
	20	7.40 ± 0.44
	30	7.54 ± 0.51
PP T2	10	4.91± 0.33
	20	6.19 ± 0.40
	30	6.67 ± 0.75

In order to better highlight the influence of fibers embedded length on the pull-out peak load, the data of Table III.4 are also plotted in Figure III.9. A sharp increase of load is recognizable from 10 to 20 mm (85, 39 and 26 % for PP, PP T1 and PP T2 fibers, respectively). On the contrary, a slight increase of pullout peak load was registered for 30 mm of embedment length. An explanation of this phenomena derives on what stated before: at

increasing fiber embedded length a greater friction during pullout is achieved.

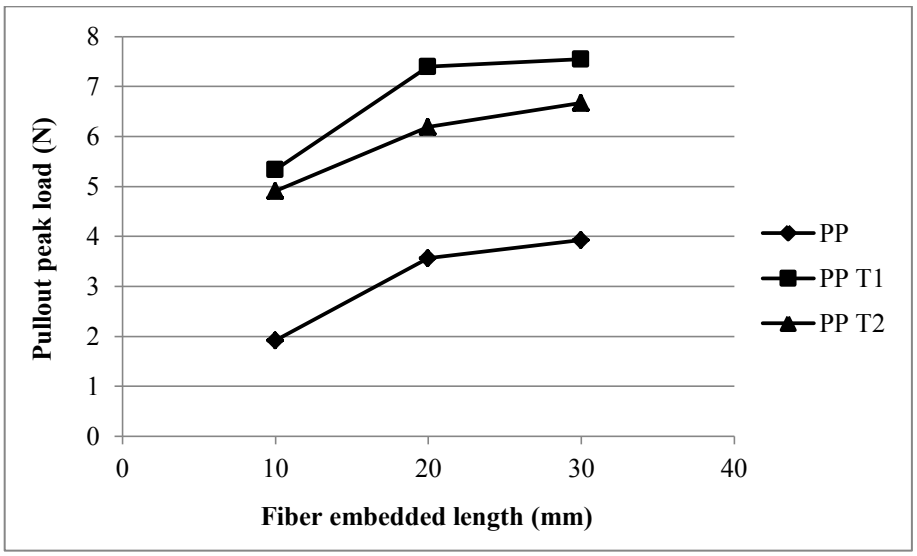

Figure III.9 *Maximum pullout load vs. embedment length (Coppola et al. 2015)*

III.2.2.2 Fiber/matrix ITZ investigations

SEM is a valid methodology to investigate fiber/matrix interactions and observe the ITZ. The different ways the fibers can interact with the cementitious matrix can be recognized from Figure III.10. The low wettability of pristine PP fibers (Figure III.10a) results in a poor adhesion with the cement paste and the formation of a high porous ITZ (Machovič et al., 2013). The presence of interlocking positions onto PP T1 fibers (Figure III.1b) contributes to have a less porous ITZ but fiber surface (as in the case of pristine PP fibers) shows a limited presence of hydration products (Figure III.10b). In the case of PP T2 fibers, not only a dense ITZ is recognizable but is evident also the high presence of hydration products on the fiber surface (Figure III.10c) due to the well-known chemical reactivity of silica particles into a cementitious matrix (Du et al., 2015; Jo et al., 2007).

On PP T2 fibers surface, at higher magnification, distinct rhombohedral shaped crystals of CaCO3 can be found in addition to the hydration products (Figure III.10d).

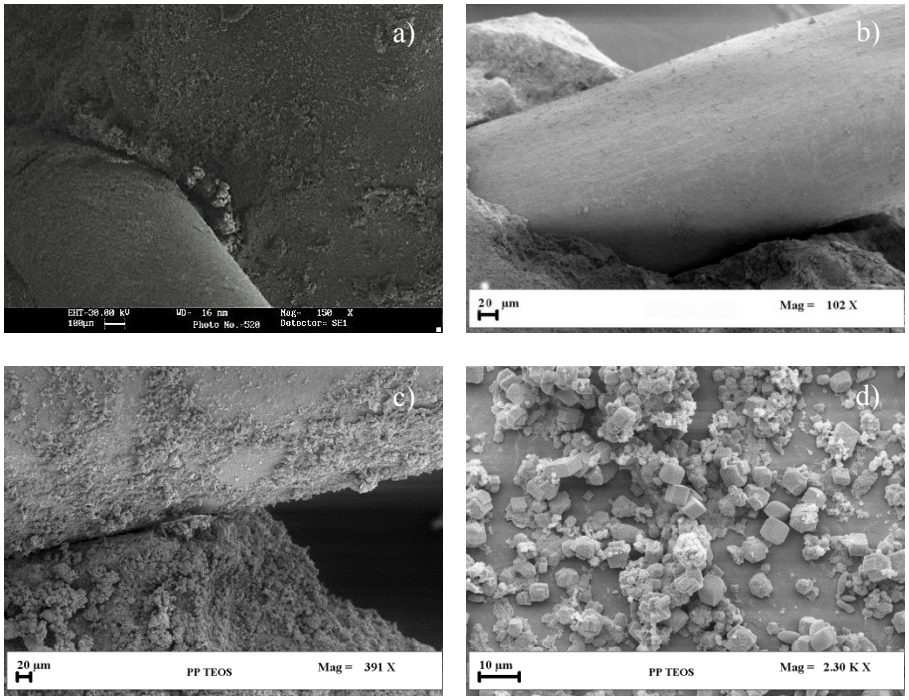

Figure III.10 *Fiber/matrix interfacial transition zone of: a) PP; b) PP T1 and c) PP T2, respectively; d) detail of hydration products and $CaCO_3$ (Coppola et al. 2015)*

III.3 Conclusions

The aim of the work discussed in this chapter was to improve the adhesion between polypropylene fibers and cementitious mortar modifying the chemical affinity by means of fibers surface chemical treatments. In fact, the poor wettability of PP fibers results in a weak bond with the cement paste and thus mechanical or chemical treatments are necessary to improve fiber bridging ability in stress transfer.

To this extent, two chemical treatments have been investigated: alkaline hydrolysis and nano-silica sol-gel particles deposition. SEM images revealed that alkaline hydrolysis increases fibers roughness while tensile tests reported a slight decrease of fibers ductility. On the contrary, sol-gel process produces nano-silica spheres particles on fibers surface and mechanical properties are not affected.

SEM pictures of ITZ reveal a poor adhesion between PP fibers and cement paste, a very porous ITZ and the absence of hydration products on fiber surface. Also for PP T1 fibers the surface is quite free of hydration products but the presence of interlocking positions contributes to have a less porous ITZ. In the case of PP T2 fibers, not only a denser ITZ was recognizable but also the high presence of hydration products on the fiber surface.

Pull-out tests confirmed the better performances of treated fibers: an higher pull-out peak load was achieved and an increase of pull-out energy was evident considering the slip-hardening behaviour showed by PP T1 and PP T2 fibers. Also bending tests report an increase of fiber reinforced mortar flexural strength over the unreinforced mortar. Slight higher values of flexural strength were reported for mortars containing PP T2 fibers respect mixes with PP T1 fibers.

Thus, the interesting results confirm the promising application of nano-silica treated fibers for improving fiber/matrix interactions. The presence of nano-silica particles not only reduces the ITZ porosity, as shown by SEM analysis, thus giving beneficial effects on mortar durability, but also improves the fiber/matrix bond increasing the stress transfer, i.e. the fiber reinforced mortar strength.

Chapter IV
Foamed fibers: characterization and use into a cementitious mortar

IV.1 Fibers characterization

IV.1.1 Fibers optimization and morphology

Foamed fibers are a new class of fibers in which a foaming agent is dry blended with polymer pellets before the extrusion process (as described previously § …) and then extruded with a traditional extruder. Since this process has never been investigated in literature before, its optimization was necessary to obtain a stable process but also to achieve an adequate surface texture. The aim was to produce foamed fibers having a rough surface, in order to increase fiber/matrix interactions. To this extent, foaming agent content and processing conditions were adapted (Table II.2) and the results are discussed as follows.

As evident from Table IV.1, fibers physical and mechanical properties are greatly affected both by processing parameters (capillary die, take-up speed, screw speed etc.) and foaming agent content. First of all, it was necessary to find the optimal foaming agent content, in order to obtain fibers with a rough surface. Using a capillary die of 2 mm, the higher foaming agent quantity the higher diameter (Table IV.1), as expected, due to the foamed strand swelling out of the extruder. Reducing the capillary die, was possible to obtain thinner fibers, but was necessary to modify processing parameters (§ II.2). Thus, the parameters that governed fibers optimization were fibers diameter and surface roughness, both investigated by SEM investigations.

As expected, elastic modulus of PP fibers (i.e. non-foamed fibers) is the highest one. It should be noticed that PP fibers used in comparison with foamed fibers are a further optimization (the aim was to have a lower diameter) of PP fibers used for chemical treatments. The addition of a low amount of foaming agent reduced fibers elastic modulus but increased

tensile strength and break at failure. The main reason is that PP fibers draw ratio (i.e. the ratio between take-up speed and extrusion speed) is higher than PP+0.5FA, resulting in more oriented fibers with higher elastic modulus but lower ductility (Table IV.1). To achieve a rougher surface, the foaming agent content was increased and, contextually, screw speed and take-up speed were decreased. Increasing the foaming agent loading, a higher quantity of gas was produced, due to its decomposition, resulting in higher diameters (Table IV.1). To overcome this drawback, it was decided to change the capillary die with a smaller one (from 2 mm to 0.5 mm). In this way, it was possible to obtain foamed fibers having a lower radius, but, at the same time, it was necessary to increase foaming agent content up to 5wt.%. Once that processing parameters were fixed for the virgin material, the foam extrusion process was performed also on the end-of-waste material. In this case, due to the material heterogeneity, a lower amount of foaming agent was necessary to obtain an adequate surface roughness.

Table IV.1 *Fibers physical and mechanical properties*

Fiber	r (mm)	P (%)	ρ (g/cm^3)	E (MPa)	σ_b (MPa)	ε_b (%)
PP	0.13	-	0.910	1007	26	813
PP+0.5FA	0.39	10	0.776	730	32	1139
PP+1FA	0.81	38	0.568	314	13	232
PP+2FA	0.84	16	0.709	327	19	816
PP+5FA	0.39	16	0.791	466	14	351
Recycled	0.22	-	0.883	250	11	283
Recycled+2FA	0.53	9	0.869	289	10	14

Concerning surface texture, non-foamed and foamed fibers with the lowest foaming agent content (PP and PP+0.5FA fiber, respectively) present a smooth surface (Figure IV.1). Increasing the foaming agent content, a greater amount of yielded gas tends to migrate on fibers external surface, achieving a rougher surface (Figure IV.2). Finally, both virgin foamed fibers (PP+5FA), with the required radius, and end-of-waste foamed fibers (Recycled+2FA), with a slightly higher radius, show an optimal surface roughness (Figure IV.3).

A more irregular surface is responsible of better fiber/matrix interactions, offering interlocking position for the cement paste. Moreover, fibers porosity and mechanical properties are strictly dependent on the different cell morphology, as discussed in the following.

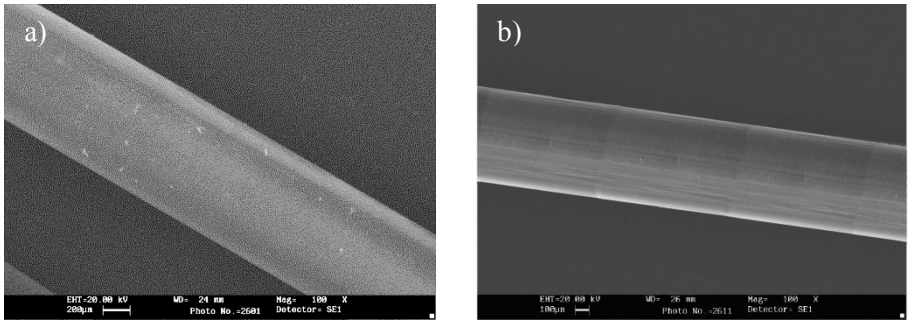

Figure IV.1 *Surface of virgin fibers and foamed virgin fibers with 0.5 wt.% of foaming agent*

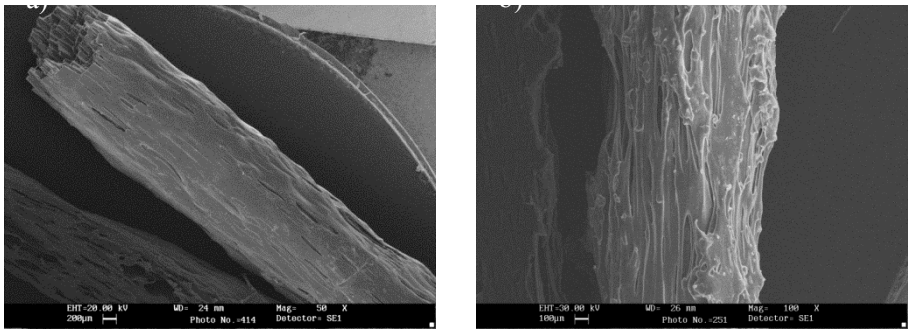

Figure IV.2 *Surface of virgin foamed fibers with 1 and 2 wt.% of foaming agent, respectively*

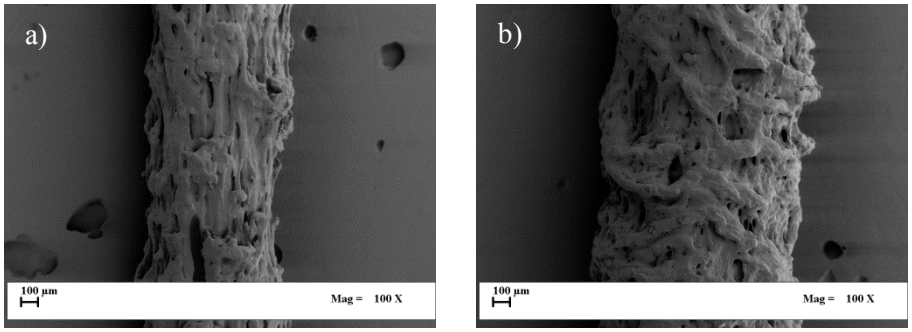

Figure IV.3 *Surface of a) virgin and b) end-of-waste foamed (with 5 and 2wt.% of foaming agent, respectively) fibers*

Also fibers internal morphology is influenced by the foam extrusion process and foaming agent content. Fibers cross section was evaluated on cryogenically broken fibers by SEM images. Non-foamed fibers have a solid circular cross-section without any pores (Figure IV.4a). A low addition of foaming agent (0.5wt.%) leads to the formation of an internal porosity, with bigger pores in the fibers core (Figure IV.4b). Such pores distribution is due to the temperature profile of the extruded filament: the temperature in the fibers core is higher than the strands surface one. Higher temperatures, in the inner part of the extruded filament, allow bubbles growth in the polymer melt while in more external fibers zones (i.e. at lower temperature) bubbles achieve the stabilization phase more rapidly. PP+1FA and PP+2FA fibers contain more voids, as clearly visible in Figure IV.5a and Figure IV.5b, respectively. Moreover, PP+1FA fibers show bigger cells than PP+2FA fibers that have more voids but with a smaller average area.

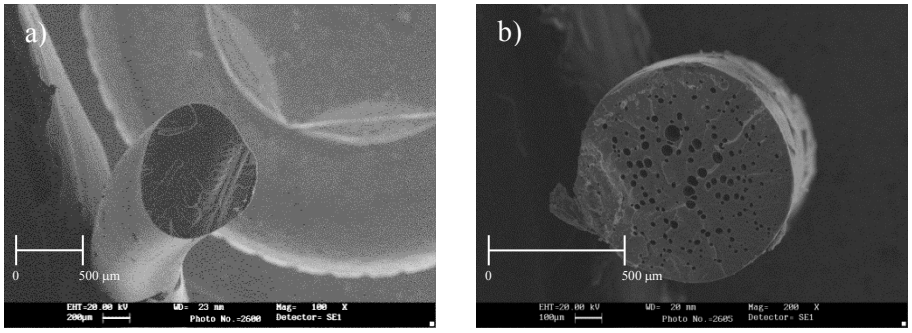

Figure IV.4 *Cross section of virgin fibers and foamed virgin fibers with 0.5 wt.% of foaming agent*

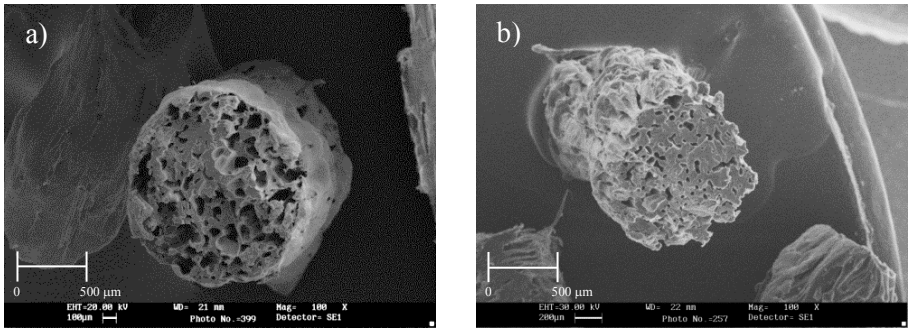

Figure IV.5 *Cross section of virgin foamed fibers with 1 and 2 wt.% of foaming agent, respectively*

Increasing the foaming agent content and changing the capillary die, internal porosity changed again (Figure IV.6a). Large pores are present in the PP+5FA fibers cross section and a very high surface porosity is also recognizable. End-of-waste foamed fibers (Figure IV.6b) present smaller pores and a more regular rough surface.

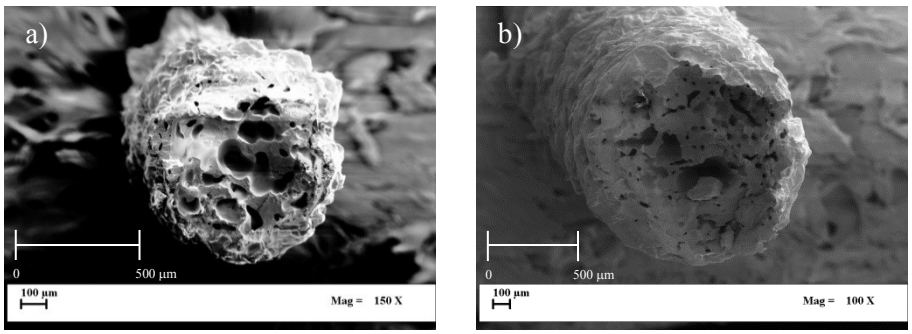

Figure IV.6 *Cross section of a) virgin and b) end-of-waste foamed (with 5 and 2wt.% of foaming agent, respectively) fibers*

IV.1.2 Fibers profile roughness

A further analysis of fibers profile was carried out using images taken with a digital camera (Figure IV.7). A roughness coefficient could be defined in terms of profile linear roughness ratio, R_l, that is the ratio between the length of the profile line, L, and the projected length of the profile line, L_0:

$$R_I = \frac{L}{L_0} \qquad \text{(IV.1)}$$

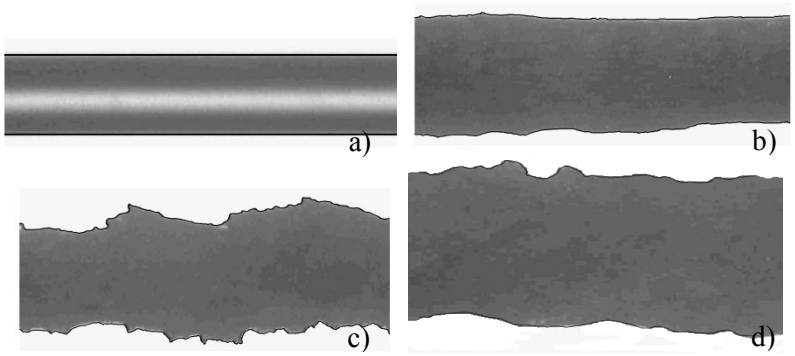

Figure IV.7 *Profile roughness of a) PP, b) PP+1FA, c) PP+2FA and d) Recycled+2FA fibers, respectively*

As evident from the images (Figure IV.7), a relevant increase of surface roughness was achieved. In particular, the increase of R_I, respect PP smooth fibers, was 1, 16, 15 and 7%, for PP+1FA, PP+2FA, PP+5FA and Recycled+2FA fibers, respectively.

IV.1.3 Fibers density

Fibers density and porosity are strictly correlated to what previously observed in terms of internal morphology (pores dimension, distribution and numbers). In general, fibers internal porosity leads to a density decrease (Table IV.1).

In particular, for PP fibers, at increasing foaming agent content, a progressive porosity increase was observed, corresponding to a linear density decrease (Figure IV.8). A maximum of porosity is reached for PP+1FA fibers (38 %) while further increasing the foaming agent content a sharp decrease of porosity was obtained and, consequently, also fibers density increased again. Moreover, for fibers with the 5wt.% of foaming agent (i.e. PP+5FA), porosity and density are the same as PP+2FA fibers (Table IV.1).

In the case of end-of-waste fibers, due to the relative low porosity (9 %), a very slight decrease of porosity was measured (1.6 %) respect non-foamed end-of-waste fibers.

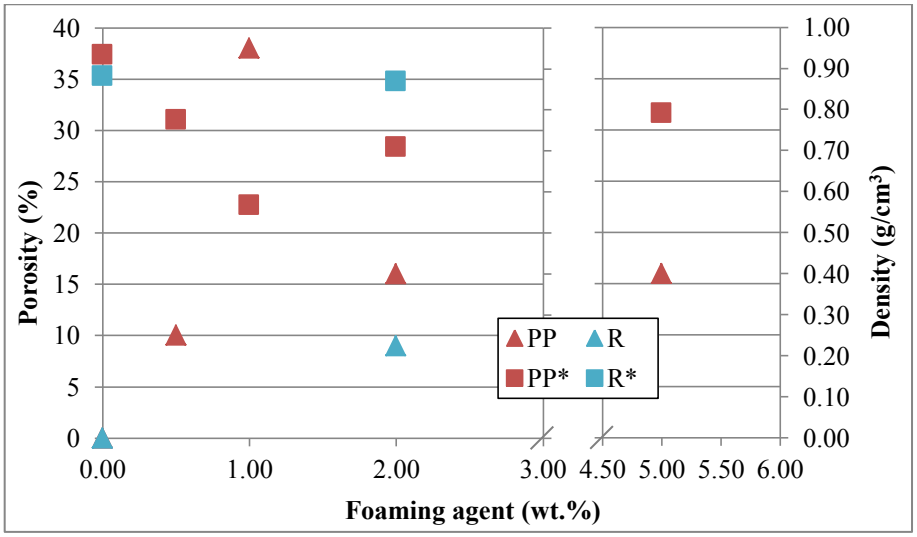

Figure IV.8 *Fibers density (□) and porosity (△) for the investigated samples at different foaming agent content*

IV.1.4 Fibers mechanical properties

Fibers mechanical properties, in particular tensile properties, are greatly affected by internal and external morphology. As a matter of fact, the foaming process leads to a decrease of elastic modulus, tensile strength and ductility except for recycled fibers (Table IV.1).

As stated before, PP+0.5FA fibers report a lower elastic modulus but an increase of ductility. Considering the different processing conditions and the different internal morphology, the increase of ductility can be explained not only by the different drawing but also by the ability of cells to deform themselves before rupture promoting the drawing of the cell walls.

The influence of porosity and cells structure is evident for PP+1FA and PP+2FA fibers where in both cases a sharp reduction of elastic modulus was observed. PP+2FA fibers are more ductile thanks to a lower porosity and a different orientation of the voids. As clear in Figure IV.9a, PP+1FA fibers cells are oriented in the flow direction and during the tensile test cells walls are broken easier. On the contrary, PP+2FA fibers have a different longitudinal section: cells are not aligned in the flow direction and pores walls are thicker (Figure IV.9b).

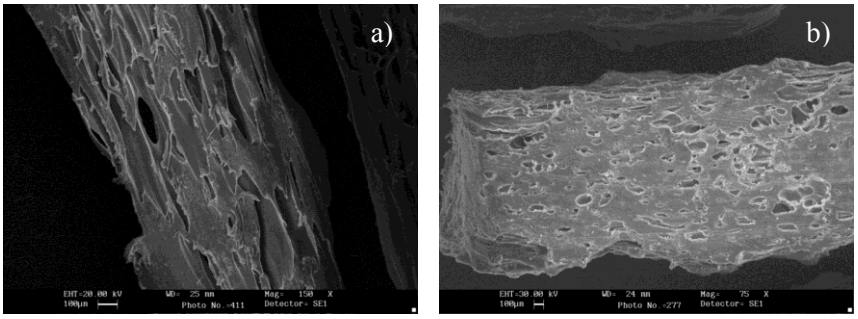

Figure IV.9 *Longitudinal section of PP+1FA and PP+2FA fibers, respectively*

Non-foamed end-of-waste fibers have very low mechanical properties compared to non-foamed fibers produced with virgin material. As previously discussed, recycled fibers are made of a polyolefin mix, in particular PP and PE. Since the incompatibility of these two polymers, in Figure IV.10 PP droplets in a continuous PE matrix are recognizable. These incompatibility represents the main reason for the unsatisfactory mechanical properties of these recycled mixed plastics.

Comparing non-foamed and foamed recycled fibers, thanks to a better dispersion of PP phase into PE ones promoted by the foaming process, a slight increase of elastic modulus was observed. On the contrary, a dramatically decrease of ductility was achieved. SEM micrographs obtained on cryogenically fractured fibers show the widespread presence of micro-

pores (Figure IV.10) with very thin walls. Such morphology combined to the incompatibility of the two polymers is responsible of fibers mechanical behavior.

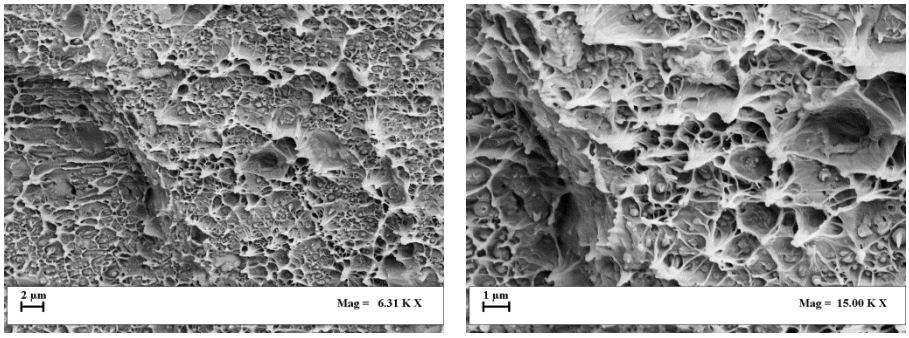

Figure IV.10 *SEM micrographs showing Recycled fibers foamed structure and PP droplets into PE matrix (Coppola et al. 2016)*

IV.1.5 Fiber intrinsic efficiency ratio (FIER)

Generally, for fibers with circular, square or rectangular geometry a paramount parameter is the aspect ratio, that is the ratio between fibers length and diameter (or equivalent diameter for non-circular fibers). However, for fibers with irregular section profile the definition of an equivalent diameter should be not suitable for expressing the improved fiber/matrix mechanical interactions. Thus, a parameter that contains the ratio of perimeter to cross sectional area could better explain the improved roughness of the fiber cross section. Antoine Naaman (Naaman, 2003) proposed a simple way to characterize the influence of the perimeter/area ratio by a variable defined as the Fiber Intrinsic Efficiency Ratio (FIER):

$$\mathrm{FIER} = \frac{\omega L}{A} \qquad \text{(IV.1)}$$

where ω is the fiber cross section perimeter (m), L is the fiber length (m) and A is the cross section area (m^2).

Considering the eq. IV.1, it was possible to determine the FIER for the investigated foamed fibers (Table IV.2). Moreover, to measure the efficiency of each foamed fiber profile, the variation of FIER respect to a smooth circular fiber was determined. As example, in Figure IV.11 are reported a PP+2FA fiber cross section and a circular fiber with the same cross section area. It is worth to mention that a higher surface roughness (i.e. a bigger perimeter) assures a higher interfacial area, that means an improved fiber/matrix adhesion

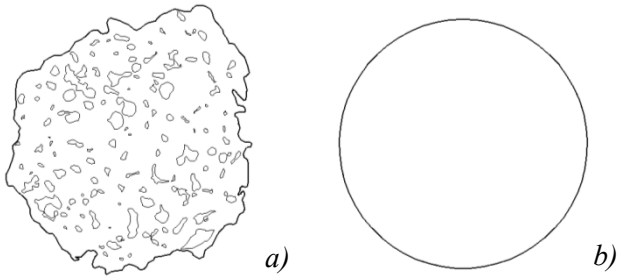

Figure IV.11 *a) PP+2FA fiber and b) circular fiber having the same cross section area*

The highest increase of the FIER parameter was measured for PP+2FA fibers (+ 58 % compared to a circular fiber with the same cross section area), but the diameter of these fibers was still too high. Varying processing parameters, capillary die and foaming agent content PP+5FA fibers were produced and these fibers have a FIER parameter +14 % higher than circular smooth fibers (Table IV.2). Comparing PP+5FA and Recycled+2FA fibers, the latter have a more irregular surface while the former present a regular order in the surface roughness. The reason of the different diameter and surface texture, lies in the processing parameters. In order to have an adequate surface roughness, take-up speed was slightly lower in the case of recycled fibers (Table II.2). As consequence of the different take-up speed, Recycled+2FA fibers diameter was higher and more gases move toward fibers surface, resulting in a more irregular texture.

Clearly, FIER and $FIER_{cf}$ are the same for circular fibers, thus ΔFIER is equal to zero.

Table IV.2 *Fiber Intrinsic Efficiency Ratio (FIER) and relative FIER variation of the investigated fibers*

Fiber	FIER	$FIER_{cf}$*	ΔFIER (%)°
PP+1FA	0.0032	0.0029	10
PP+2FA	0.0046	0.0029	58
PP+5FA	0.0065	0.0057	14
Recycled+2FA	0.0043	0.0034	26

* $FIER_{cf}$ is the FIER of a circular fiber with a cross section area equal to the foamed fiber area;

° ΔFIER is the increase of foamed fibers FIER respect to the $FIER_{cf}$.

IV.2 Fiber reinforced mortar characterization

Once that the optimization of fibers surface texture and diameters was done, foamed and non-foamed fibers were used into a cementitious mortar. Rheological, mechanical and durability properties of the fiber reinforced mortar were investigated in order to study the influence of fibers addition. Moreover, due to the different surface roughness, both the interfacial transition zone (ITZ) and pull-out resistance were studied.

IV.2.1 Rheological properties

The rheological behavior of cementitious materials is particular decisive in terms of their workability, which is usually characterized by means of performing slump and/or spread tests. These tests, however, only address a limited regime of shear rates, i.e. very low ones. Few investigations have focused at higher shear rates. Such rates can be attained in rheometers and may allow for characterizing the impact of admixtures, fine particles or fibers, by means of measuring the torque upon mixing. Fibers parameters (i.e. volume fraction, diameter, length, stiffness etc.) greatly affect cementitious materials workability. To this extent, flow table tests and rheological tests using a rheometer were performed.

IV.2.1.1 Flow table test

Considering the spreading of the mortar on the table, consistency of fiber reinforced and reference samples was measured (according to the procedure described previously, § II.7.1.2). All the mixtures were prepared with a w/c ratio of 0.5 and a sand/binder ratio of 3, according to EN 196-1. The investigated samples nomenclature, fiber length and content are reported in Table IV.3. Rheological properties of mortars containing only PP and PP+5FA fibers were studied after that some preliminary results led to effects very similar to their corresponding end-of-waste fibers (Recycled and Recycled+2FA, respectively).

In general, fibers addition leads to an overall workability decrease, more pronounced for non-foamed fibers (Figure IV.14). In order to better understand fibers influence, some pictures of the flow table test are reported for comparison (Figures IV.12-13). The reference mortar (i.e. without fibers) is reported in Figure IV.12a.

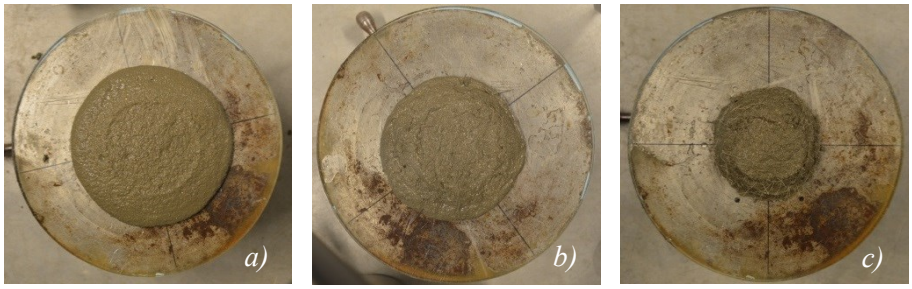

Figure IV.12 *Spreading on the table of the (a) reference, (b) FPP-FRMC30 and (c) PP-FRMC30 samples, respectively*

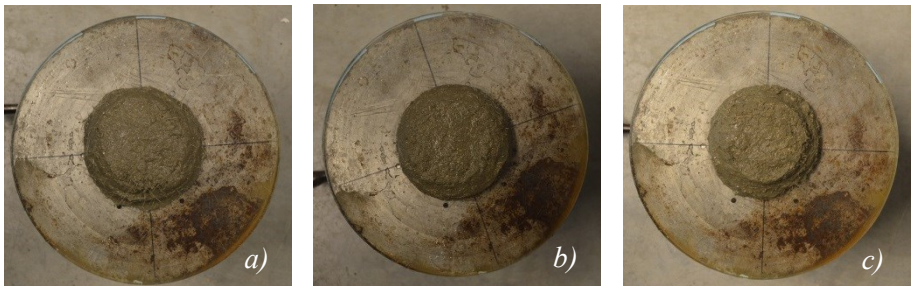

Figure IV.13 *Spreading on the table of the (a) PP-FRMB30, (b) FPP-FRMC15 and (c) PP-FRMC15 samples, respectively*

As expected, at increasing fibers volume fraction, a decrease of consistency was obtained (Figure IV.14). Mortars reinforced with foamed fibers reported always a higher consistency, compared to mortars reinforced with non-foamed fibers, at fixed volume fraction. Foamed fibers lower density and higher diameter result in a lower amount of fibers, at fixed volume fraction, respect non-foamed fibers (Figure IV.21) producing a more workable mortar.

Moreover, longer fibers influence differently mortar consistency: PP-FRMC15 mortar has a slight higher consistency respect to PP-FRMC30; on the contrary, FPP-FRMC15 mortar has a lower consistency than FPP-FRMC30. PP fibers are more flexible than FPP ones and easily weave together to form fibers bundles; such drawback is more pronounced for longer fibers.

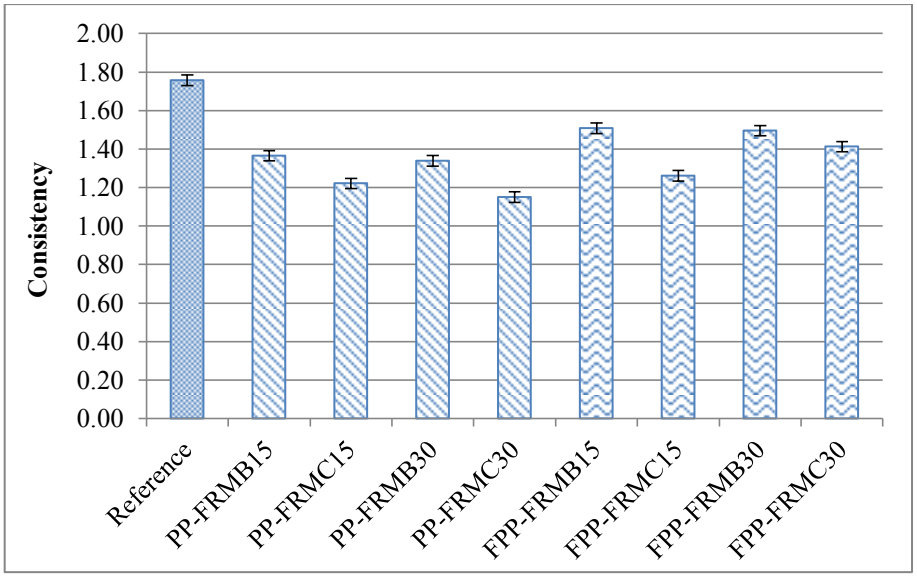

Figure IV.14 *Consistency of the reference and fiber reinforced investigated samples*

IV.2.1.2 Rheometer (RheoCAD)

For this test, only preliminary results are reported because other tests are in course, in order to ensure reproducibility. Flow curves were obtained according the procedure described in § II.7.1.3. An example of flow curve is reported in Figure IV.15.

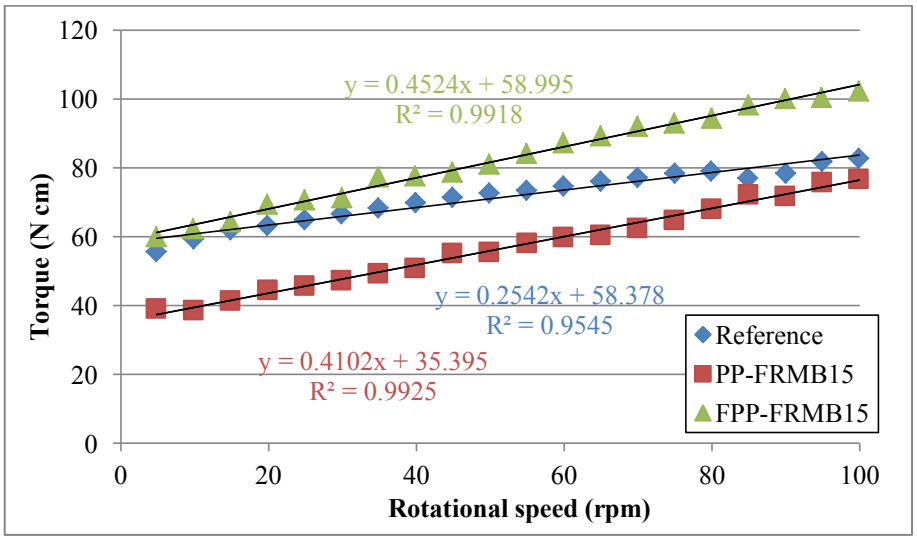

Figure IV.15 *Flow curve (torque vs. rotational speed) of Reference mortar and mortars reinforced with 1% of PP and FPP fibers 15 mm length*

As evident, data are well interpolated by the simple model of Bingham. Moreover, according to eq. II.12, the slope of the flow curve is proportional to plastic viscosity and the constant term is proportional to yield stress. As expected, plastic viscosity of the reference mortar is lower than plastic viscosity of the fiber reinforced samples. The torque is proportional to the shear stress and the necessary torque to activate the rotation is proportional to the yield stress. In the case of PP-FRMB15 a lower yield stress was measured compared to the reference mortar and FPP-FRMB15. Due to the high amount of fibers in FPP-FRMB15 thus a relevant fiber/aggregates/matrix interaction, a lower torque was necessary to activate the movement of the mortar in the rheometer

The influence of fibers on the thixotropic behavior was assessed measuring the torque at a fixed rpm. As evident in Figure IV.16, torque reduction for the Reference mortar (i.e. without fibers) is more pronounced than the torque of PP-FRMB15 fiber reinforced mortar.

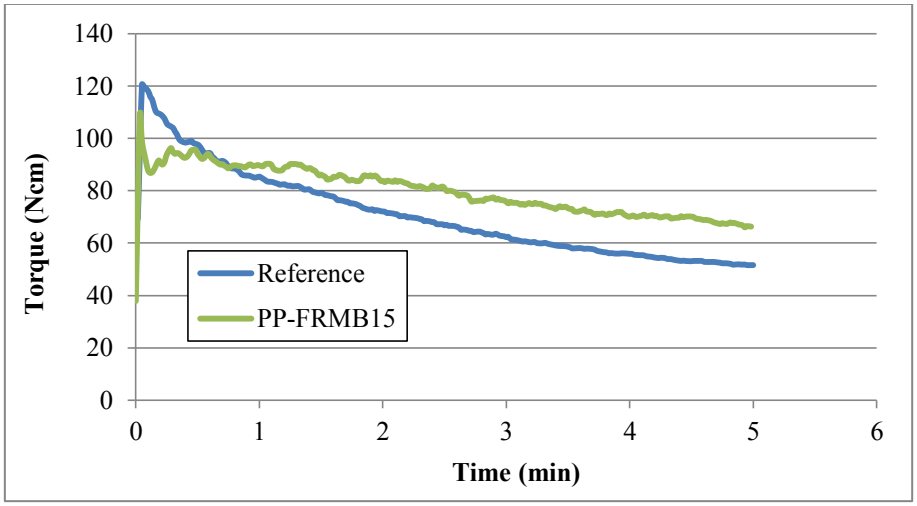

Figure IV.16 *Torque variation at constant rpm*

Further analysis are ongoing in order to study the influence of fibers length and volume fraction.

IV.2.2 Mechanical properties

To determine flexural strength, 25 mixtures were prepared and tested (1 as reference, i.e. without fibers, and 24 fiber reinforced), according the procedure described in § II.7.2.1. Nomenclature of the tested samples is reported in Table IV.3.

Table IV.3 *Investigated compositions: nomenclature, fibers length and volume fractions*

Name	Fiber	Fiber length (mm)	Fiber volume fraction (%)°
Reference	-	-	-
PP-FRMA15	PP	*15*	*0.50*
PP-FRMB15	PP	*15*	*1.00*
PP-FRMC15	PP	*15*	*2.00*
PP-FRMA30	PP	*30*	*0.50*
PP-FRMB30	PP	*30*	*1.00*
PP-FRMC30	PP	*30*	*2.00*
FPP-FRMA15	PP+5FA	*15*	*0.50*
FPP-FRMB15	PP+5FA	*15*	*1.00*
FPP-FRMC15	PP+5FA	*15*	*2.00*
FPP-FRMA30	PP+5FA	*30*	*0.50*
FPP-FRMB30	PP+5FA	*30*	*1.00*
FPP-FRMC30	PP+5FA	*30*	*2.00*
R-FRMA15	R	*15*	*0.50*
R-FRMB15	R	*15*	*1.00*
R-FRMC15	R	*15*	*2.00*
R-FRMA30	R	*30*	*0.50*
R-FRMB30	R	*30*	*1.00*
R-FRMC30	R	*30*	*2.00*
FR-FRMA15	R+2FA	*15*	*0.50*
FR-FRMB15	R+2FA	*15*	*1.00*
FR-FRMC15	R+2FA	*15*	*2.00*
FR-FRMA30	R+2FA	*30*	*0.50*
FR-FRMB30	R+2FA	*30*	*1.00*
FR-FRMC30	R+2FA	*30*	*2.00*

IV.2.2.1 Flexural strength

Taking into account the non-structural use of the investigated fibers, flexural strength was investigated to highlight if fibers addition and the different fibers morphology can affect mechanical properties.

In general, flexural strength is not influenced by fibers addition and the average value is 6.76 ± 0.32 MPa. As example, flexural strength of PP-FRXY (X is fibers volume fraction and Y fibers length) samples are reported in Figure IV.17. Considering the relative low elastic modulus of the investigated synthetic fibers (both foamed and non-foamed) no increase of flexural strength was expected.

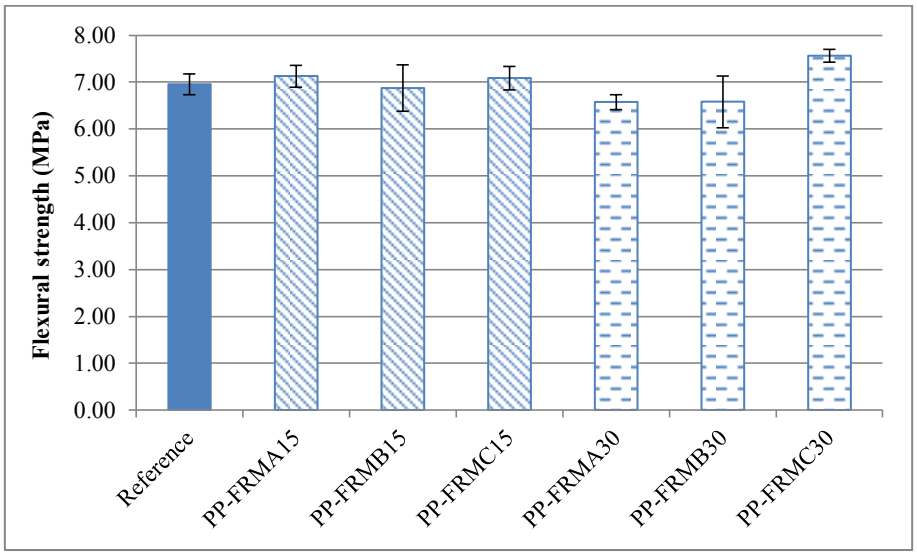

Figure IV.17 *Flexural strength of mortars reinforced with PP fibers*

On the contrary, post-cracking behavior was greatly influenced by fibers addition as the presence of a post-cracking branch was clearly recognizable. In Figure IV.18 the load/deflection curves of fiber reinforced mortar samples, at fixed fibers volume fraction (i.e. 2 %), are reported as example. Residual strength of mortars reinforced with PP fibers is higher than that of mortars containing Recycled fibers because former fibers have higher elastic modulus and tensile strength than the latter. In Figure IV.18 is also clear that longer fibers give rise to higher residual strength than shorter ones, for mortars reinforced with PP fibers. Fibers mechanical properties affect samples residual strength because after cracking fibers tensile properties are involved in the load transmission. Moreover, fiber/matrix adhesion is of widespread importance in the fibers bridging across cracks.

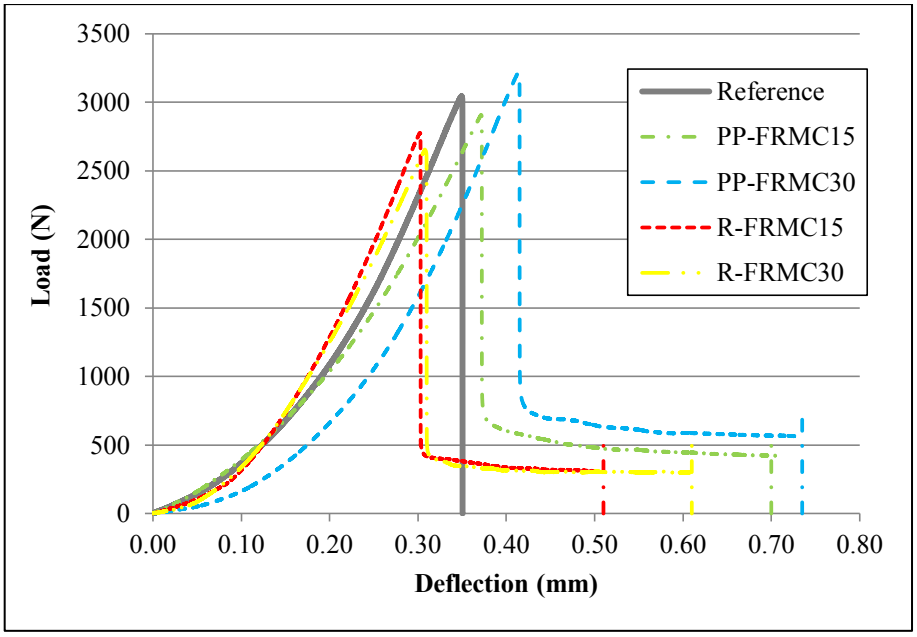

Figure IV.18 *Example of load/deflection curve at fixed volume fraction (2.0 %) varying fibers length (15 and 30 mm, respectively)*

In order to investigate the influence of fibers length, material, volume fraction and morphology on post-cracking behavior, residual strengths of the studied samples are compared in Figures IV.19-20.

Cementitious materials have a low tensile strength resulting in a brittle failure. As consequence, the reference mortar reports no residual strength after cracking. On the contrary, at increasing fibers volume fraction, an increase of residual strength was obtained. As expected, mortars containing 2% of fibers have the higher residual strength. In general, PP fibers (both foamed and non-foamed) give rise to higher residual strength, due to the higher mechanical properties of fibers. Moreover, mortars reinforced with foamed fibers have always better performances except for PP-FRMC30 where the high amount of non-foamed fibers prevail on the improved adhesion. Thus, despite the lower amount of fibers in the cross section and fibers mechanical properties, the improved fiber/matrix interaction allowed better load transfers. In the case of FPP-FRMA30 probably the very low quantity of fibers was not able to give a residual strength. Furthermore, is clear that longer fibers are more efficient than shorter ones.

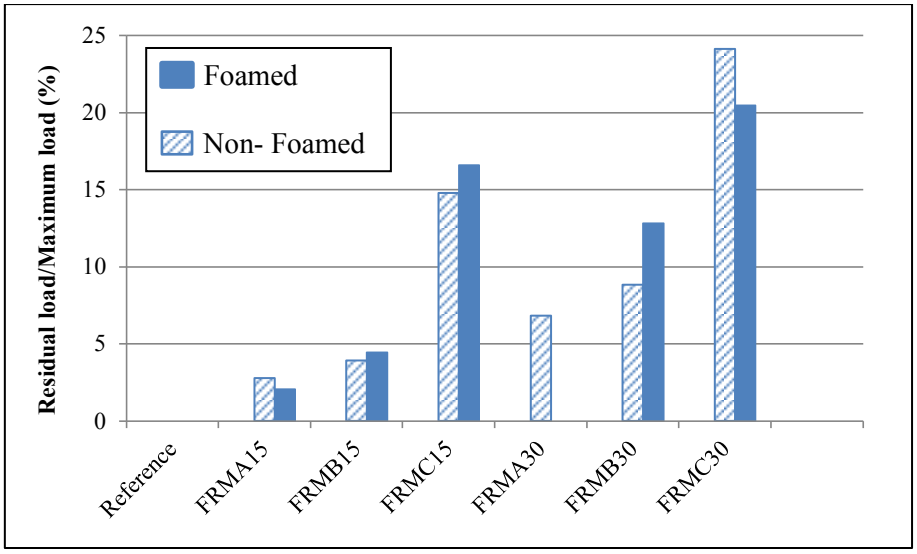

Figure IV.19 *Ratio between residual strength and maximum load of mortar samples reinforced with foamed and non-foamed PP fibers*

Regarding the use of end-of-waste foamed fibers, due to their very low mechanical properties, mortars reinforced with such fibers present approximatively the same residual strength, independently from fibers length and volume fraction. In particular, the main drawback is fibers very low elongation at break.

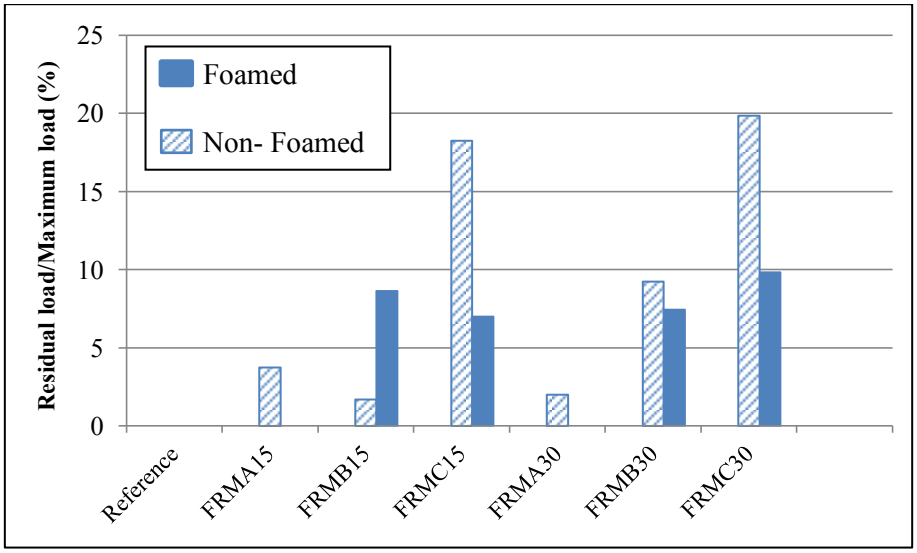

Figure IV.20 *Ratio between residual strength and maximum load of mortar samples reinforced with foamed and non-foamed Recycled fibers*

As stated previously, concerning fiber reinforced mortar workability, due to the different density and diameter of the investigated fibers, at fixed fiber volume fraction the amount of fibers to be used is dramatically different using foamed and non-foamed fibers. In Figure IV.21 are reported, as examples, the fibers used to produce PP-FMC15 (Figure IV.21a) and FPP-FRMC15 (Figure IV.21b), respectively. As clear, at fixed fibers length and volume fraction, the quantity of fibers to be used is considerably different. The significant lower amount of foamed fibers gives rise to more workable mortars and improved post-cracking behavior, as showed for FPP-FRMs. PP+5FA fibers diameter is 3 times higher than PP fibers one, as reported in Table IV.1.

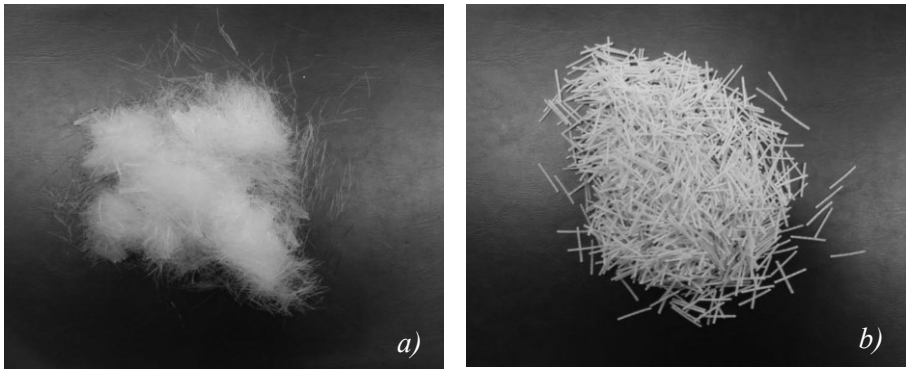

Figure IV.21 *Fibers amount for the production of a) PP-FRMC15 and b) FPP-FRMC15*

To further confirm what previously stated, after flexural tests, polished cross sections were observed by an optical microscope to investigate fibers dispersion and quantity in mortar samples. As expected, the ratio between fibers area and specimen cross section is approximatively corresponding to the fibers volume fraction. At fixed volume fraction and fibers length (2% and 15 mm, respectively), a quantity of fibers lower than 85 % is observed for mortars containing foamed fibers (Figure IV.22). Such important difference contributed for the obtainment of a better workability while on post-cracking behavior were determinant fibers mechanical properties.

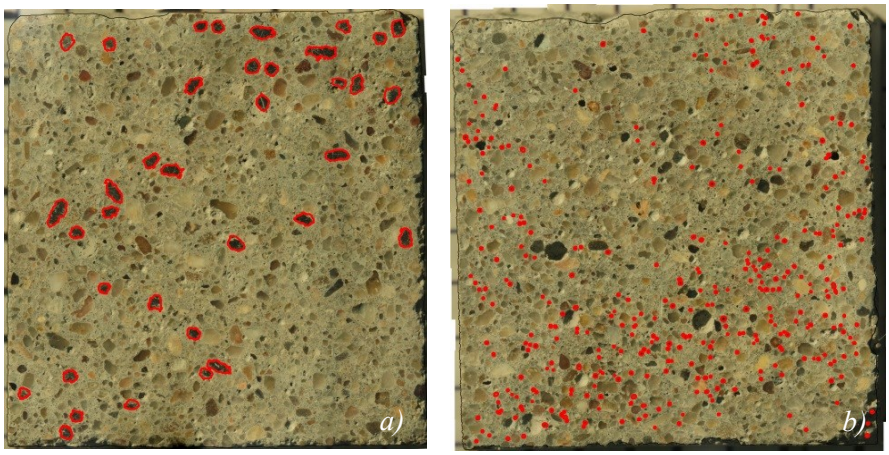

Figure IV.22 *Fibers quantity in a) FR-FRMC15 and b) PP-FRMC15 polished cross sections after flexural test*

IV.2.2.2 Compressive strength

Also for compressive strength, as for the flexural one, any meaningful influence of fibers (both foamed and non-foamed) was observed on it and the average value is 70.12 ± 4.47 MPa.

A slight decrease (8-10 %) was observed only for mortars containing high fibers volume fraction (2 %) and longer fibers (30 mm). These results are mainly explained considering the reduced workability, resulting in a worse compaction and thus an increased porosity, as reported in the following.

On the contrary, the fibers presence is very important for the compression failure mode (Figure IV.23). For the reference mortar, the typical hourglass shaped rupture was observed (Figure IV.23a) while the reinforced sample showed a multiple-cracking without specimen disintegration (Figure IV.23b).

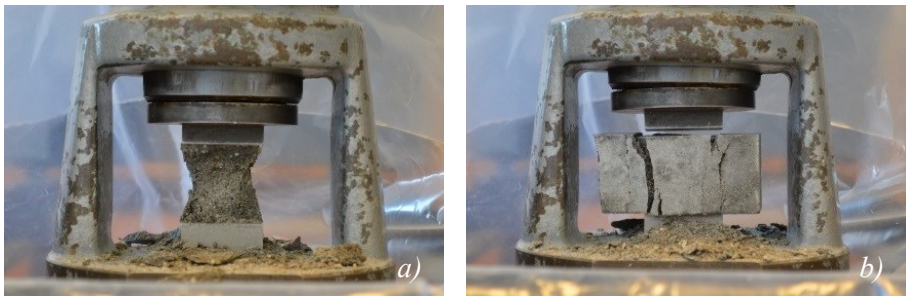

Figure IV.23 *Compression failure of mortar specimen: a) reference sample, hourglass shaped failure; b) fiber reinforced sample, multi-cracking failure*

IV.2.3 Fiber/matrix interactions

IV.2.3.1 Single fiber pull-out

Single fiber pull-out tests were carried out on PP, PP+1FA and PP+2FA fibers, respectively. Two fiber embedment lengths were investigated (10 and 20 mm, respectively). Pull-out tests of PP fibers were already discussed previously (§ III.2.2.1). The complete debonding of PP fibers was observed due to the poor adhesion, as they present a smooth surface. Concerning foamed fibers, pull-out tests were performed on PP+1FA and PP+2FA fibers, in order to study the influence of the different morphology and mechanical properties on the pull-out resistance. In both cases, it was not observed fibers debonding. As clear in Figure IV.24, two different behavior were recognizable: a tensile failure was observed for PP+1FA fibers (Figure IV.24a) while stretching occurred for PP+2FA fibers (Figure IV.24b). The different failure mode is mainly due to the different strain at failure of the investigated fibers (Table IV.1). PP+2FA fibers have not only a slight higher elastic modulus and tensile strength compared to PP+1FA fibers, but also a significantly higher strain at failure (816 % respect 232 % of PP+1FA fibers).

Pull-out curves are useful to obtain information about the maximum pull-out load and the interfacial toughness. The pull-out curves of the investigated fibers are reported in Figure IV.25.

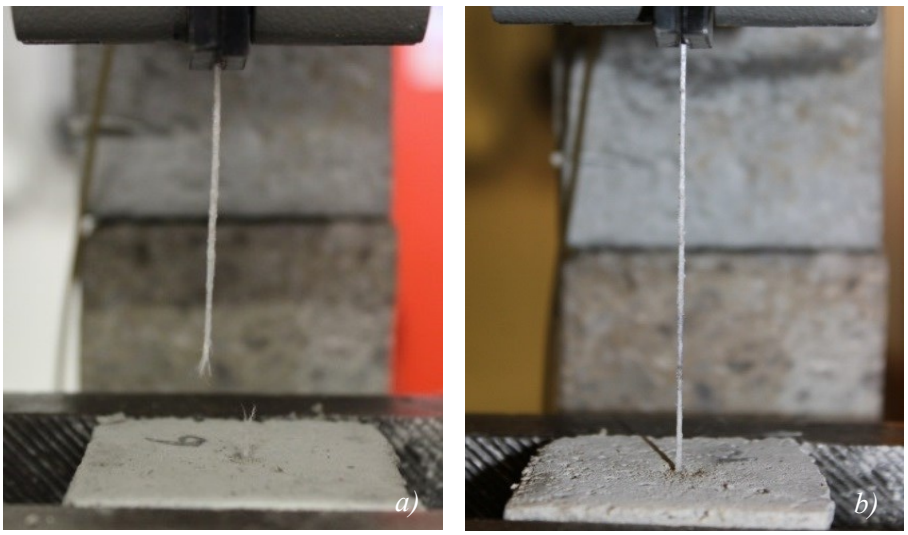

Figure IV.24 *Pullout of a) PP+1FA fiber and b) PP+2FA from a mortar sample*

The improved behavior of foamed fibers can be recognized comparing pullout curves. For smooth fibers slipping occurs after the peak load that is, for PP fibers, significantly lower compared to the maximum pull-out load of foamed fibers. On the other hand, foamed fibers, whose surface roughness offers interlocking positions, show higher adhesion to the cement paste. Thus, after the peak load, fibers start to be stretched. These phenomena have a key role for the behavior of the composite because determine the achievement of the maximum contribute of fibers. Moreover, the improved adhesion will results in a better fiber bridging during crack opening. As evident from Figure IV.25, maximum pullout load for foamed fibers increases considerably, particularly for PP+2FA fibers.

Considering the post-peak branch, is evident for PP fibers a strain hardening behavior mainly due to fiber abrasion and the presence of debris, that increase friction during pull-out. In the case of foamed fibers, after the peak load a plateau is recognizable, corresponding to the fiber stretching.

The interfacial toughness, that is the energy absorbed during pullout, is represented by the area under the pullout curve. Considering the area up to 3 mm (before that fibers start to be stretched) it is clear the remarkable increase of interfacial toughness.

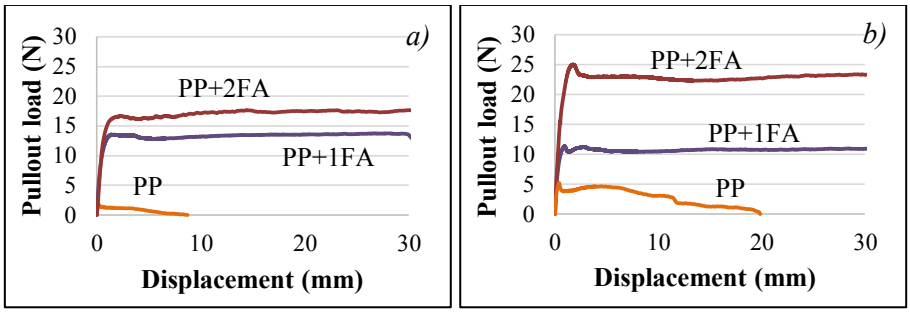

Figure IV.25 *Pull-out curves, embedment length of a) 10 mm and b) 20 mm, respectively*

IV.2.3.2 Fiber/matrix ITZ investigations

The different surface textures result into different fiber/matrix interactions. First of all, PP fibers are completely separated from the cement paste (Figure IV.26a). Moreover, the low interaction implies also an increase of interface porosity (Figure IV.26b). Fibers surface does not show the presence of hydration products. ITZ is mainly constituted by needles of ettringite and pores. The thickness ranges between 120 and 205 μm.

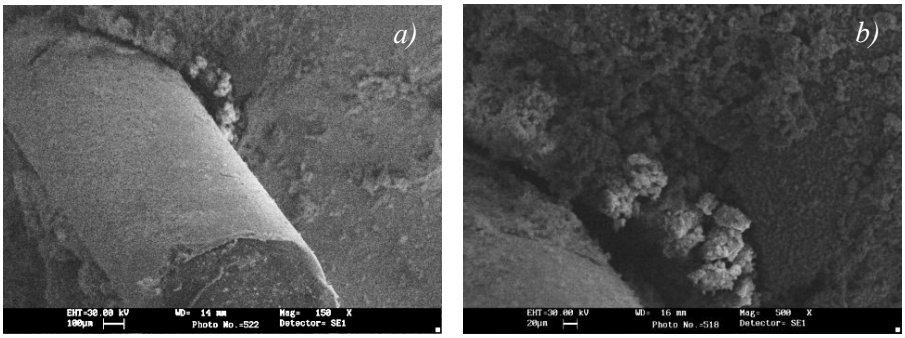

Figure IV.26 *Interfacial transition zone between a PP fiber and mortar*

In the case of foamed fibers the different interface arrangement is clearly shown in Figure IV.27. The irregular surface offers interlocking positions for the cement paste, resulting in a better adhesion. Moreover, also mechanical bond is improved, as demonstrated by pull-out tests.

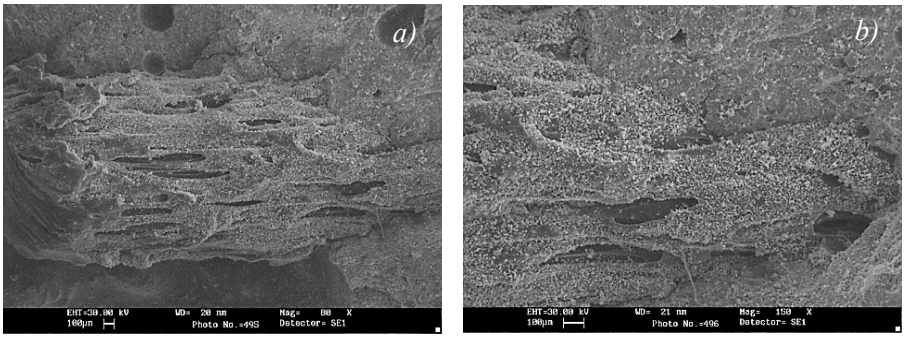

Figure IV.27 *Interfacial transition zone between PP+2% HCF fiber and mortar*

IV.2.4 Durability of fiber reinforced mortars

IV.2.4.1 Water absorption

Cementitious materials are characterized by a wide range of pores, of different dimensions, and water can penetrates through the material pores in several ways. Building materials usually contain an amount of physically bound water without affecting their durability. But if the material's moisture content is above a certain percentage, the deterioration effect of moisture is activated causing numerous issues. Thus, the knowledge of the water movement within cementitious materials is of great importance to determine the degradation ability of a material.

Tests were performed on reference and fiber reinforced samples according the nomenclature reported in Table IV.3. In particular, mortar samples containing 0.5 and 1 % volume fraction of non-foamed fibers and 1 and 2% volume fraction of foamed fibers were investigated. In order to investigate not only the influence of the different morphology, but also the different material both PP and Recycled fibers were used.

IV.2.4.1.1 Capillary water absorption

According to the standard EN 13057, water absorbed per surface unit versus the square root of the testing time was reported in graph. One of the curves is reported in Figure IV.28 as example. As evident, the behavior is clearly non-linear.

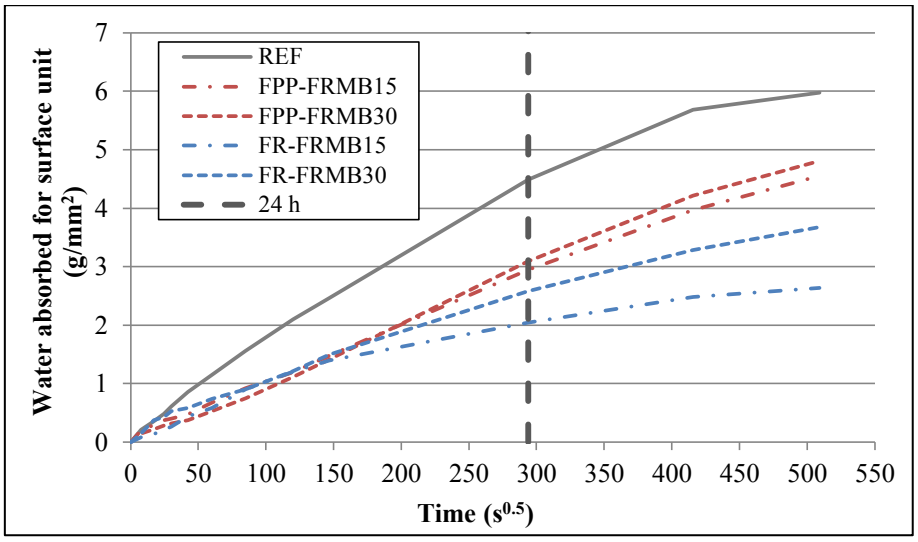

Figure IV.28 *Water absorbed for surface unit versus time (square root of testing time)*

Due to the non-linearity, the water capillary absorption coefficient was calculated at 24 h and the results are reported in Figure IV.29. As evident, fibers addition greatly influenced water absorption. In particular, considering non-foamed fibers, the presence of shorter fibers increases capillary water absorption coefficient respect the reference mortar while mortars reinforced with longer non-foamed fibers have approximatively the same value, of this parameter, compared to the reference sample. The great influence of fibers length could be explained in terms of fibers quantity. At fixed fibers volume fraction, mortars reinforced with 15 mm fibers contain the double amount of fibers compared to mortars containing 30 mm length fibers, as previously stated (§ IV.2.2.1). At fixed non-foamed fibers length, at increasing volume fraction a slight increase of water absorption was measured. Considering mortars containing foamed fibers, an opposite trend is recognizable: at increasing fibers length, an increase of capillary water absorbed water was observed. A more evident influence exists, concerning capillary water absorption, at increasing fibers volume fraction. As evident also from fiber reinforced mortars consistency (Figure IV.14), at increasing foamed fibers content, a sharper decrease of consistency was achieved, compared to mortars containing non-foamed fibers. Consistency influences mortar compaction and thus porosity, as will be later discussed. Moreover, mortars containing foamed recycled fibers have always lower water absorption coefficient than the reference sample thanks to a slight bigger diameter.

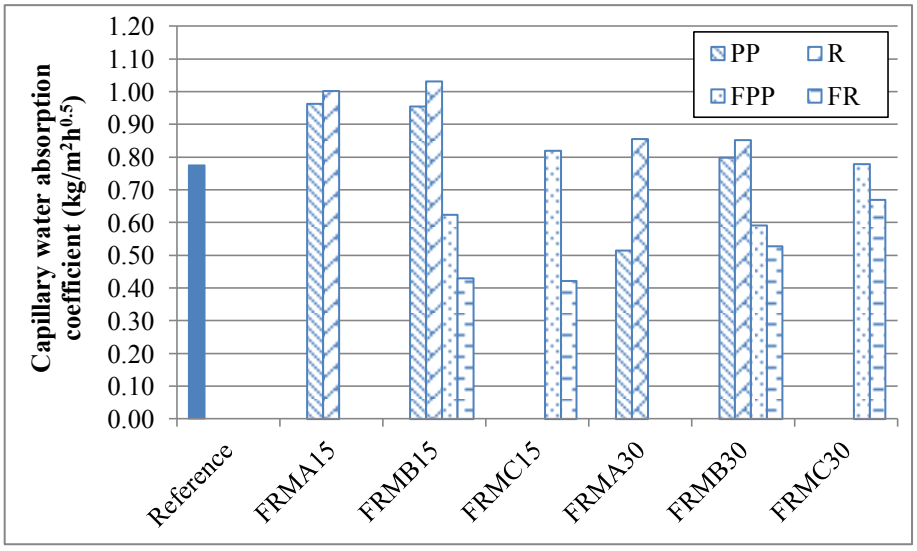

Figure IV.29 *Absorption coefficient of the investigated fiber reinforced mortars after 24 h*

The better behavior of foamed fibers is mainly due to the higher workability (thus the obtainment of a better compaction) of mortars reinforced with foamed fibers, that leads to a lower number of capillary pores. Moreover, the good adhesion between foamed fibers and cement paste avoids the formation of a porous ITZ, as discussed previously (Figures IV.27-28).

Concerning the capillary rise, in Figure IV.30 is shown a picture of some specimens during the test and capillary rise values are reported in Figure IV.31. According to what previously stated for the water absorption coefficient, two different behavior are recognizable for mortars containing foamed and non-foamed fibers, respectively. In particular, for mortars reinforced with non-foamed fibers, at increasing fibers length a decrease of capillary rise was observed. Moreover, samples containing Recycled fibers have a lower capillary rise than mortars containing PP fibers. PP and Recycled fibers have a different diameter (Table IV.1) that influences the amount of fibers but also the pores network in the specimen. On the contrary, for foamed fibers reinforced samples, at increasing fibers length an increase of capillary rise was recognizable. As evident both from Figure IV.29 and Figure IV.31, capillary rise of mortars containing fibers with a bigger diameter is lower.

Figure IV.30 *Example of water capillary raise in mortar specimens*

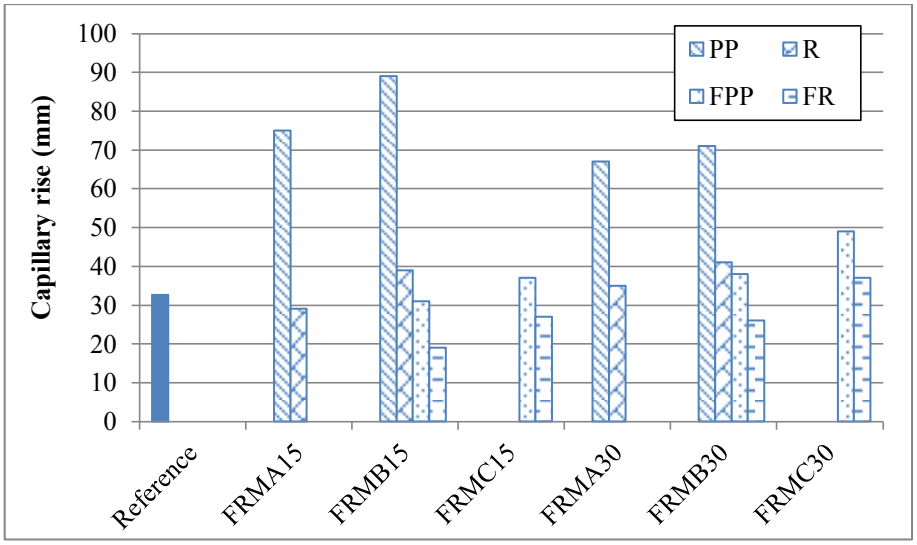

Figure IV.31 *Capillary rise of the investigated fiber reinforced mortar samples after 24 h of testing*

It is possible to conclude that in general, at increasing fibers volume fraction an increase of capillary water absorption coefficient was observed, more pronounced for non-foamed fibers. Furthermore, 15 mm length fibers are preferable in the case of foamed fibers while mortar samples containing non-foamed fibers 30 mm length have a lower water uptake than samples with 15 mm length non-foamed fibers.

IV.2.4.1.2 Total immersion absorption

Water absorption and porosity of the investigated samples are reported in Figure IV.32 and Figure IV.33, respectively. An overall decrease of water absorption and, consequently, of porosity were observed for all the fiber reinforced samples compared to the reference sample. The only exception is represented by mortars containing foamed recycled fibers 30 mm length (i.e. FR-FRMB30 and FR-FRMC30) whose water absorption and porosity were approximatively equal to the reference values.

Water absorption of mortars containing non-foamed fibers decreases at increasing fibers length, similarly to what previously observed in the case of capillary water absorption. Moreover, at fixed non-foamed fibers length and increasing fibers volume fraction, the water absorption is constant for mortars reinforced with PP fibers while decreases for R-FRMs.

Mortars containing foamed fibers have higher water absorption values compared to mortars reinforced with non-foamed fibers, but anyway lower than the reference sample (except the cases mentioned before). It is worth to mention that in this case (i.e. total immersion in water), is the total porosity

that plays an important role in the water absorption. As already stated (§ IV.2.1.1) non-foamed fibers are more flexible than foamed ones, thus the compaction of these mortars could be worse, despite the better fiber/matrix adhesion and the higher consistency of mortars containing foamed fibers.

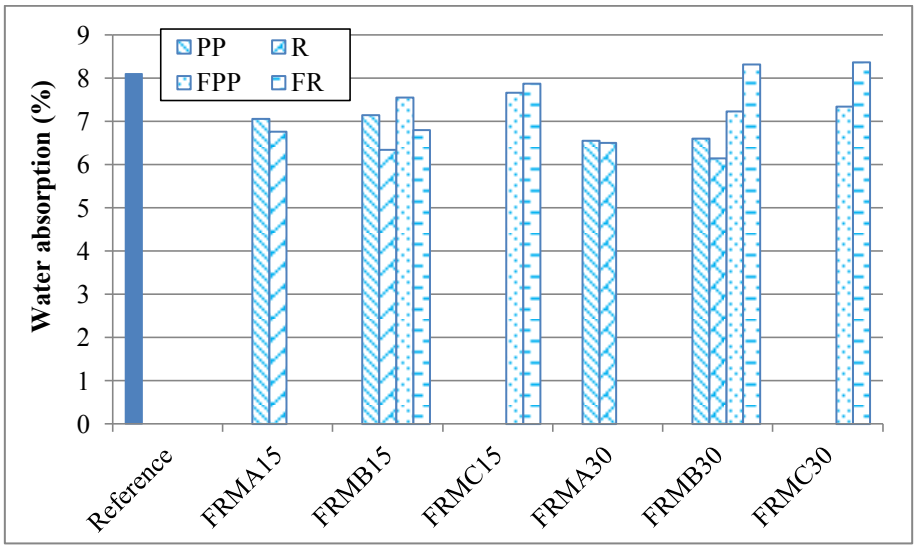

Figure IV.32 *Water absorption of the investigated mortars*

The porosity measured after total water immersion test is the porosity open to water, that is the porosity that allows water to penetrate (in our case under atmospheric pressure) (Figure IV.33).

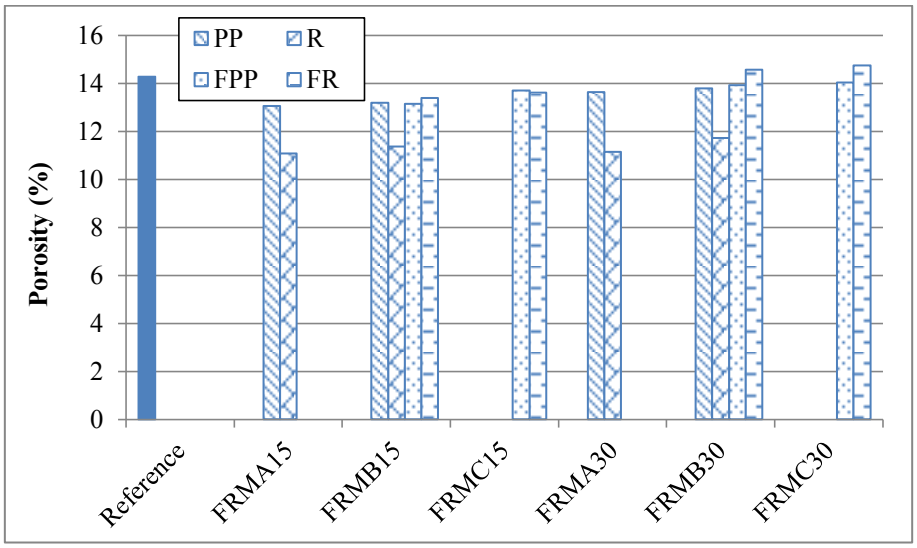

Figure IV.33 *Porosity of the investigated mortars*

There are no significant changes among the investigated samples, except for R-FRMs that show a lower porosity (independently from fibers length and volume fractions). Moreover, among the fiber reinforced samples, the mortars containing longer fibers (30 mm) at high volume fraction (2 %) have the highest porosity, coherently with the slight reduction of compressive strength observed for such samples.

IV.2.4.2 Sulfate attack

In this test, the mass variation of mortar specimens during sulfate attack cycles was evaluated. In particular, a negative variation was measured for mortars containing non-foamed fibers, meaning a loss of mass due to the formation of expansive products (i.e. ettringite). At increasing fibers length and volume fraction a mass decrease was obtained. On the contrary, an increase of mass was registered for samples containing foamed fibers. The different behavior can be explained considering the different fiber/matrix interactions. The interlocking positions onto foamed fibers avoid mortar loss despite the ongoing degradation. Thus, even if mortars reinforced with foamed fibers are more porous than the other fiber reinforced samples (as discussed in the previous paragraph), such fibers are more able to keep together mortars parts under expansion and degradation, due to sulfate attack. A further confirmation of this hypothesis derives from the reference mortar (i.e. without fibers) that has the highest mass loss.

Also a visual analysis was carried out on the investigated samples, in order to estimate the superficial degradation of the specimens. As example, the degradation analysis of mortars containing PP and FPP fibers are reported in Figure IV.34 and Figure IV.35, respectively. The initial shape and geometry of the sample are better preserved in the case of mortars containing foamed fibers.

Figure IV.34 *Comparison of the superficial degradation of PP fiber reinforced mortars at different cycles*

Figure IV.35 *Comparison of the superficial degradation of FPP fiber reinforced mortars at different cycles*

IV.2.4.3 Shrinkage cracking test

Shrinkage cracking tests were performed on the reference mortar and mortars reinforced with recycled fibers both foamed and non-foamed. Figure IV.36 shows the average rate of evaporation for all the performed tests. Several authors refer as a critical limit a rate of evaporation equal to1 $kg/m^2/h$. In our study, this value was reached after 3 hours but all the samples reported cracks after the second hour of test. After the third hour, as the critical limit is exceeded and thus shrinkage induced stresses increase, a consequent sharp increase of cracks width was noticed.

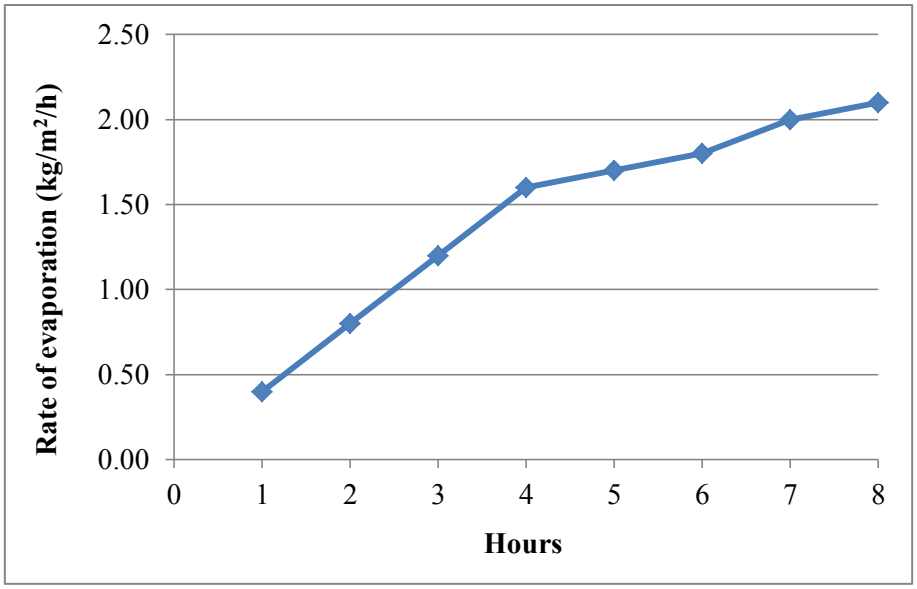

Figure IV.36 *Average rate of evaporation of water from mortar slabs (Coppola et al. 2016b)*

Figures IV.38-42 show the crack pattern at the end of the test (8 hours) for the investigated samples. In particular, Figure IV.37 shows the reference sample at the end of the test and the relative crack pattern, as example of the implemented procedure.

Figure IV.37 *Reference panel at the end of the test (8 hours) (Coppola et al. 2016b)*

Fibers addition has several advantages in controlling cracks opening. First of all, a reduction of the number of cracks on the slab surface was achieved. In particular, the higher the fiber volume fraction the lower is the number of cracks. In addition, longer fibers lead to a lower number of cracks. Moreover, using longer fibers, the diagonal cracks that connect the inner square (formed by cracks) to the outer one disappeared. Finally, also cracks width is influenced both by fiber length and volume fraction. Fibers volume fraction influences also cracks length and width. At increasing volume fraction, a reduction of cracks length is obtained. The presence of an higher fibers quantity hinders cracks propagation, resulting in micro-cracks openings.

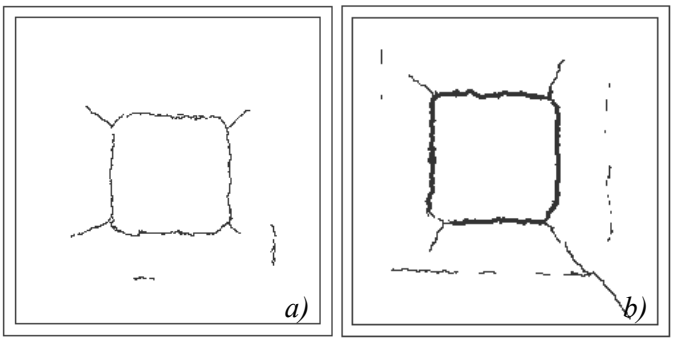

Figure IV.38 *a) FR-FRMA15 and b) R-FRMA15 at the end of the test (8 hours) (Coppola et al. 2016b)*

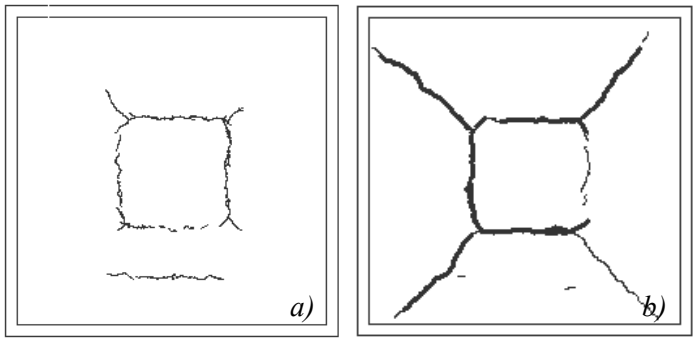

Figure IV.39 *a) FR-FRMB15 and b) R-FRMB15 at the end of the test (8 hours) (Coppola et al. 2016b)*

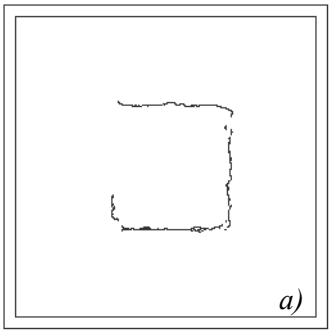

b)

Figure IV.40 *a) FR-FRMA30 and b) R-FRMA30 at the end of the test (8 hours) (Coppola et al. 2016b)*

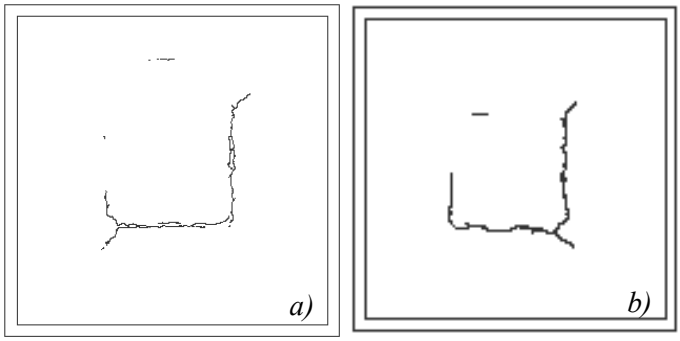

Figure IV.41 *a) FR-FRMB30 and b) R-FRMB30 at the end of the test (8 hours) (Coppola et al. 2016b)*

As expected, all the mortars containing fibers show a lower cracks width compared to the reference sample. Comparing foamed fibers to smooth fibers is possible to highlight several important results. In general, fibers addition delays cracks opening and their growth. Figure IV.42 and Figure IV.43 show the relationship between different fiber volume fractions and related cracks width. In particular, shorter fibers (Figure IV.42) are less efficient than longer ones (Figure IV.43). Moreover, due to the better fiber/matrix adhesion, foamed fibers lead to a lower crack width for the investigated volume fractions. Foamed fibers (15 mm length) were able to reduce cracks width by 28 and 33%, for 0.5 and 1.0% volume fraction, respectively. On the contrary, cracks width reduction for smooth fibers was 20 and 26%. Longer foamed fibers (30 mm) reduced cracks width of 33 and 38% whilst smooth fibers of 25 and 32%.

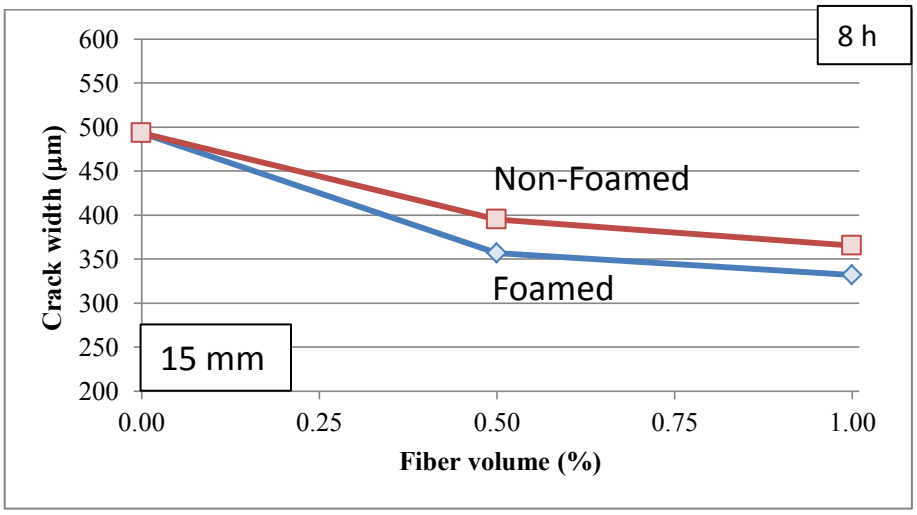

Figure IV.42 *Relationship between fiber volume fraction (l_f = 15mm) and crack width after 8h (Coppola et al. 2016b)*

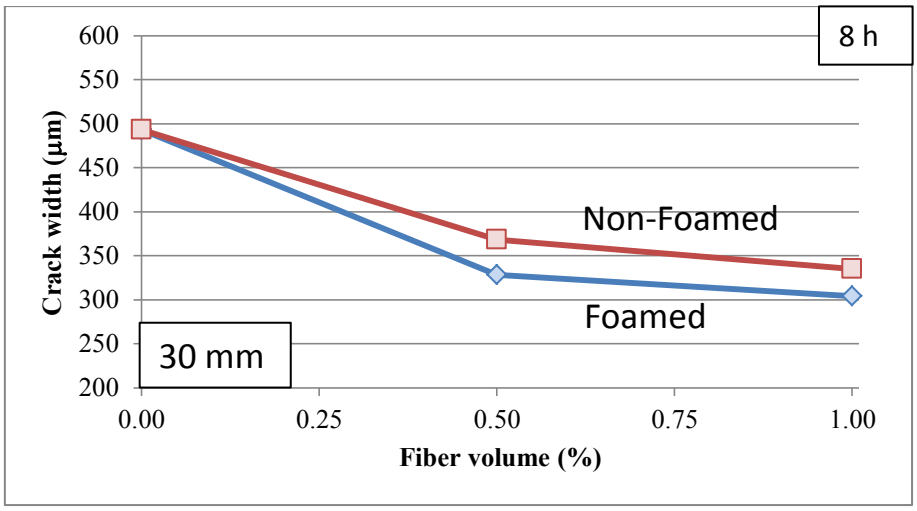

Figure IV.43 *Relationship between fiber volume fraction (l_f = 30mm) and crack width after 8h (Coppola et al. 2016b)*

For the investigated parameters (fibers length and volume fraction), foamed fibers show a higher efficiency (Figure IV.44). With reference to the combined effects of fiber length and volume fraction, it can be observed that both for foamed and smooth fibers, cracks width reduction is the same when 15 mm length fibers at 1.0% and 30 mm length fibers at 0.5% are added. Coherently with all the results, the best performance was exhibits by FR-FRMB30, i.e. the mortar sample containing 30 mm foamed fibers at 1.0% volume fraction.

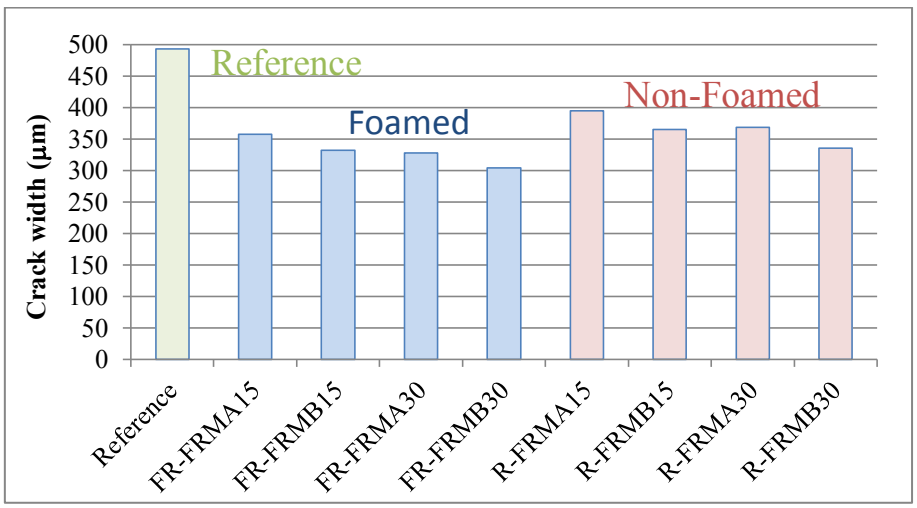

Figure IV.44 *Relationship between fiber parameters (length and volume fractions) and crack width (Coppola et al. 2016b)*

IV.3 Conclusions

The use of fibers both in concrete and mortar is a common and efficient practice to improve not only mechanical properties but also to reduce shrinkage cracking. One of the main drawback of synthetic fibers, in particular of polyolefin fibers, is the weak bond between these fibers and the cementitious matrix. In the previous chapter the fibers chemical surface modification was presented as a possible solution. Another way to overcame the weak interactions between fibers and the cement paste is the improvement of mechanical friction. To this extent, a foam extrusion process was carried out to manufacture polymeric fibers having a rougher surface than the traditional smooth one.

Moreover, due to the increasing environmental issues linked to plastic production and disposal, the possibility to produce fibers starting from an end-of-waste material was investigated.

Experimental investigations demonstrated that foam cell dimensions and distribution can be controlled by foaming agent content and processing conditions. In particular, optimizing foaming agent quantity and processing parameters was possible to produce fibers having an adequate surface texture, suitable for mortar reinforcement. The foam extrusion produced fibers with increased surface roughness but a reduction of fibers mechanical properties was obtained. The optimal foamed fibers were produced using a capillary die of 0.5 mm; 5 wt.% and 2 wt.% of foaming agent for PP and Recycled fibers, respectively. The foaming process produced fibers with a reduced density, due to the internal porosity, resulting in a tensile properties decay. Only recycled fibers reported a slight higher elastic modulus tanks to a better dispersion of the constituent phases (i.e. PP, LDPE and HDPE).

Concerning fiber reinforced mortars at the fresh state, fibers addition leads to an overall workability decrease, more pronounced for mortars containing non-foamed fibers. Moreover, as expected, at increasing fibers volume fraction, a decrease of consistency was obtained. Also the increase of fibers length influenced workability, increasing and decreasing consistency in the case of foamed and non-foamed fibers, respectively.

Fiber reinforced mortars mechanical properties, flexural and compressive strength, were not influenced by fibers addition nor their morphology. A residual strength was observed both using foamed fibers and non-foamed fibers. In particular, at increasing volume fraction and fibers length an increase of residual load was measured. The effectiveness of foamed fibers rough surface is evident as PP foamed fibers reinforced samples have the same residual strength of PP non-foamed FRMs despite their lower mechanical properties and reduced number in the specimens cross-section. Regarding the use of recycled foamed fibers, a very low residual strength was measured, due to their low elongation at break.

SEM images show the different interaction between smooth fibers, i.e. PP

fibers, and foamed fibers. The rougher surface gives rise to a better fiber/matrix adhesion as confirmed by pull-out tests which showed a considerable increase of maximum pull-out load and consequently interface toughness. Pull-out tests have shown that the use of fibers with a good mechanical bond with the cement paste, implies a significant improvement of total energy absorption due to the increased contact area.

Capillary water absorption tests demonstrated the effectiveness of fibers in reducing capillary water absorption coefficient, in particular for mortars containing shorter foamed fibers. The same evidence was found for water absorption after total immersion in water under atmospheric pressure.

Fibers length and volume fraction are key parameters in controlling plastic shrinkage cracking. To this extent, mortar slabs containing both smooth and foamed fibers were prepared using two fibers length (15 and 30 mm, respectively) and two volume fractions (0.5 and 1.0%, respectively). Fibers addition is able to influence cracks number, length and width. In particular, increasing fibers volume fraction a decrease of cracks number and length was achieved whilst longer fibers are more efficient in reducing cracks width. Moreover, mortar samples containing foamed fibers reported a better control of shrinkage cracking: cracks opening was delayed and also crack pattern changed. In particular, the improved fiber/matrix bond was able to reduce crack width, compared to mortar slabs containing smooth fibers.

The results of this study demonstrate the possibility to optimize fibers volume fraction in cementitious mortars using foamed fibers, that are engineered fibers with an improved fiber/matrix bond, by simply changing the manufacturing process. In addition, using end-of-waste materials a more sustainable product can be obtained. Benefits could be not only in the control of plastic shrinkage cracking but also in the workability of fresh mortars, mechanical strength and durability of the hardened composite.

Chapter V
Foamed aggregates: characterization and use into a cementitious mortar

V.1 Aggregates characterization

Aggregates represent about the 70 % of the volume of cementitious composites (He et al., 2015; León and Ramírez, 2010) and is clear the great influence that also low volume fraction substitutions could have on the properties of the end product. Thus, a complete characterization of the artificial aggregates is necessary before their use into a cementitious mortar.

Moreover, the possibility to use an end-of-waste material to produce plastic aggregates represent an important choice in the perspective of a sustainable development.

After the optimization of foaming extrusion process to produce rough fibers (as discussed in the previous chapter), the same principle was used to produce foamed strands subsequently grinded to became aggregates.

V.1.1 Morphological properties

A satisfactory aggregate should be well graded with a good proportion between rounded and angular particles and a surface texture not too smooth. Natural weathering and abrasion processes confer to quartz sand a smooth surface and result in round particles as shown in Figure V.1. On the contrary, artificial aggregates present an elongated shape (Figure V.2), i.e. cylindrical shape, as a result of the manufacturing process: extrusion produces foamed strands (§ II.8) that later are grinded to became aggregates. Moreover, artificial aggregates present a surface porosity not present in the case of natural aggregates. Surface cavities and the rough texture resulting from the foam extrusion process, increase cement paste ability to adhere and penetrate inside superficial voids and cavities, as will be later discussed.

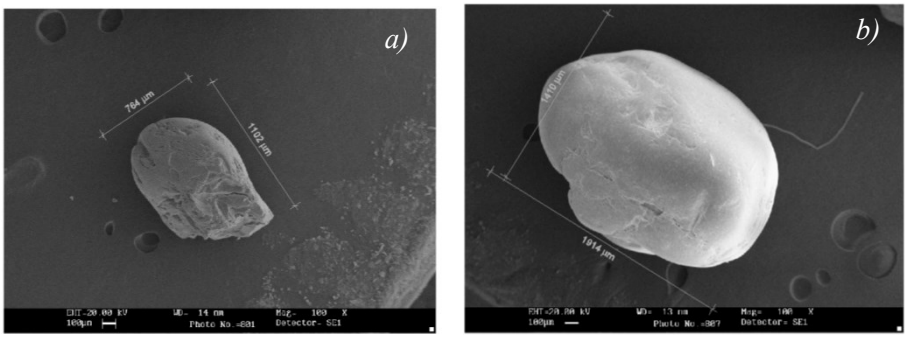

Figure V.1 *SEM pictures of natural quartz sand grains (Coppola et al. 2016)*

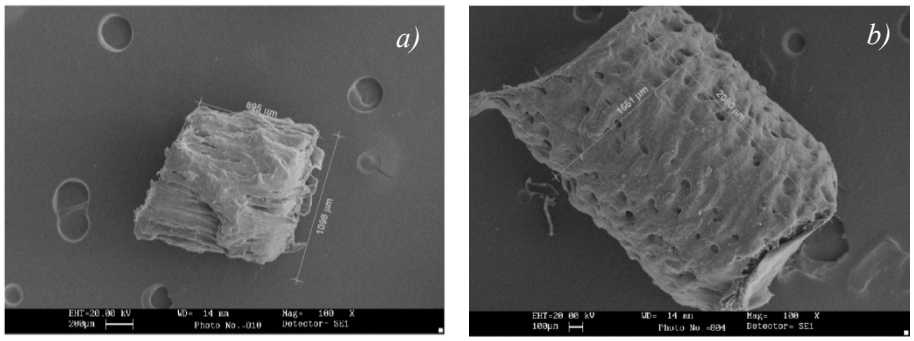

Figure V.2 *Lightweight aggregates (LWAs) SEM pictures(Coppola et al. 2016)*

As clear from Figures V.3, at fixed particle size, natural sand grains are irregular and inhomogeneous while artificial plastic aggregates are regular and homogenous (Figure V.4). The different morphology is important because rounder particles have a lower specific surface area; on the contrary, elongated particles, as in the case of foamed aggregates, have a greater specific surface area, that means a higher need of cement paste to have the same workability.

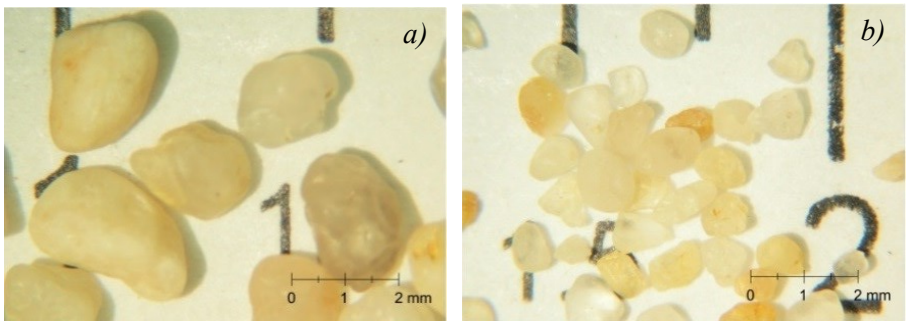

Figure V.3 *Natural sand: a) 1.40/2.00 and b) 0.50/1.00*

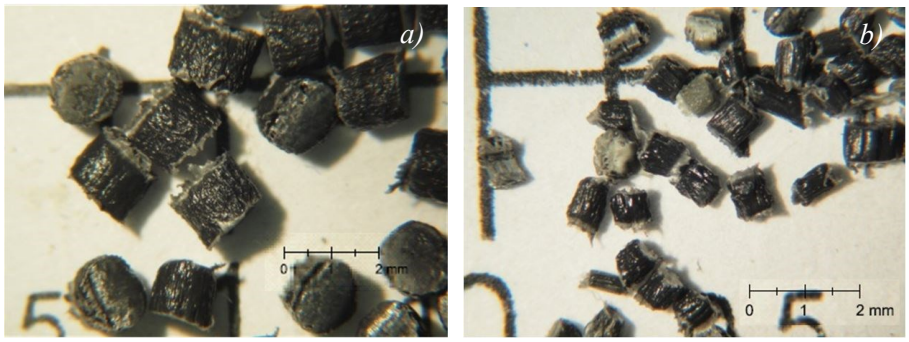

Figure V.4 *Artificial aggregates: a) 1.40/2.00 and b) 0.50/1.00*

V.1.2 Physical properties

One of the main advantages in the use of plastic aggregates is their low density resulting in a lightweight composite material. As a consequence, the risk of aggregates segregation due to plastic particles buoyancy is very high. It is worth to mention that a reduction of aggregates weight reduces the overall dead weight of the structure, resulting in cost savings and reduced seismic loads.

Particle and bulk density of LWAs were investigated and results are reported in Table V.1. At increasing particle size lower values of particle density were measured: fine aggregates are slightly heavier than coarse ones. The reason is that bigger particles are more porous than smaller ones, due to the ability of bubbles to growth and stabilize inside a thicker foamed strand. As reported by several authors (Albano et al., 2009; Kan et al., 2009; Marzouk et al., 2007; Madandoust et al., 2011), one of the main issue is LWAs dispersion due to the low density which causes aggregates floating if not well dispersed into the matrix. Bulk density shows the same behavior: fine particles have a higher bulk density than coarser ones. Artificial aggregates density is lower than natural quartz sand density of 65% approximately, considering an average particle density of 913 kg/m^3 for LWAs.

Table V.1 *LWAs particle and bulk density (Coppola et al. 2016)*

Mesh size (mm)	LWA	
	Particle density (kg/m^3)	Bulk density (kg/m^3)
1.40/2.00	897	348
1.00/1.40	914	361
0.50/1.00	920	387
0.18/0.50	922	402

V.2 Lightweight mortar characterization

After natural and artificial aggregates characterization, lightweight and reference (i.e. without plastic aggregates) mortars were prepared. Natural quartz sand was substituted by volume.

The nomenclature and composition of the investigated lightweight mortar samples are reported in Table V.2. Three different water to cement (w/c) ratios (0.30, 0.45 and 0.50, respectively) and four lightweight aggregates (LWAs) volume fractions (5, 10, 25 and 50 %, respectively) were investigated. Moreover, LWAs were used both in saturated and unsaturated conditions. Mixtures preparations and further details are discussed in § ….

Depending on the property of interest, appropriate mixtures were investigated.

Table V.2 *Nomenclature and composition of lightweight mortar samples (IC = Internal Curing water; S = Saturated; Sp = SuperPlasticizer)*

Mortar	w/c	LWA (%)	Saturated	Sp (wt.% of cem)
Reference/0.30 Sp	0.30	-	-	4.5
Reference/0.45 Sp	0.45	-	-	0.5
Reference/0.45	0.45	-	-	-
Reference/0.50	0.50	-	-	-
LWM5-IC/0.30 Sp	0.30	5	x	4.5
LWM5-IC/0.45 Sp	0.45	5	x	0.5
LWM10-IC/0.30 Sp	0.30	10	x	4.5
LWM10-IC/0.45 Sp	0.45	10	x	0.5
LWM10-S/0.45	0.45	10	x	-
LWM10-S/0.50	0.50	10	x	-
LWM10/0.50	0.50	10	-	-
LWM25-IC/0.30 Sp	0.30	25	x	4.5
LWM25-IC/0.45 Sp	0.45	25	x	0.5
LWM25-S/0.45	0.45	25	x	-
LWM25-S/0.50	0.50	25	x	-
LWM25/0.50	0.50	25	-	-
LWM50/0.50	0.50	50	-	-

V.2.1 Rheological properties

Flow table tests were performed for all the mixtures except for those containing superplasticizer because their consistency was fixed in order to have a mortar with a good workability. Pictures of the flow tests are reported in Figures V.5-7. Mortar workability is affected both by LWAs shape and porous surface. The porous structure of LWAs influences workability of fresh mortar due to the absorption of both mixing water and cement paste inside pores (Kan et al., 2009). On the contrary, as discussed before, natural quartz sand has a smooth surface and water absorption is close to zero. Moreover, also aggregates shape affects mortar rheology: rounder particles produce a more workable mortar while elongated particles, as LWAs, give rise to higher friction and reduce consistency. To partially overcome these drawbacks, LWAs could be soaked and saturated into part of mixing water before mixtures preparation. For both w/c ratios, at increasing LWAs content a reduction of workability was observed and it was proportional to LWAs substitution. Considering the already reduced workability of mortars prepared with saturated LWAs and a w/c of 0.45, mortars containing unsaturated LWAs and w/c of 0.45 were not prepared. On the contrary, saturating LWAs, in the case of w/c ratio of 0.50, was possible to decrease the loss in consistency of about 3% (Figure V.8).

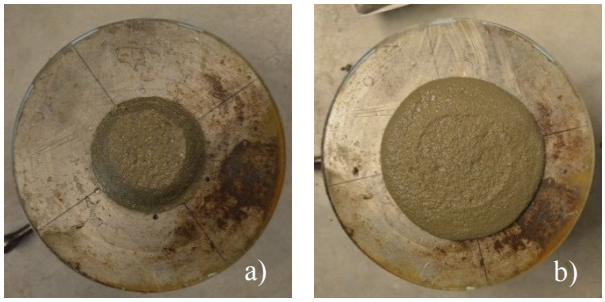

Figure V.5 *a) Reference/0.45 and b) Reference/0.50 (Coppola et al. 2016)*

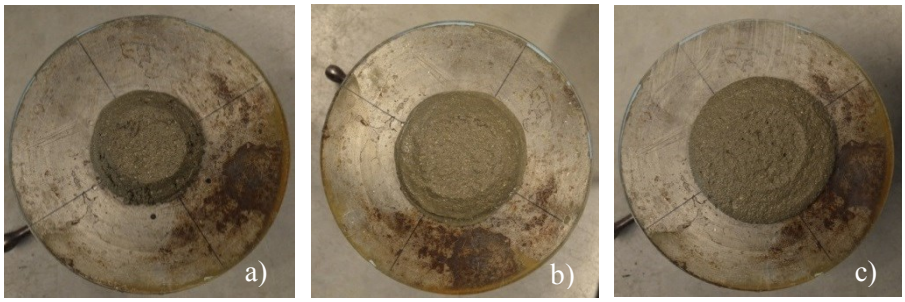

Figure V.6 *a) LWM10-S/0.45 ; b) LWM10/0.50 and c) LWM10-S/0.50 (Coppola et al. 2016)*

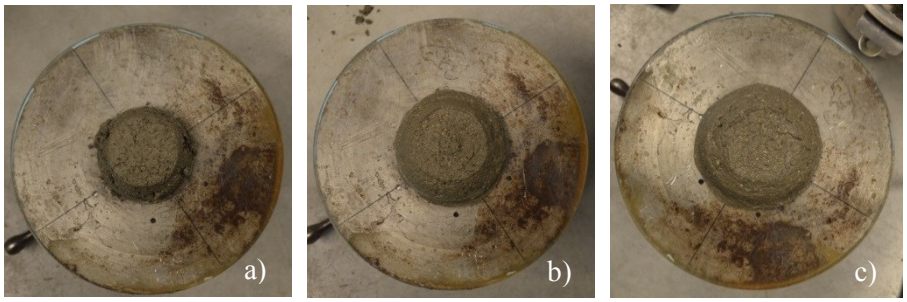

Figure V.7 *a) LWM25-S/0.45; b) LWM25/0.50 and c) LWM25-S/0.50 (Coppola et al. 2016)*

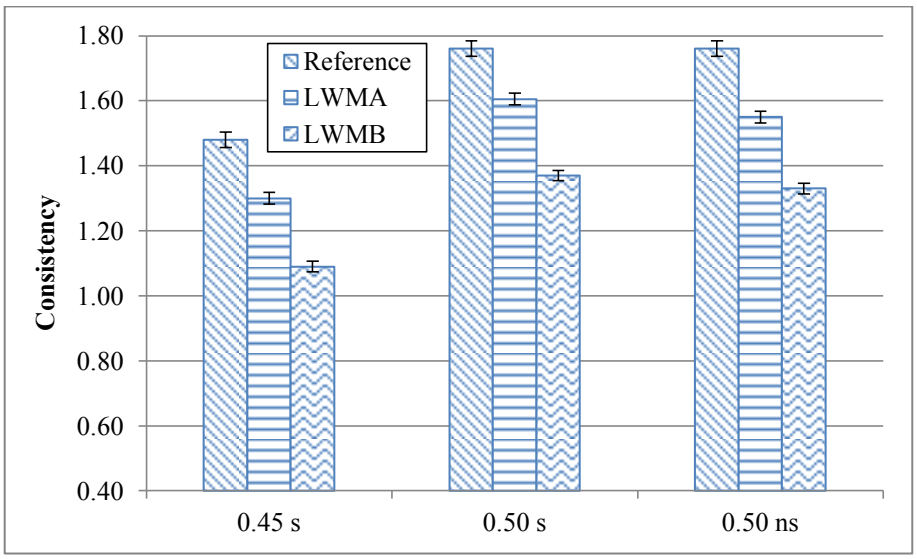

Figure V.8 *Fresh mortar consistency vs. w/c ratios (s = saturated and ns = non saturated) (Coppola et al. 2016)*

V.2.2 Physical properties

V.2.2.1 Density of lightweight mortar

Dry density values, ρ_d, of hardened mortar are reported in Table V.3. Natural aggregates replacement leads to a sharp decrease of density, in particularly for mortars with the highest w/c ratio and saturated aggregates. It is generally known that lower w/c ratios correspond to denser cementitious pastes resulting in heavier mortars. Considering the w/c ratio of 0.5, when LWAs are not saturated (i.e., LWM10/0.50 and LWM25/0.50), density decrease is lower due to the porous structure of aggregates which absorb water reducing the free water respect the mixtures in which aggregates are saturated. On the contrary, when LWAs are saturated, part of the water

contained into pores is given back to the mixture increasing porosity and weakening the interfacial transition zone (ITZ). These assumptions are confirmed by the lower compressive strength and higher porosity (Table V.3) of mortars with saturated aggregates. In all the investigated mortar samples, at increasing sand replacement a linearly decrease of dry density was observed (Figures V.9-10) and mixtures with non-saturated aggregates have an effective w/c of 0.46, considering as 8 % aggregates porosity. As results of the lower effective w/c ratio and higher density, an improvement of mechanical properties was achieved (§ V.2.3). Considering the mixtures containing additional water for the internal curing (§ V.3) a slight decrease of density and increase of porosity were measured, indicating that water is actually released increasing the porosity, but this water, at the same, promotes a further hydration of the cement since the compressive strength of these mortars is slightly higher (Table V.3).

As expected, the lowest values of porosity were measured for mortars prepared with w/c = 0.30. As a consequence, at fixed sand volume replacement, these mortars were also the most heaviest.

Table V.3 *Mortars physical and mechanical properties (ρ_d = dry density; R_f = flexural strength and R_c = compressive strength)*

Mortar	ρ_d (g/cm^3)	Porosity (%)	R_f (MPa)	R_c (MPa)
Reference/0.30 Sp	2.197	13	9.17	74.17
Reference/0.45 Sp	2.092	17	7.55	59.53
Reference/0.45	2.212	17	6.93	58.38
Reference/0.50	2.143	16	6.88	51.97
LWM5-IC/0.30 Sp	2.148	14	9.06	72.15
LWM5-IC/0.45 Sp	1.995	18	6.42	46.52
LWM10-IC/0.30 Sp	2.085	14	7.96	62.09
LWM10-IC/0.45 Sp	1.933	17	6.21	38.91
LWM10-S/0.45	1.994	16	5.33	37.69
LWM10-S/0.50	1.923	18	5.04	32.13
LWM10/0.50	1.981	16	5.09	35.56
LWM25-IC/0.30 Sp	1.969	14	7.15	43.78
LWM25-IC/0.45 Sp	1.804	19	4.88	25.52
LWM25-S/0.45	1.809	17	4.38	24.61
LWM25-S/0.50	1.756	19	4.19	21.02
LWM25/0.50	1.805	17	3.84	22.97
LWM50/0.50	1.374	23	2.87	14.05

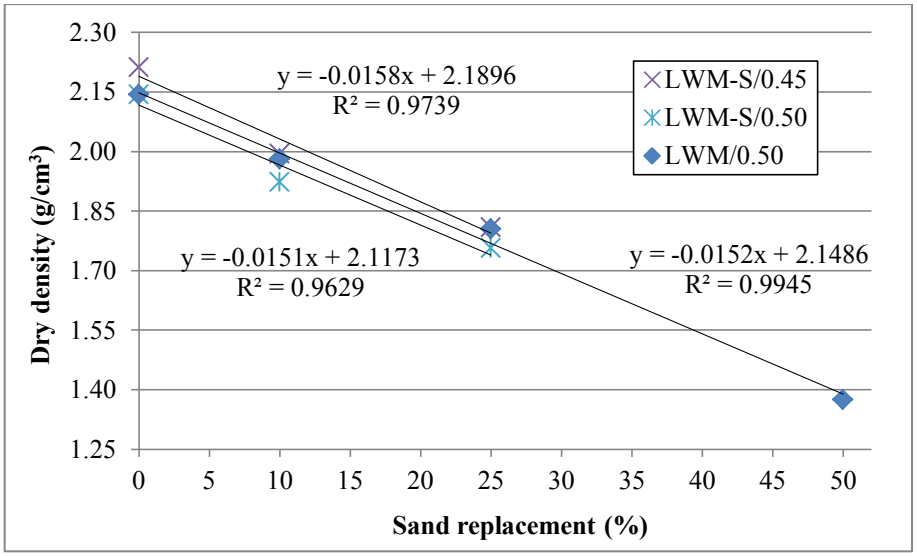

Figure V.9 *Lightweight mortars (containing saturated and unsaturated aggregates) dry density reduction varying the volume of natural sand replacement*

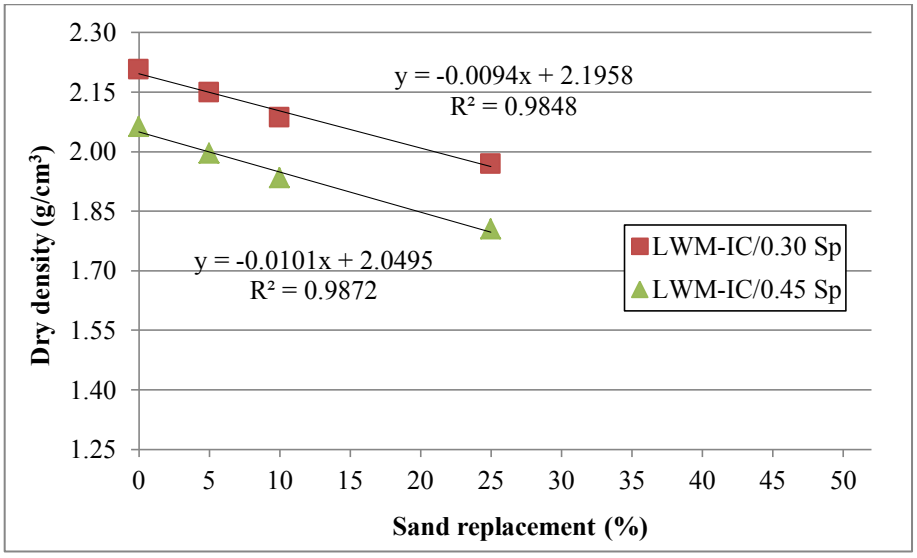

Figure V.10 *Lightweight mortars (containing additional water for internal curing and superplasticizer) dry density reduction varying the volume of natural sand replacement*

V.2.2.2 Thermal conductivity

The incorporation of plastic aggregates in mortar or concrete, generally leads to a quite sharp decrease of thermal conductivity. Moreover, if porous aggregates (plastic or not) are used, the air contained in the aggregates pores contributes to lower thermal conductivity (Mounanga et al., 2008). It is worth to mention that air thermal conductivity is 0.026 W/m K (at 20 °C and atmospheric pressure) while for a typical insulating material, i.e. expanded polystyrene (EPS) is 0.035 W/m K.

Tests to determine thermal conductivity were performed on mortar samples containing different artificial aggregates volume fractions (Reference/0.50, LWM10/0.50, LWM25/0.50 and LWM50/0.50) according to the procedure described in § ….

Thermal conductivity is inversely proportional to the gradient of temperature (eq. V.1) existing between the two surfaces of the investigated specimen (mortar slab in this case):

$$\boldsymbol{\lambda = \frac{Fs}{A\Delta T}} \qquad \text{(V.1)}$$

where λ is the thermal conductivity (W/m K), F is the heat flow rate (W), s is the specimen thickness (m), A is the measurement area (m^2) and ΔT is the thermal gradient between specimens surfaces.

Considering the thermal flux constant, thermal conductivity (λ) and temperature gradient (ΔT) are represented by an equilateral hyperbola (i.e. with perpendicular asymptotes) with Cartesian axes as asymptotes (Figure V.11).

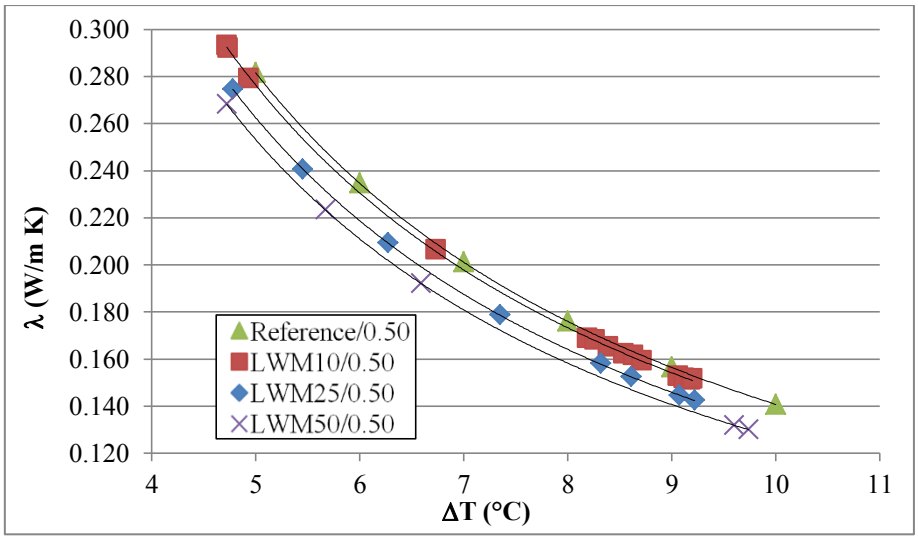

Figure V.11 *Thermal conductivity of the investigated lightweight mortars at different temperature gradients*

As expected, at increasing natural sand replacement, a decrease of thermal conductivity was measured. Moreover, seen the relationship between thermal conductivity and temperature gradient (eq. V.1), at increasing ΔT a decrease of λ was registered. Thermal conductivities for ΔT of 1°C and 10°C (λ and λ_{10}, respectively) of the investigated samples are reported in Table V.4. Five tests were performed for each mortar sample to ensure the reproducibility.

Table V.4 *Thermal conductivity of investigated lightweight mortars*

Specimen	λ (W/m K)	λ_{10} (W/m K)	$\Delta\lambda_{10}$ (%)
Reference/0.50	1.408	0.141	-
LWM10/0.50	1.365	0.136	3
LWM25/0.50	1.311	0.131	7
LWM50/0.50	1.266	0.127	10

A reduction of thermal conductivity of 3, 7 and 10 % was obtained replacing 10, 25 and 50% of natural quartz sand, respectively. Lightweight insulating mortars can be used as plaster or rendering mortars. A lower thermal conductivity means that using a lightweight mortar, instead of the reference one, at fixed thickness, a better thermal insulation will be achieved. On the contrary, to obtain the same thermal insulation, a lower thickness of mortar will be necessary, reducing the material consumption (i.e. reducing costs).

Moreover, a linear relationship is recognizable between thermal conductivity and both sand volume replacement and dry density (Figure V.12). As stated previously, at increasing sand replacement, a decrease of dry density was achieved. The lightweight mortar with the lowest dry density and thermal conductivity, as expected, is LWM50/0.50 (i.e. the mortar with the highest sand replacement). In literature, also other authors reported linear relationships between thermal conductivity and sand volume replacements or dry density (Nguyen et al., 2014; Corinaldesi et al., 2015).

It should be noticed, that when more porous aggregates are used (i.e. the air content in pores is higher) a more pronounced decrease of thermal conductivity is achieved. At the same time, it is necessary to consider that the gain in thermal insulation is paid by a decrease in compressive strength as widely reported in literature (Nguyen et al., 2014; Mounanga et al., 2008; Corinaldesi et al., 2011; Ferrándiz-Mas et al., 2014; Corinaldesi et al., 2015). Thus an optimization of the balance between mechanical properties and physical properties should be found.

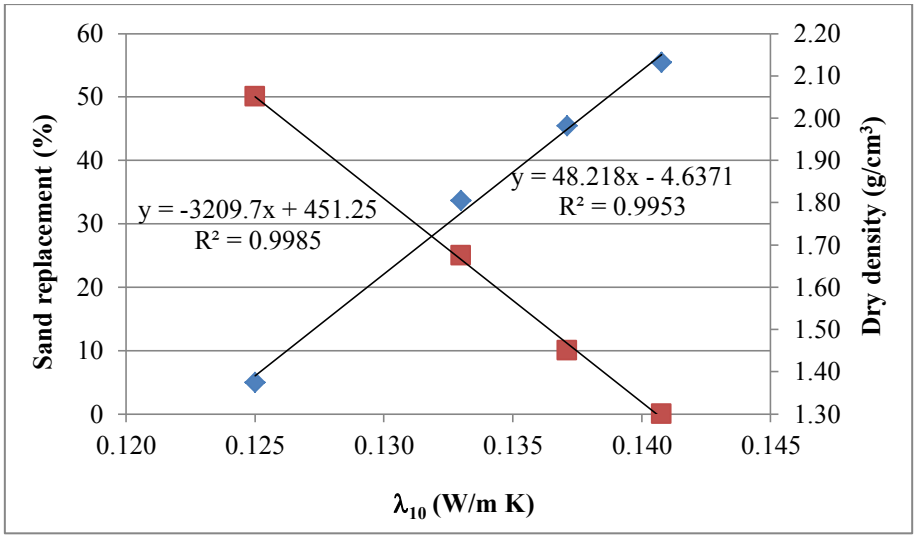

Figure V.12 *Thermal conductivity (λ_{10}) of lightweight investigated mortars versus sand replacement (■) and dry density (◆)*

V.2.2.2 Water vapor permeability

In order to obtain information about the effect of the natural sand replacement on the water vapor transmission rate of the mortar, water vapor permeability tests were performed on the reference sample, used as control, and on three lightweight mortars (LWM10/0.50, LWM25/0.50 and LWM50/0.50, respectively).

Representing the mass variation versus time during water vapor permeability tests (Figure V.13), it is possible to determine water vapor transmission rate per surface unit (WVT) that is the slope of the line fittings data points dived for the sample test area. The linear relationships existing between the mass variation over time of the lightweight mortar samples, ensure the steady state condition (i.e. the water vapor that flows through the sample is constant in time).

At increasing artificial aggregates content, the slope of the fitting lines increases, meaning an increase of WVT (i.e. a decrease of the water vapor transmission resistance).

These observations are in accordance to the water vapor permeability (W_{vp}) and resistance (μ) of the investigated samples, calculated according the standard EN 1015-19 (§ II.9.4.5) and reported in Table V.5. Moreover, several authors reported about the reduction of water vapor resistance of lightweight mortars (Gadea et al., 2010; Corinaldesi et al., 2015; Pedro et al., 2013; Iucolano et al., 2013).

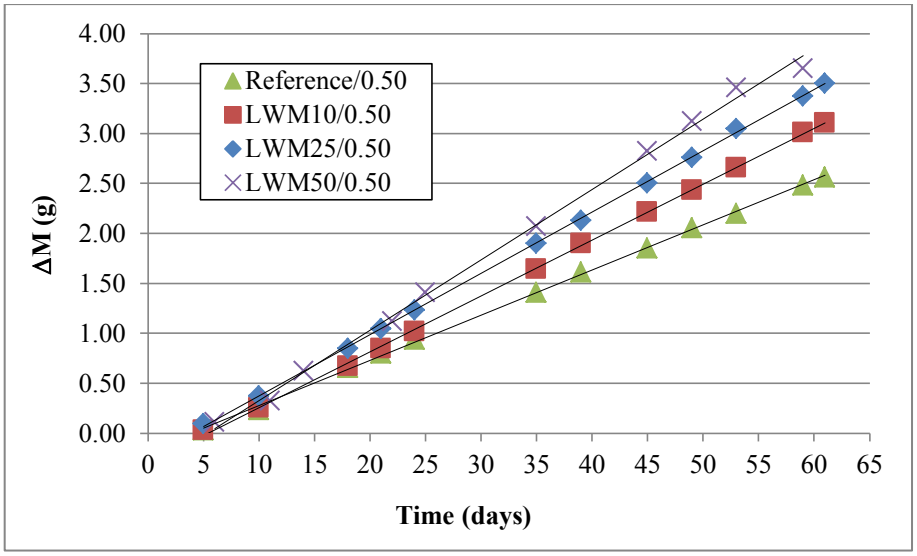

Figure V.13 *Mass variation versus time during water vapor permeability test for the investigated lightweight mortars*

The progressive increase in permeability is proportional to natural sand replacement. In particular, a reduction of water vapor permeability of 13, 25 and 48 % was measured for lightweight mortars containing 10, 25 and 50 % of plastic aggregates. The linear relationship existing between water vapor resistance and sand replacement is recognizable in Figure V.14.

Although the low porosity variation (Table V.3), significant only for LWM50/0.50 samples, water vapor permeability changes significantly. It means that artificial aggregates addition influence mostly other ranges of pores than that open to water (in fact, the porosity reported in Table V.3 is the porosity open to water). Probably the capillary pores network increased due to the reduced workability of lightweight mortars. Moreover, aggregates have a porous structure that can facilitate water vapor transport through the mortar.

Table V.5 *Water vapor permeability (W_{vp}), resistance (μ) and resistance variation, compared to reference mortar, of the investigated specimens*

Specimen	W_{VP} (kg/m s Pa)	μ	$\Delta\mu$ (%)
Reference/0.50	$2.97 \cdot 10^{-11}$	6.56	-
LWM10/0.50	$3.60 \cdot 10^{-11}$	5.72	13
LWM25/0.50	$3.97 \cdot 10^{-11}$	4.90	25
LWM50/0.50	$5.88 \cdot 10^{-11}$	3.38	48

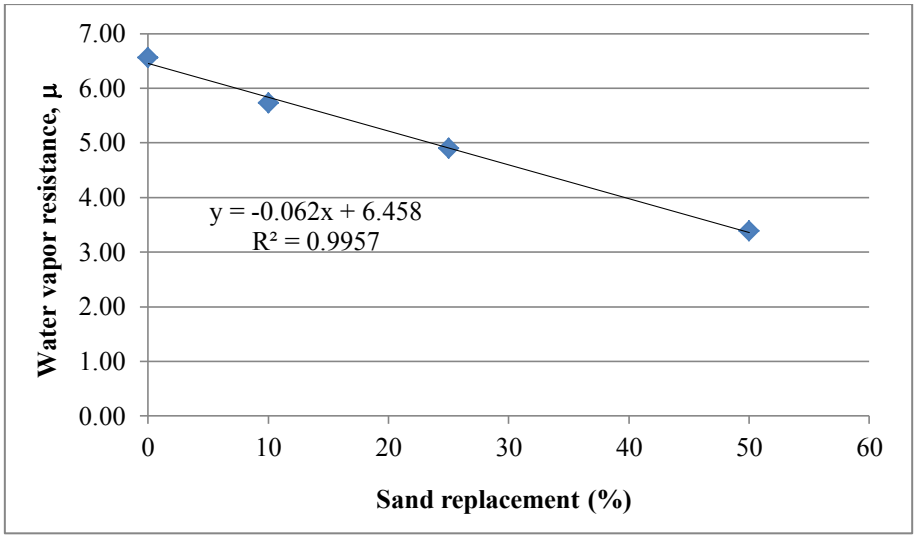

Figure V.14 *Water vapor resistance of the investigated lightweight mortars at different natural sand volume replacement*

V.2.3 Mechanical properties

The replacement of natural silica sand with artificial plastic aggregates greatly influences mortar mechanical properties. As widely reported in literature, generally mechanical properties decrease due to the lower mechanical properties of the plastic aggregates or the weak adhesion between plastic aggregates and cement paste (Ferrándiz-Mas et al., 2014; Corinaldesi et al., 2011; Saikia and de Brito, 2012; Pedro et al., 2013; Correia et al., 2010; da Silva et al., 2014). The results of mechanical tests, i.e. flexural and compressive strength, are reported in Table V.3.

V.2.3.1 Flexural strength

As expected, at increasing plastic content a decrease of mechanical properties was obtained. Figure V.15 reports an example of load/deflection curves acquired during flexural test: at increasing LWAs content a less brittle behavior was recognizable but a sharp decrease of flexural strength was attained. The area under the load-displacement curve represents the energy absorbed during the test: the increase of this area means the increase of toughness of lightweight mortars at increasing natural sand volume replacement. The same evidence was also found by other authors (Li et al., 2004; Hannawi et al., 2010). Aggregates saturation is not particularly influent on flexural strength while are of great importance w/c ratio and the use of superplasticizer (Table V.3). At increasing w/c ratio a decrease of flexural strength was obtained (for example, from 9.17 MPa of

Reference/0.30 Sp to 6.88 MPa of Reference/0.50). Moreover, at fixed w/c ratio, the use of a superplasticizer increased the flexural strength (for example, from 6.93 MPa of Reference/0.45 to 7.55 MPa of Reference/0.45 Sp).

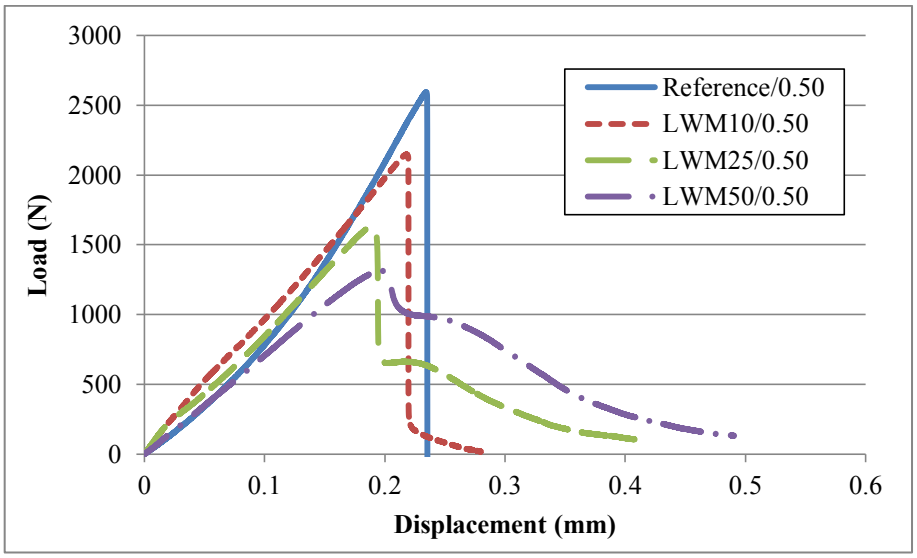

Figure V.15 *Example of load/displacement curve obtained from flexural test (Coppola et al. 2016)*

V.2.3.2 Compressive strength

Compressive strength decrease is mainly due to natural aggregates substitution as results of LWAs lower mechanical properties. Moreover, also porosity variation among the different investigated samples is responsible of compressive strength decay. Comparing flexural and compressive strength results reported in Table V.3 is possible to appreciate the different behavior exhibited by investigated lightweight mortar samples. Flexural strength decrease is less pronounced than compressive one because for flexural strength plays an important role the good adhesion between aggregates and cement paste but also artificial aggregates higher deformability. On the contrary, for compressive strength, are relevant porosity and aggregates mechanical properties. Thus, to enhance compressive strength is necessary to modify mortar porosity and/or aggregates mechanical properties. As a consequence, compressive strength of LWMs with the lowest w/c (i.e. 0.30) have is higher than that of LWMs produced with w/c equal to 0.45 or 0.50.

Compressive strength decrease is proportional to LWAs content and LWMs dry density, as reported in Figures V.16-17.

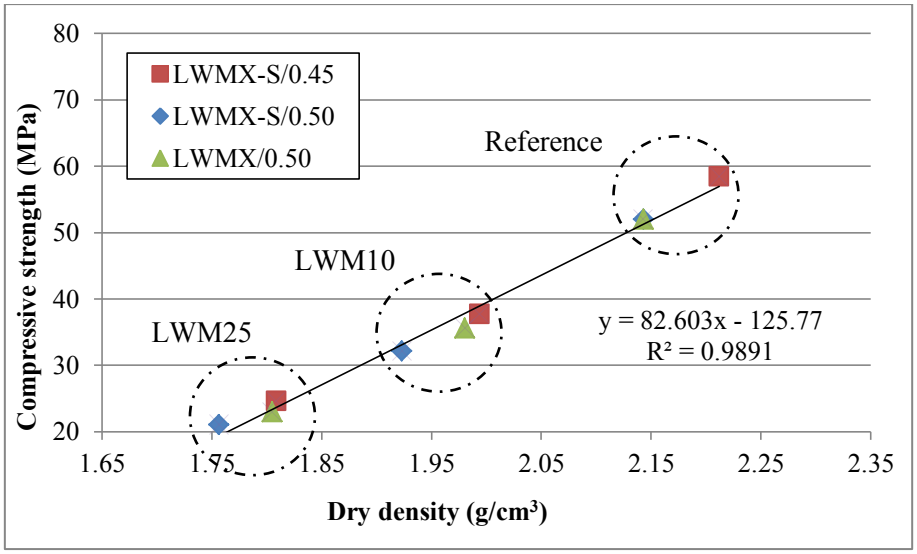

Figure V.16 *Compressive strength vs. dry density of lightweight mortars with w/c 0.50 and 0.45 (Coppola et al. 2016)*

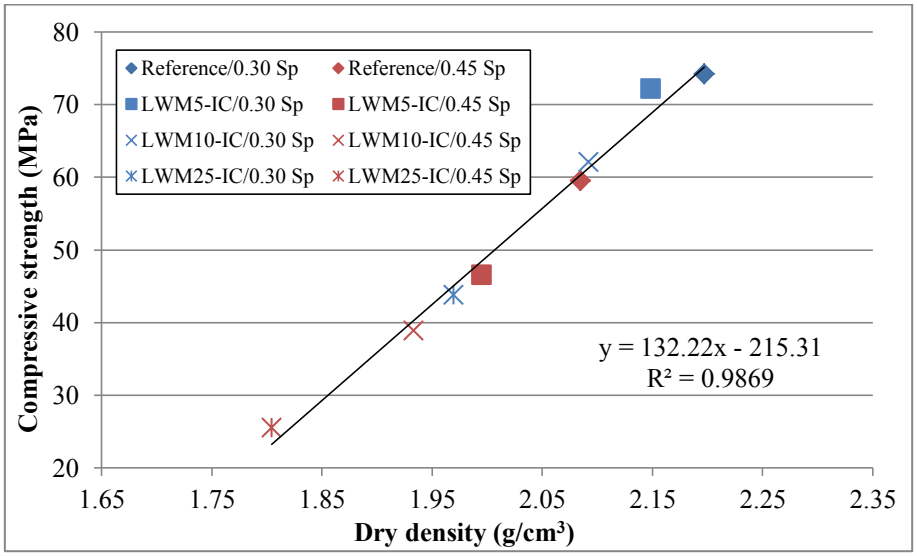

Figure V.17 *Compressive strength vs. dry density of lightweight mortars with w/c 0.45 and 0.30, containing internal curing water (IC) and superplasticizer (Sp). For nomenclature § Table V.2*

Moreover, reporting on the same graph (Figure V.18) the compressive strength values versus dry densities of all the investigated mortars, a power law relationship can be recognized as reported in literature also by Babu et al. (2006) and Tittarelli et al. (2016).

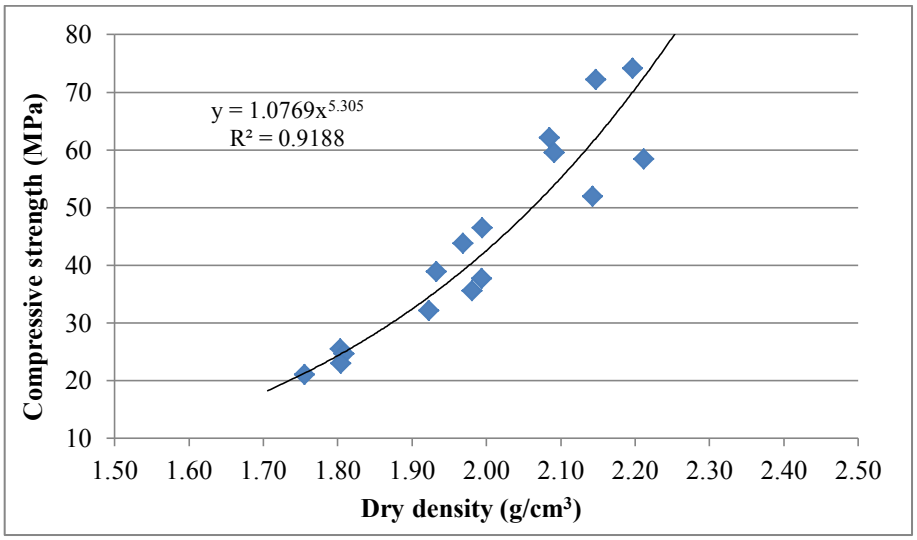

Figure V.18 *Compressive strength vs. dry density of all the investigated lightweight mortars*

Flexural and compressive strength are strictly correlated and a linear relationship could be found between these properties (Figure V.19).

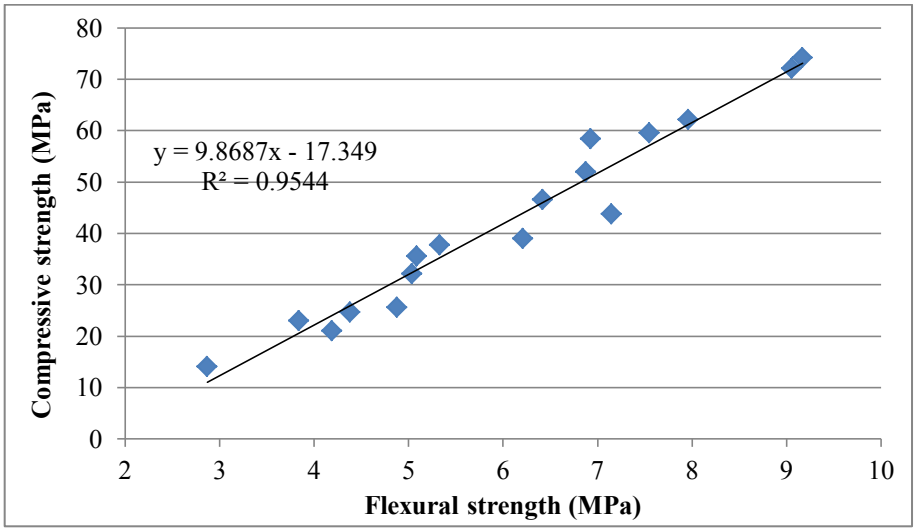

Figure V.19 *Compressive strength vs. flexural strength of all the investigated lightweight mortars*

It should be noticed that compressive strength of LWMs was always higher than minimum requirements for rendering and plastering mortars (Table V.6) or masonry mortars (Table V.7). All of the LWMs are of CS IV type, according to EN 998-1. Considering masonry mortars classification (EN 998-2, Table V.7), all the LWMs have a compressive strength higher than 20 MPa (Table V.3) except LWM50/0.50 whose compressive strength is 14.05 MPa.

Table V.6 *Rendering and plastering mortar classification in accordance with EN 998-1*

Property	Type	Mean values
Compressive strength at 28 days (MPa)	CS I	0.4-2.5
	CS II	1.5-5.0
	CS III	3.5-7.5
	CS IV	> 6
Capillary water absorption ($kg/min^{0.5}\ m^2$)	W 0	Not specified
	W 1	≤ 0.40
	W 2	≤ 0.20
Thermal conductivity (W/m K)	T 1	≤ 0.1
	T 2	≤ 0.2

Table V.7 *Masonry mortar classification in accordance with EN 998-2*

Class	Compressive strength (MPa)
M 20	20
M 15	15
M 10	10
M 5	5
M 2.5	2.5
M 1	1

V.2.4 Aggregates/matrix interactions

The low density of artificial aggregates may lead to segregation or not good dispersion of artificial aggregates. As the occurrence of this phenomenon can compromise final properties of the composite mortar, it is interesting to study specimens cross section. For this purpose one cross section of each mix was investigated by an optical microscope on polished surfaces. Figure V.20 shows that an homogeneous dispersion of artificial aggregates (artificial aggregates are the black particles) was achieved. Moreover, despite the reduction in workability, a good compacity is recognizable as well as an optimal distribution of the different aggregate sizes.

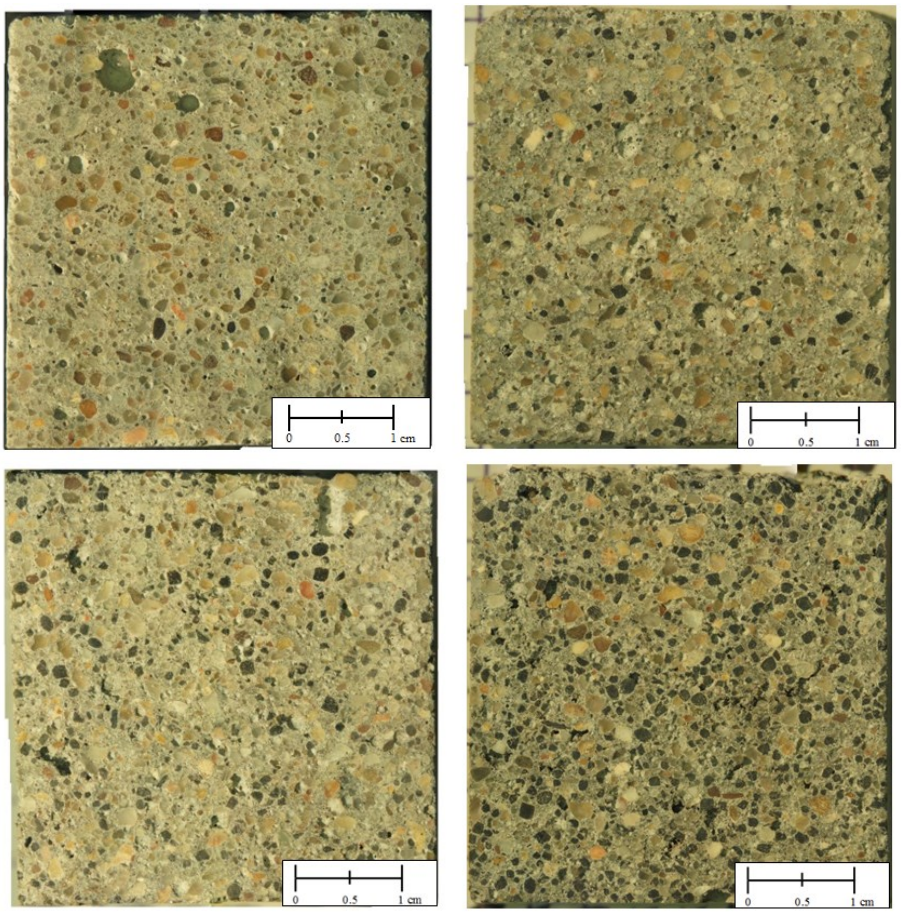

Figure V.20 *Cross section analysis (clockwise from top left): Reference/0.50, LWM10/0.50, LWM25/0.50 and LWM50/0.50*

A more detailed analysis is reported in Figure V.21 that shows the natural and artificial aggregates (NA and LWA, respectively) distribution for LWM25/0.50 sample taken by optical and scanning electron microscope on a polished specimen.

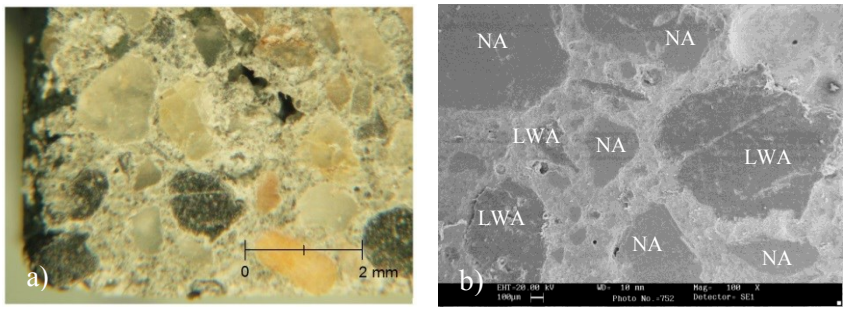

Figure V.21 *a) LWM25/0.50 polished surface (optical microscope) and b) SEM picture of aggregates distribution in the same mortar sample (Coppola et al. 2016)*

Many authors (Hannawi et al., 2010; Saikia and de Brito, 2014; Gadea et al., 2010; Choi et al., 2005) reported a weak adhesion between artificial aggregates and cement paste due to the increase of water content at the interface: a weak adhesion is generally responsible of porosity increase and decay of mechanical properties. As shown by Figure V.22a, natural and LWAs present the same ITZ without any increase in distance between artificial aggregates surface and cement paste. Moreover, Figure V.22b shows the increase of interfacial adhesion between LWAs and matrix, due to the interlocking positions offered by aggregates surface roughness.

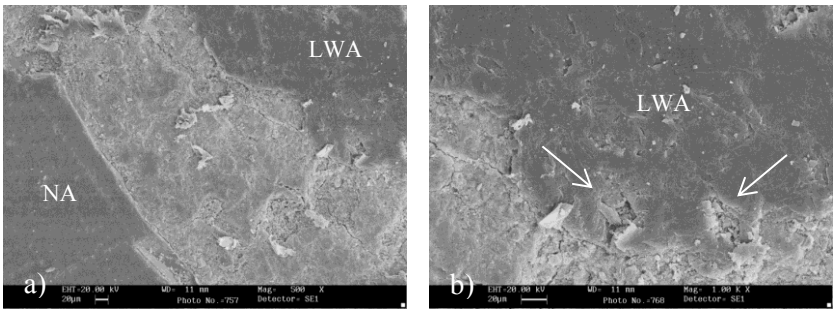

Figure V.22 *a) Natural and artificial aggregates ITZ and b) detail of cement paste penetrated into LWA (Coppola et al. 2016)*

SEM pictures taken on fractured surfaces confirm what stated before: the ITZ between natural aggregates and cement paste (Figure V.23) is the same than for artificial aggregates (Figure V.24). Moreover, LWAs, offer interlocking positions while natural aggregates are smoother and only in the case of surface irregularities cement paste adhere onto them.

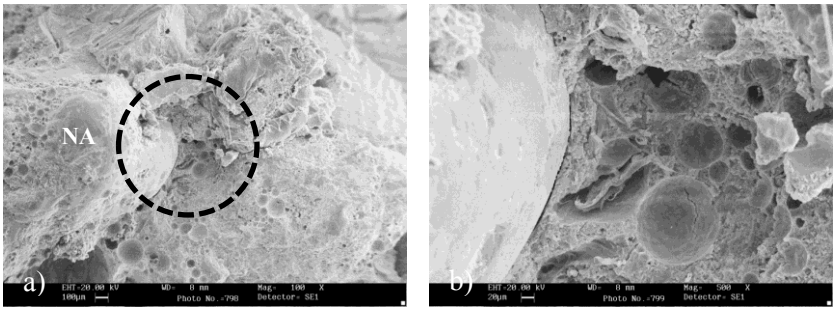

Figure V.23 *a) ITZ between natural aggregate (NA) and cement paste (fractured surface) and b) detail (Coppola et al. 2016)*

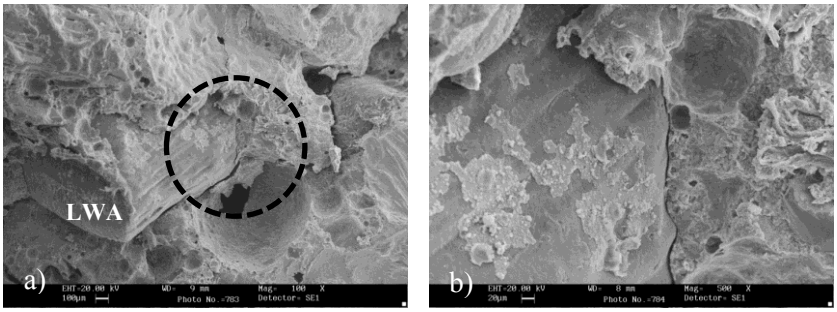

Figure V.24 *a) ITZ between lightweight aggregate (LWA) and cement paste (fractured surface) and b) detail (Coppola et al. 2016)*

At higher magnifications (Figure V.25) details of the hydration products grown into aggregates pores are shown.

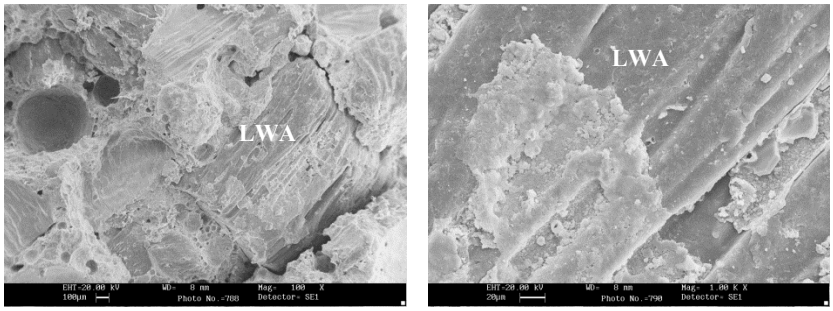

Figure V.25 *Detail of the hydration products grown into LWAs surface pores (Coppola et al. 2016)*

V.3 Use of foamed aggregates as internal curing reservoir

For this investigation, only preliminary results are reported, because tests are still in course. Shrinkage tests are considering the use of artificial aggregates as reservoir for internal curing water. In particular, two different w/c ratios (0.30 and 0.45) and two different tests (autogenous and total shrinkage) are ongoing.

As example, specimens length variation is reported in Figure V.26. It is clear the great influence of aggregates saturation on the dimensional stability. Moreover, at increasing volume sand replacement, a decrease of shrinkage was measured. Thus, despite the different rigidity of plastic aggregates, the saturation can reduce total shrinkage.

Other studies are evaluating the influence of w/c ratio and the amount of length variation due to the autogenous shrinkage.

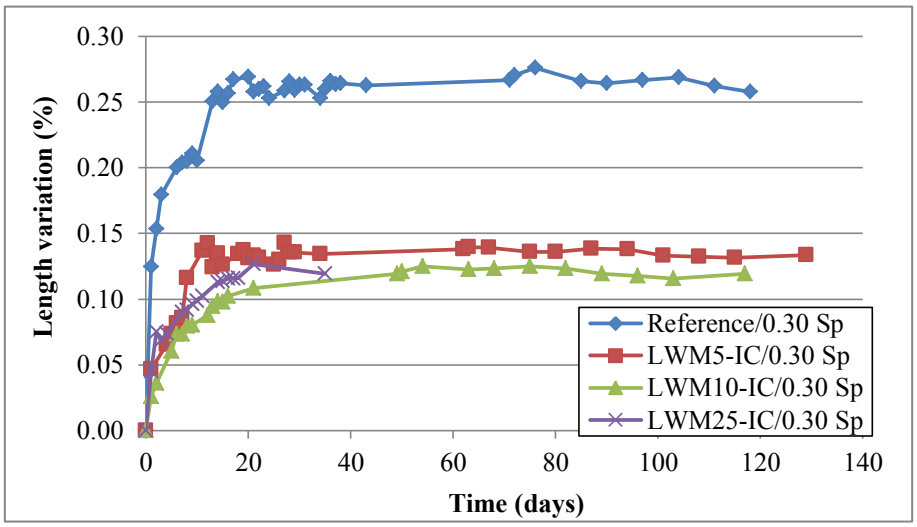

Figure V.26 *Length variation due to total shrinkage (w/c =0.30)*

V.4 Conclusions

In this chapter, the possibility to use foamed plastic wastes for the production of artificial aggregates was investigated. Using plastic waste aggregates was possible to obtain a lighter and sustainable mortar. Aggregates were manufactured by a foam extrusion process, in order to have artificial aggregates with a rough surface. In particular, lightweight aggregates (LWAs) present a cylindrical shape, due to manufacturing process, and an irregular surface texture. On the contrary, natural aggregates are smooth and well rounded. The different shape and surface texture influence mortar workability reducing the consistency but saturating aggregates is possible to slight overcame to this drawback. Increasing LWAs content, a sharp decrease of density was achieved, proportional to LWAs volume fraction. The presence of free water, when aggregates are saturated, produces an increase of porosity and consequently a decrease of compressive strength respect to mixtures containing unsaturated aggregates. At increasing LWAs content a decrease of mechanical properties was achieved but a less brittle behavior was recognizable. However, for all the investigated lightweight mixtures, compressive strength values were higher than the minimum requirements for masonry and repair mortars. LWAs saturation is not influent on flexural strength while a small influence has the use of a lower w/c ratio. Although LWAs low density (65% lower than natural quartz sad) a good dispersion was obtained. Moreover, SEM investigations revealed the presence of interlocking positions onto aggregates surface due to the high porosity and rough surface of foamed aggregates. Thermal conductivity and water vapor resistance decrease at increasing natural sand substitutions and proportionally to mortars density. Finally, the possibility to use aggregates porosity as reservoir of internal curing water was investigated, resulting in promising preliminary results.

Conclusions

This Ph.D. thesis faced the principles and the experimental practice of improving the fiber/cement matrix adhesion in cementitious mortars. In particular, two different methods were attempted: i) the chemical treatments of smooth fibers and ii) the production (by the customization of the extrusion-foaming process) of fibers with a rough surface texture and high porosity. Moreover, also lightweight artificial aggregates were produced and used into a cementitious mortar. Both for fibers and aggregates production, an end-of-waste material was used. In particular, the end-of-waste plastic consists of a polyolefin blend (PE and PP). In order to improve fiber/matrix chemical affinity, two chemical treatments were investigated while to promote fiber/matrix mechanical bond, a foam extrusion process was implemented, in order to produce foamed fibers.

In the first phase of the research, two chemical treatments have been investigated: alkaline hydrolysis and nano-silica sol-gel particles deposition. The first treatment increases fibers roughness while tensile tests reported a slight decrease of fibers ductility; the latter produces nano-silica spherical particles on fibers surface and mechanical properties are not affected. As expected, PP fibers have a very poor adhesion with the cement paste, resulting in a porous ITZ. Alkaline hydrolysis promoted the creation of interlocking positions on fiber surface but the best behavior was recognized for fibers with nano-silica particles on the surface. In this case, a denser ITZ and a great amount of hydration products were observed by SEM investigations. Pull-out tests confirmed the better performances of treated fibers: a higher pull-out peak load was achieved and an increase of pull-out energy was evident.

Subsequently, the possibility to improve fiber/matrix adhesion producing synthetic fibers with a surface texture different from the traditional smooth one was investigated. A foam extrusion process was used to manufacture polymeric fibers with a rough surface, in order to improve mechanical bonding with the cementitious matrix. Moreover, foamed fibers were produced using both a virgin polymer and an end-of-waste material. Optimizing foaming agent quantity and processing parameters was possible to produce fibers having adequate surface texture and diameter, suitable for mortar reinforcement. The optimal foamed fibers were produced using a capillary die of 0.5 mm; 5 wt.% and 2 wt.% of foaming agent for virgin PP

and Recycled fibers, respectively. Concerning fiber reinforced mortars at the fresh state, fibers addition leads to an overall workability decrease, more pronounced for mortars containing non-foamed fibers. Fibers with increased surface roughness showed a reduction of mechanical properties. However mechanical properties, (both flexural and compressive strength) of fiber reinforced mortars, were not influenced by fibers addition nor their morphology. A residual flexural strength was observed both using foamed fibers and non-foamed fibers. In particular, at increasing volume fraction and fibers length an increase of residual load was measured. The effectiveness of rougher surface is evident as samples reinforced with PP foamed fibers have the same residual strength of PP non-foamed FRMs (despite their lower mechanical properties and reduced number of fibers in the specimens cross-section). As expected, the rougher surface gives rise to a better fiber/matrix adhesion, as confirmed by pull-out tests which showed a considerable increase of maximum pull-out load and, consequently, interface toughness.

Durability investigations on the fiber reinforced mortars reported good results for capillary water absorption, sulfate attack and plastic shrinkage cracking. In particular, fibers length and volume fraction are key parameters in controlling plastic shrinkage cracking: increasing fibers volume fraction, a decrease of cracks number and length was achieved whilst longer fibers are more efficient in reducing cracks width. Moreover, mortar samples containing foamed fibers reported a better control of shrinkage cracking because cracks opening was delayed and the improved fiber/matrix bond was able to reduce crack width, compared to mortar slabs containing smooth fibers.

Finally, once that the foaming process was optimized for the end-of-waste material, lightweight artificial aggregates were produced, starting from foamed strands. At increasing LWAs substitution, a sharp decrease of density was achieved. Also workability and mechanical properties decrease, but a more ductile behavior was recognizable. Thanks to the porous and rough surface texture, aggregates buoyancy was avoided and a good aggregates/cement paste ITZ was achieved. Thermal conductivity and water vapor resistance decrease at increasing natural sand substitutions and proportionally to mortars density. Moreover, the possibility to use aggregates porosity as reservoir of internal curing water showed promising preliminary results.

In conclusion, the results of this study demonstrate the possibility to optimize fibers volume fraction in cementitious mortars using engineered fibers with an improved fiber/matrix bond. Surface roughness improvement obtained in foamed fibers resulted to be more effective respect to the chemical treatments. Benefits could be seen not only in the control of plastic shrinkage but also in the workability of fresh mortars, mechanical strength and durability of the hardened composite. Finally, concerning the materials sustainability, it was demonstrated that fibers and light weight aggregates, characterized by high compatibility with cementitious matrix, can be produced from end-of-waste materials.

References

Abbas Y. M. and Khan M. I. (2016) Fiber–Matrix Interactions in Fiber-Reinforced Concrete: A Review. *Arab. J. Sci. Eng.*, **41**, 1183-1198.

Afroughsabet V. and Ozbakkaloglu T. (2015) Mechanical and durability properties of high-strength concrete containing steel and polypropylene fibers. *Constr. Build. Mater.*, **94**, 73-82.

Albano C., Camacho N., Hernandez M., Matheus A. and Gutierrez, A. (2009) Influence of content and particle size of waste pet bottles on concrete behavior at different w/c ratios. *Waste Manage.*, **29**, 2707-2716.

Alizade E., Alaee F. J. and Zabihi S. (2016) Effect of steel fiber corrosion on mechanical properties of steel fiber reinforced concrete. *Asian Journal Of Civil Engineering* (BHRC), **17**, 147-158.

Al-Salem S. M., Lettieri P. and Baeyens J. (2010) The valorization of plastic solid waste (PSW) by primary to quaternary routes: From re-use to energy and chemicals. *Prog. Energ. Combust.*, **36**, 103-129.

Aly T., Sanjayan J. and Collins F. (2008) Effect of polypropylene fibers on shrinkage and cracking of concretes. *Mater. Struct.,* **41**, 1741-1753.

Al-Zboon K. K. and Al-Zou'by J. (2016) Effect of volcanic tuff on the characteristics of cement mortar. *Eur. J. Environ. Civ. En.*, **20**, 520-531.

Aprianti E. (2016) A huge number of artificial waste material can be supplementary cementitious material (SCM) for concrete production–a review part II. *J. Clean. Prod.*, **142**, 4178–4194.

Audo M., Mahieux P. Y. and Turcry P. (2016) Utilization of sludge from ready-mixed concrete plants as a substitute for limestone fillers. *Constr. Build. Mater.*, **112**, 790-799.

Babu D. S., Babu K. G. and Tiong-Huan W. (2006) Effect of polystyrene aggregate size on strength and moisture migration characteristics of lightweight concrete. *Cem. Concr. Compos.*, **28**, 520-527.

Babu K. G. and Babu D. S. (2003) Behaviour of lightweight expanded polystyrene concrete containing silica fume. *Cem. Concr. Res.*, **33**, 755-762.

Banfill P. F. G. (2006) *Rheology of fresh cement and concrete*. Rheology reviews, 2006, 61-130.

Banthia N. and Gupta R. (2006) Influence of polypropylene fiber geometry on plastic shrinkage cracking in concrete. *Cem. Concr. Res.,* **36**, 1263-1267.

Basheer L., Kropp J. and Cleland D. J. (2001) Assessment of the durability of concrete from its permeation properties: a review. *Constr. Build. Mater.*, **15**, 93-103.

Bentur A. and Mindess S. (2006) *Fibre reinforced cementitious composites*. CRC Press.

Bentz D. P., Lura P. and Roberts J. W. (2005) Mixture proportioning for internal curing. *Concr. Int.*, **27**, 35-40.

Bertin, S. and Robin J. J. (2002) Study and characterization of virgin and recycled LDPE/PP blends. *Eur. Polym. J.*, **38**, 2255-2264.

Blander M. and Katz J. L. (1975) Bubble nucleation in liquids. *AIChE Journal*, **21**, 833-848.

Bogas J. A. and Gomes T. (2015) Mechanical and Durability Behaviour of Structural Lightweight Concrete Produced with Volcanic Scoria. *Arab. J. Sci. Eng.*, **40**, 705-717.

Borg R. P., Baldacchino O. and Ferrara L. (2016) Early age performance and mechanical characteristics of recycled PET fibre reinforced concrete. *Constr. Build. Mater.*, **108**, 29-47.

Butera S., Christensen T. H. and Astrup T. F. (2015) Life cycle assessment of construction and demolition waste management. *Waste Manage.*, **44**, 196-205.

Cai G., Noguchi T., Degée H., Zhao J. and Kitagaki R. (2016) Volcano-related materials in concretes: a comprehensive review. *Environ. Sci. and Pollut. R.*, **23**, 7220-7243.

Cardoso R., Silva R. V., de Brito J. and Dhir R. (2016) Use of recycled aggregates from construction and demolition waste in geotechnical applications: A literature review. *Waste Manage.*, **49**, 131-145.

Castro J., Keiser L., Golias M. and Weiss J. (2011) Absorption and desorption properties of fine lightweight aggregate for application to internally cured concrete mixtures. *Cem. Concr. Compos.*, **33**, 1001-1008.

Chan Y.-W. and Li V. C. (1997) Effects of transition zone densification on fiber/cement paste bond strength improvement. *Adv. Cem. Based Mater.,* **5**, 8-17.

Chang T. P., Shih J. Y., Yang K. M. and Hsiao T. C. (2007) Material properties of Portland cement paste with nano-montmorillonite. *J. Mater. Sci.*, **42**, 7478-7487.

Chen Z., Xu J., Chen Y. and Lui E. M. (2016) Recycling and reuse of construction and demolition waste in concrete-filled steel tubes: A review. *Constr. Build. Mater.*, **126**, 641-660.

Choi Y. W., Moon D. J., Chung J. S. and Cho S. K. (2005) Effects of waste PET bottles aggregate on the properties of concrete. *Cem. Concr. Res.*, **35**, 776-781.

Choi Y. W., Moon D. J., Kim Y. J. and Lachemi M. (2009) Characteristics of mortar and concrete containing fine aggregate manufactured from recycled waste polyethylene terephthalate bottles. *Constr. Build. Mater.*, **23**, 2829-2835.

Coppola B., Courard L., Michel F., Incarnato L. and Di Maio L. (2016) Investigation on the use of foamed plastic waste as natural aggregates replacement in lightweight mortar. Compos. Part B-Eng., **99**, 75-83.

Coppola B., Di Maio L., Courard L., Scarfato P. and Incarnato L., (2016b) Development and use of foamed recycled fibers to control shrinkage cracking of cementitious mortars. *In Proceedings of the 4rd Workshop "The New Boundaries of Structural Concrete"*. 167-174.

Coppola B., Di Maio L., Scarfato P. and Incarnato L. (2015) Use of polypropylene fibers coated with nano-silica particles into a cementitious mortar. *In Polymer Processing With Resulting Morphology And Properties: Feet in the Present and Eyes at the Future: Proceedings of the GT70 International Conference* (Vol. 1695, p. 020056). AIP Publishing.

Coppola B., Scarfato P., Incarnato L. and Di Maio L. (2014) Durability and mechanical properties of nanocomposite fiber reinforced concrete. *CSE-City Safety Energy*, **2**, 127-136.

Corcella C. M., Tavano S. and Canonico F. (2004) Analisi reologica delle prestazioni dei superfluidificanti acrilici al variare delle caratteristiche chimico-mineralogiche del cemento (In Italian).

Corinaldesi V., Donnini J. and Nardinocchi A. (2015) Lightweight plasters containing plastic waste for sustainable and energy-efficient building. *Constr. Build. Mater.*, **94**, 337-345.

Corinaldesi V., Mazzoli A. and Moriconi G. (2011) Mechanical behaviour and thermal conductivity of mortars containing waste rubber particles. *Mater. Design*, **32**, 1646-1650.

Correia J. R., Lima J. S. and de Brito J. (2014) Post-fire mechanical performance of concrete made with selected plastic waste aggregates. *Cem. Concr. Compos.*, **53**, 187-199.

Correia S. L., Partala T., Loch F. C. and Segadães A. M. (2010) Factorial design used to model the compressive strength of mortars containing recycled rubber. *Compos. Struct.*, **92**, 2047-2051.

da Silva A. M., de Brito J. and Veiga R. (2014) Incorporation of fine plastic aggregates in rendering mortars. *Constr. Build. Mater.*, **71**, 226-236.

Dintcheva N. T., La Mantia F. P., Trotta F., Luda M. P., Camino G., Paci M., Di Maio L. and Acierno D. (2001) Effects of filler type and processing apparatus on the properties of the recycled "light fraction" from municipal post-consumer plastics. *Polym. Advan. Technol.*, **12**, 552-560.

Du H., Du S. and Liu X. (2015) Effect of nano-silica on the mechanical and transport properties of lightweight concrete. *Constr. Build. Mater.*, **82**, 114-122.

Dubois S. and Lebeau F. (2015) Design, construction and validation of a guarded hot plate apparatus for thermal conductivity measurement of high thickness crop-based specimens. *Mater. Struct.*, **48**, 407-421.

Ferrándiz-Mas V., Bond T., García-Alcocel E. and Cheeseman C. R. (2014) Lightweight mortars containing expanded polystyrene and paper sludge ash. *Constr. Build. Mater.*, **61**, 285-292.

Ferraris C. F., Obla K. H. and Hill R. (2001) The influence of mineral admixtures on the rheology of cement paste and concrete. *Cem. Concr. Res.*, **31**, 245-255.

Ferreira L., de Brito J. and Saikia N. (2012) Influence of curing conditions on the mechanical performance of concrete containing recycled plastic aggregate. *Constr. Build. Mater.*, **36**, 196-204.

Feys D., Verhoeven R. and De Schutter G. (2008) Fresh self compacting concrete, a shear thickening material. *Cem. Concr. Res.*, **38**, 920-929.

Fraternali F., Ciancia V., Chechile R., Rizzano G., Feo L. and Incarnato L. (2011) Experimental study of the thermo-mechanical properties of recycled PET fiber-reinforced concrete. *Compos. Struct.*, **93**, 2368-2374.

Gadea J., Rodríguez A., Campos P. L., Garabito J. And Calderón, V. (2010) Lightweight mortar made with recycled polyurethane foam. *Cem. Concr. Compos.*, **32**, 672-677.

Garofalo E., Claro M., Scarfato P., Di Maio L. and Incarnato L. (2015) Upgrading of recycled plastics obtained from flexible packaging waste by adding nanosilicates. In *Polymer Processing With Resulting Morphology And Properties: Feet in the Present and Eyes at the Future: Proceedings of the GT70 International Conference* (Vol. 1695, p. 020053). AIP Publishing.

Golias M., Castro J. and Weiss J. (2012) The influence of the initial moisture content of lightweight aggregate on internal curing. *Constr. Build. Mater.*, **35**, 52-62.

Grünewald S. (2012) Fibre reinforcement and the rheology of concrete. In Roussel Nicolas, *Understanding the rheology of concrete*. Elsevier.

Gutiérrez-González S., Gadea J., Rodríguez A., Junco C. and Calderón V. (2012) Lightweight plaster materials with enhanced thermal properties made with polyurethane foam wastes. *Constr. Build. Mater.*, **28**, 653-658.

Hannawi K., Kamali-Bernard S. and Prince W. (2010) Physical and mechanical properties of mortars containing PET and PC waste aggregates. *Waste Manage.*, **30**, 2312-2320.

Hassanpour M., Shafigh P. and Mahmud H. B. (2012) Lightweight aggregate concrete fiber reinforcement–a review. *Constr. Build. Mater.*, **37**, 452-461.

He H., Stroeven P., Pirard E. and Courard L. (2015) On the shape simulation of aggregate and cement particles in a DEM system. *Advances in Materials Science and Engineering*.

Henry P. (2016) *Circular Economy package–what's in it*.

Hernández-Olivares F., Bollati M. R., Del Rio M. and Parga-Landa, B. (1999) Development of cork–gypsum composites for building applications. *Constr. Build. Mater.*, **13**, 179-186.

Horvath A. (2004) Construction materials and the environment. *Annu. Rev. Environ. Resour.*, **29**, 181-204.

Ignatyev I. A., Thielemans W. and Vander Beke B. (2014) Recycling of polymers: a review. *ChemSusChem*, **7**, 1579-1593.

Imbabi M. S., Carrigan C. and McKenna S. (2012) Trends and developments in green cement and concrete technology. *Int. J. Sust. Built Environ.*, **1**, 194-216.

Intini F. and Kühtz S. (2011) Recycling in buildings: an LCA case study of a thermal insulation panel made of polyester fiber, recycled from post-consumer PET bottles. *Int. J. Life Cycle Assess.*, **16**, 306-315.

Iucolano F., Liguori B., Caputo D., Colangelo F. and Cioffi R. (2013) Recycled plastic aggregate in mortars composition: Effect on physical and mechanical properties. *Mater. Design*, **52**, 916-922.

Jayapalan A. R., Lee B. Y. and Kurtis K. E. (2013) Can nanotechnology be 'green'? Comparing efficacy of nano and microparticles in cementitious materials. *Cem. Concr. Compos.,* **36**, 16-24.

Jensen O. M. and Hansen P. F. (2001) Water-entrained cement-based materials: I. Principles and theoretical background. *Cem. Concr. Res.*, **31**, 647-654.

Jo B. W., Kim C. H., Tae G. H. and Park J. B. (2007) Characteristics of cement mortar with nano-SiO 2 particles. *Constr. Build. Mater.*, **21**, 1351-1355.

Kakooei S., Akil H. M., Jamshidi M. and Rouhi J. (2012) The effects of polypropylene fibers on the properties of reinforced concrete structures. *Constr. Build. Mater.,* **27**, 73-77.

Kan A. and Demirboğa R. (2009) A novel material for lightweight concrete production. *Cem. .Concr. Compos.*, **31**, 489-495.

Kan A. and Demirboğa R. (2009a) A novel material for lightweight concrete production. *Cem. Concr. Compos.*, **31**, 489-495.

Kan A. and Demirboğa R. (2009b) A new technique of processing for waste-expanded polystyrene foams as aggregates. *J. Mater. Process. Tech.*, **209**, 2994-3000.

Kim J.-H. J., Park C.-G., Lee S.-W., Lee S.-W. and Won J.-P. (2008) Effects of the geometry of recycled PET fiber reinforcement on shrinkage cracking of cement-based composites. *Compos. Part B-Eng.*, **39**, 442-450.

Kim S. B., Yi N. H., Kim H. Y., Kim J.-H. J. and Song Y.-C. (2010) Material and structural performance evaluation of recycled PET fiber reinforced concrete. *Cem. Concr. Compos.*, **32**, 232-240.

Knoeri C., Sanyé-Mengual E. and Althaus H. J. (2013) Comparative LCA of recycled and conventional concrete for structural applications. *Int. J. Life Cycle Assess.*, **18**, 909-918.

Kong L., Zhang B. and Yuan J. (2009) Effect of lightweight aggregate pre-wetting on microstructure and permeability of mixed aggregate concrete. *J. Wuhan Univ. Technol.-Mater. Sci. Ed.*, **24**, 838-842.

Kraai P. P. (1985) A proposed test to determine the cracking potential due to drying shrinkage of concrete. *Concrete Constr.*, **30**, 775-778.

Lancaster L. C. (2005) *Concrete vaulted construction in Imperial Rome: innovations in context*. Cambridge University Press.

Lanzoni L., Nobili A. and Tarantino A. M. (2012) Performance evaluation of a polypropylene-based draw-wired fibre for concrete structures. *Constr. Build. Mater.*, **28**, 798-806.

Lee S. T. and Park C. B. (2014) *Foam extrusion: principles and practice*. CRC press.

Lee S. T. and Ramesh N. S. (2004) *Polymeric foams: mechanisms and materials.* CRC press.

Lee S. T., Park C. B. and Ramesh N. S. (2007). *Polymeric foams: science and technology.* CRC Press.

León M. P. and Ramírez F. (2010) Morphological characterization of concrete aggregates by means of image analysis. *J. Constr. Eng.*, **25**, 215-240.

Li G., Stubblefield M. A., Garrick G., Eggers J., Abadie C. and Huang B. (2004) Development of waste tire modified concrete. *Cem. Concr. Res.*, **34**, 2283-2289.

Libre N. A., Shekarchi M., Mahoutian M. and Soroushian P. (2011) Mechanical properties of hybrid fiber reinforced lightweight aggregate concrete made with natural pumice. *Constr. Build. Mater.*, **25**, 2458-2464.

Liguori B., Iucolano F., Capasso I., Lavorgna M. and Verdolotti L. (2014) The effect of recycled plastic aggregate on chemico-physical and functional properties of composite mortars. *Mater. Design*, **57**, 578-584.

López-Buendía A. M., Romero-Sánchez M. D., Climent V. and Guillem C. (2013) Surface treated polypropylene (PP) fibres for reinforced concrete. *Cem. Concr. Res.*, **54**, 29-35.

Ma Q., Guo R., Zhao Z., Lin Z. and He K. (2015) Mechanical properties of concrete at high temperature-a review. *Constr. Build. Mater.*, **93**, 371-383.

Machovič V., Lapčák L., Borecka L., Lhotka M., Andertova J., Kopecký L. and Mišková L. (2013) Microstructure of interfacial transition zone between PET fibres and cement paste. *Acta Geodyn. Geomater*., **10**, 121–127.

Madandoust R., Ranjbar M. M. and Mousavi S. Y. (2011) An investigation on the fresh properties of self-compacted lightweight concrete containing expanded polystyrene. *Constr. Build. Mater.*, **25**, 3721-3731.

Martinie L., Rossi P. and Roussel N. (2010) Rheology of fiber reinforced cementitious materials: classification and prediction. *Cem. Concr. Res.*, **40**, 226-234.

Marzouk O. Y., Dheilly R. M. and Queneudec M. (2007) Valorization of post-consumer waste plastic in cementitious concrete composites. *Waste Manage.*, **27**, 310-318.

Meyer C. (2009) The greening of the concrete industry. *Cem. Concr. Compos.*, **31**, 601-605.

Mora E. P. (2007) Life cycle, sustainability and the transcendent quality of building materials. *Build. Environ.*, **42**, 1329-1334.

Mounanga P., Gbongbon W., Poullain P. and Turcry, P. (2008) Proportioning and characterization of lightweight concrete mixtures made with rigid polyurethane foam wastes. *Cem. Concr. Compos.*, **30**, 806-814.

Naaman A. E. (2003) Engineered steel fibers with optimal properties for reinforcement of cement composites. *J. Adv. Concr. Technol.*, **1**, 241-252.

Napolano L., Menna C., Graziano S. F., Asprone D., D'Amore M., de Gennaro R. and Dondi M. (2016) Environmental life cycle assessment of lightweight concrete to support recycled materials selection for sustainable design. *Constr. Build. Mater.*, **119**, 370-384.

Nehdi M., Mindess S. and Aıtcin P. C. (1998) Rheology of high-performance concrete: effect of ultrafine particles. *Cem. Concr. Res.*, **28**, 687-697.

Neville A. M. (1995) *Properties of concrete*.

Nóvoa P. J. R. O., Ribeiro M. C. S., Ferreira A. J. M. and Marques A. T. (2004) Mechanical characterization of lightweight polymer mortar modified with cork granulates. *Compos. Sci. Technol.*, **64**, 2197-2205.

Ochi T., Okubo S. and Fukui K. (2007) Development of recycled PET fiber and its application as concrete-reinforcing fiber. *Cem. Concr. Compos.*, **29**, 448-455.

Ossa A., García J. L. and Botero E. (2016) Use of recycled construction and demolition waste (CDW) aggregates: A sustainable alternative for the pavement construction industry. *J. Clean. Prod.*, **135**, 379-386.

Ozger O. B., Girardi F., Giannuzzi G. M., Salomoni V. A., Majorana C. E., Fambri, L., Baldassino N. and Di Maggio R. (2013) Effect of nylon fibres on mechanical and thermal properties of hardened concrete for energy storage systems. *Mater. Design*, **51**, 989-997.

Pacheco-Torgal F. and Jalali S. (2011) Cementitious building materials reinforced with vegetable fibres: A review. *Constr. Build. Mater.*, **25**, 575-581.

Panesar D. K. and Shindman B. (2012) The mechanical, transport and thermal properties of mortar and concrete containing waste cork. *Cem. Concr. Compos.*, **34**, 982-992.

Pedro D., de Brito J. and Veiga R. (2012) Mortars made with fine granulate from shredded tires. *J. Mater. Civil Eng.*, **25**, 519-529.

Pei M., Wang D., Zhao Y., Hu X., Xu Y., Wu J. and Xu D. (2004) Surface treatments of subdenier monofilament polypropylene fibers to optimize their reinforcing efficiency in cementitious composites. *J. Appl. Polym. Sci.*, **92**, 2637-2641.

Pešić N., Živanović S., Garcia R. and Papastergiou P. (2016) Mechanical properties of concrete reinforced with recycled HDPE plastic fibres. *Constr. Build. Mater.*, **115**, 362-370.

Ramachandran V. S. and Beaudoin J. J. (2000) *Handbook of analytical techniques in concrete science and technology: principles, techniques and applications*. Elsevier.

Rashad A. M. (2016) Vermiculite as a construction material–A short guide for Civil Engineer. *Constr. Build. Mater.*, **125**, 53-62.

Ries J. P. and Holm T. A. (2004) A Holistic Approach to Sustainability For the Concrete Community—Lightweight Concrete-Two Millennia of Proven Performance. *Information Sheet*, **7700**, 1-15.

Rigamonti L., Grosso M., Møller J., Sanchez V. M., Magnani S. and Christensen T. H. (2014) Environmental evaluation of plastic waste management scenarios. *Resour. Conserv. Recy.*, **85**, 42-53.

Robichaud L. B. and Anantatmula V. S. (2010) Greening project management practices for sustainable construction. *J. Manage. Eng.*, **27**, 48-57.

Rottstegge J., Han C. C. and Hergeth W. D. (2006) Compatibility Investigations on Polymer-Fiber-Reinforced Cements Modified with Polymer Latexes. *Macromol. Mater. Eng.*, **291**, 345-356.

Sabnis G. M. (2015) *Green Building with Concrete: Sustainable Design and Construction*. CRC Press.

Saikia N. and de Brito J. (2014) Mechanical properties and abrasion behaviour of concrete containing shredded PET bottle waste as a partial substitution of natural aggregate. *Constr. Build. Mater.*, **52**, 236-244.

Saikia N. and de Brito J. (2014) Mechanical properties and abrasion behaviour of concrete containing shredded PET bottle waste as a partial substitution of natural aggregate. *Constr. Build. Mater.*, **52**, 236-244.

Sauceau M., Fages J., Common A., Nikitine C. and Rodier E. (2011) New challenges in polymer foaming: A review of extrusion processes assisted by supercritical carbon dioxide. *Prog. Polym. Sci.*, **36**, 749-766

Schoon J., Buysser K. D., Driessche I. V. and Belie, N. D. (2014) Feasibility study of the use of concrete sludge as alternative raw material for Portland clinker production. *J. of Mater. Civil Eng.*, **27**, 04014272.

Shah S. P., Hou P. and Cheng X. (2015) Durability of Cement-Based Materials and Nano-particles: A Review. *In Nanotechnology in Construction* (pp. 15-24). Springer International Publishing.

Shanks R. A., Li J. and Yu L. (2000) Polypropylene–polyethylene blend morphology controlled by time–temperature–miscibility. *Polymer*, **41**, 2133-2139.

Shannag M. J., Brincker R. and Hansen W. (1997) Pullout behavior of steel fibers from cement-based composites. *Cem. Concr. Res.*, **27**, 925-936.

Sharma R. and Bansal P. P. (2016) Use of different forms of waste plastic in concrete–a review. *J. Clean. Prod.*, **112**, 473-482.

Singh A., Berghorn G., Joshi S. and Syal M. (2010) Review of life-cycle assessment applications in building construction. *Journal of Architectural Engineering*, **17**, 15-23.

Singh S., Shukla A. and Brown R. (2004) Pullout behavior of polypropylene fibers from cementitious matrix. *Cem. Concr. Res.*, **34**, 1919-1925.

Singh, L. P., Agarwal S. K., Bhattacharyya S. K., Sharma U. and Ahalawat S. (2011) Preparation of silica nanoparticles and its beneficial role in cementitious materials. *Nanomater. Nanotechno*., **1**, 44-51.

Song P. S., Hwang S. and Sheu B. C. (2005) Strength properties of nylon- and polypropylene-fiber-reinforced concretes. *Cem. Concr. Res.*, **35**, 1546-1550.

Spadea S., Farina I., Carrafiello A. and Fraternali F. (2015) Recycled nylon fibers as cement mortar reinforcement. *Constr. Build. Mater.*, **80**, 200-209.

Thong C. C., Teo D. C. L. and Ng C. K. (2016) Application of polyvinyl alcohol (PVA) in cement-based composite materials: A review of its engineering properties and microstructure behavior. *Constr. Build. Mater.*, **107**, 172-180.

Tittarelli F., Giosuè C., Mobili A., di Perna C. and Monosi S. (2016) Effect of Using Recycled Instead of Virgin EPS in Lightweight Mortars. *Procedia Eng.*, **161**, 660-665.

Turk J., Cotič Z., Mladenovič A. and Šajna A. (2015) Environmental evaluation of green concretes versus conventional concrete by means of LCA. *Waste Manage.*, **45**, 194-205.

Uhlmann D. R. and Chalmers B. (1965) The energetics of nucleation. *Ind. Eng. Chem.*, **57**, 19-31.

Uno P. J. (1998) Plastic shrinkage cracking and evaporation formulas. *ACI Mater. J.*, **95**, 365-375.

Wang R. and Meyer C. (2012) Performance of cement mortar made with recycled high impact polystyrene. *Cem. Concr. Compos.*, **34**, 975-981.

Westerholm M., Lagerblad B., Silfwerbrand J. and Forssberg E. (2008) Influence of fine aggregate characteristics on the rheological properties of mortars. *Cem. Concr. Compos.*, **30**, 274-282.

Wu H.-C. and V. C. Li (1999) Fiber/cement interface tailoring with plasma treatment. *Cem. Concr. Compos.,* **21**, 205-212.

Yang Z., Liu J., Liu J., Li C. and Zhou H., Silica modified synthetic fiber for improving interface property in FRCC, in *8th RILEM International Symposium on Fiber Reinforced Concrete: challenges and opportunities* (BEFIB 2012), edited by J. A. O. Barros (RILEM Publications SARL, 2013), pp. 347-357

Yin S., Tuladhar R., Shanks R. A., Collister T., Combe M., Jacob M., Tian M. and Sivakugan N. (2015b) Fiber preparation and mechanical properties of recycled polypropylene for reinforcing concrete. *J. Appl. Polym. Sci.*, **132**.

Yin S., Tuladhar R., Sheehan M., Combe M. and Collister T. (2016) A life cycle assessment of recycled polypropylene fibre in concrete footpaths. *J. Clean. Prod.*, **112**, 2231-2242.

Yin S., Tuladhar R., Shi F., Combe M., Collister T. and Sivakugan N. (2015a) Use of macro plastic fibres in concrete: a review. *Constr. Build. Mater.*, **93**, 180-188.

Yu J. (2013) Development and application of expanded polypropylene foam. *J. Wuhan Univ. Technol.-Mater. Sci. Ed.*, **28**, 373-379.

Yu J. (2013) Development and application of expanded polypropylene foam. *J. Wuhan Univ. Technol.-Mater. Sci. Ed.*, **28**, 373-379.

Zollo R. F. (1997) Fiber-reinforced concrete: an overview after 30 years of development. *Cem. Concr. Compos.*, **19**, 107-122.

Zuo J. and Zhao Z. Y. (2014) Green building research–current status and future agenda: A review. *Renew. Sust. Energ. Rev.*, **30**, 271-281.

Standards:

EN 196-1, Methods of testing cement: Determination of strength. September 1996.

EN 206-1, Concrete: Specification, performance, production and conformity. March 2006.

EN 933-1, Tests for geometrical properties of aggregates: Determination of particle size distribution, sieving method. April 1999.

EN 998-1, Specification for mortar for masonry: Rendering and plastering mortar, March 2004.

EN 998-2, Specification for mortar for masonry: Masonry mortar, March 2004.

EN 1015-3, Methods of test for mortar for masonry: Determination of consistence of fresh mortar (by flow table). June 2000.

EN 1015-19, Methods of test for mortar for masonry: Determination of water vapour permeability of hardened rendering and plastering mortars, June 2000.

EN 1097-3, Tests for mechanical and physical properties of aggregates: Determination of loose bulk density and voids. October 1999.

EN 1097-6, Tests for mechanical and physical properties of aggregates: Determination of particle density and water absorption. August 2013.

EN 12350-2, Testing fresh concrete: Slump-test, June 2009.

EN 12390-7, Testing hardened concrete: Density of hardened concrete, May 2009.

EN 12667, Thermal performance of building materials and products: Determination of thermal resistance by means of guarded hot plate and heat flow meter methods. Products of high and medium thermal resistance, March 2001.

ASTM C 1557-03, Standard Test Method for Tensile Strength and Young's Modulus of Fibers, 2014.

ISO 8302, Thermal insulation - Determination of steady-state thermal resistance and related properties - Guarded hot plate apparatus, 1991.

ISO 14040, Environmental management - Life cycle assessment - Principles and framework, 2006.

Directive 2008/98/EC, Waste Framework Directive, November 2008.

ACI 201.2R-01, Guide to Durable Concrete.

IUCN, World Conservation Strategy, 1980.

Japanese JCI SF-8, Method of testing for bonds of fibers, Japan Concrete Institute Committee on Fiber Reinforced Concrete, Tokyo, Japan.

Brundtland G., Khalid M., Agnelli S., Al-Athel S., Chidzero B., Fadika L., ... and Singh, M. (1987). Our common future (or "Brundtland report").

United Nations Conference on Environment and Development (1992: Rio de Janeiro, Brazil). Agenda 21: Programme of Action for Sustainable Development: Rio Declaration on Environment and Development: Statement of Forest Principles. New York: United Nations, 1993.

Report EUR 26843 EN, Villanueva and Eder 2014, End-of-waste criteria for waste plastic for conversion.

List of Symbols and Abbreviations

DSC	Differential Scanning Calorimetry
E	Elastic Modulus
FIER	Fiber Intrinsic Efficiency Ratio
FRC	Fiber Reinforced Cementitious Materials
FTIR	Fourier-Transform Infrared
GHP	Guarded Hot Plate
HDPE	High Density Polyethylene
ITZ	Interfacial Transition Zone
LCA	Life Cycle Assessment
LDPE	Low Density Polyethylene
LEED	Leadership in Energy and Environmental Design
LWAs	Lightweight Aggregates
PP	Polypropylene
r	Radius
RC	Reinforced Concrete
SEM	Scanning Electron Microscope
TGA	Thermogravimetric Analysis
W_{vp}	Water Vapor Permeability
WVT	Water Vapor Transmission rate
ε_b	Deformation at break
λ	Thermal conductivity
ρ	Density
σ_b	Tensile strength